The Institute of Paper Chemistry

Appleton, Wisconsin

Doctor's Dissertation

An Autoradiographic Study of Pentosan Deposition in the Cell Walls of *Populus tremuloides* Michx.

R. H. Mullis

June, 1975

AN AUTORADIOGRAPHIC STUDY OF PENTOSAN DEPOSITION IN THE CELL WALLS OF *POPULUS TREMULOIDES* MICHX.

A thesis submitted by

R. H. Mullis

B.S. 1967, North Carolina State University

M.S. 1969, Lawrence University

in partial fulfillment of the requirements
of The Institute of Paper Chemistry
for the degree of Doctor of Philosophy
from Lawrence University
Appleton, Wisconsin

June, 1975

TABLE OF CONTENTS

SUMMARY

Genetically identical, first-year plantlets of Populus tremuloides Michx. were infusion-fed solutions of radioactive sugars, L-arabinose-1-^{3}H (A), D-glucose-6-^{3}H (G6), and D-glucose-1-^{3}H (G1). Samples of xylem tissue from stem segments were removed after various periods of growth and examined by radiochemical and autoradiographic means.

Radiochemical studies indicated that sugar A specifically labeled the xylosyl and arabinosyl units of the wood polysaccharides with only minor labeling of the lignin. Similar studies indicated that radioactive cellulose, lignin, and pentosan were formed in the woody tissue fed sugar G1 while only cellulose and lignin were significantly labeled in the developing wood fed sugar G6.

Light and electron microscope autoradiography localized the newly synthesized wall material both on a macroscale (among the various xylem cells) and on a microscale (within individual cell walls). Comparative autoradiographic examinations of woody tissues fed sugars A and G6 revealed relatively large amounts of labeled pentosan in the cell walls of ray and pith parenchyma. In addition, the "protective layer" in ray cells adjacent to vessel elements contained considerable amounts of labeled pentosan.

Analyses of grain distributions in electron micrographs of individual woody fiber cells revealed the deposition patterns of labeled wall components. Grain density gradients across the fiber walls were calculated with the aid of a digital computer. Raw autoradiographic data consisted of grain and wall interface coordinates that were digitized directly from the electron micrographs. Model distributions of grain density predicted for autoradiographs of band sources of radioactivity were fitted to the computed distributions.

The locations of the model band sources were then used to indicate the positions of labeled cell wall components.

Autoradiographs of fiber cells analyzed in this manner included not only cells of developing wood administered sugars A and G6, but also cells of woody tissue fed sugar G6 and subsequently delignified. These analyses indicated that cellulose and pentosan were added to the secondary wall by apposition while lignin was deposited by intussusception.

INTRODUCTION

The wood cell wall is composed primarily of a cellulose framework embedded in a matrix of noncellulosic polysaccharides and lignin. The noncellulosic polysaccharides are often collectively called hemicelluloses. Most of the hemicelluloses have now been isolated and characterized by various analytical techniques. In addition, biochemical investigations have added much to our knowledge of the enzymatic reactions leading to hemicellulose biosynthesis. The manner of polymerization and deposition of hemicelluloses during formation of the thick cell walls of wood, however, has been mostly a matter of speculation. The object of this thesis research was to localize a major wood hemicellulose and to study, *in situ*, the dynamics of its deposition in the developing fiber cell wall.

HISTORICAL REVIEW

HEMICELLULOSE DISTRIBUTION IN WOOD

Although a number of methods have been used in efforts to determine the distribution of various components within woody tissue, the localization of the hemicelluloses within the cell wall has not been established with certainty. Fractionation of cells by size has indicated, however, that hemicellulose content varies according to cell type. Perilä (1) found that the ray parenchyma cells of *Betula pendula* (*B. verrucosa*) wood, for example, contained nearly twice as much xylan as the fibers and vessel elements.

Direct microscopic and histochemical methods can differentiate lignin from carbohydrate in the cell wall, but the histochemical methods used to localize specific polysaccharides are few and usually based on nonspecific or unknown reactions. It was suggested by Meier (2) that the best technique

for studying the location of the hemicelluloses would be the microdissection of single fibers with chemical analysis of the separated wall layers. Bailey (3) succeeded in physically isolating and analyzing a small amount of material derived from the compound middle lamella of Douglas-fir wood, but with the exception of the gelatinous layer in aspen tension wood (4), the various layers of the secondary cell wall have not yet been partitioned into discrete fractions for analysis.

The results of studies by Meier (5-6) on polysaccharide distributions in fiber and tracheid cell walls of three woody species have been included in various wood chemistry texts (2,7-11). Employing a similar but more elegant method than that used earlier by Sultze (12,13), Meier chemically examined fractions of developing xylem tissue at different stages of maturation. By assuming successive deposition of the wall components layer upon layer, i.e., by apposition, he deduced a distribution gradient for each polysaccharide across the cell wall. Such distributions should be accepted with reservation, however, since appositional deposition of polysaccharides has not been proven and wall composition may change with time as evidenced by the short-lived nature of the mucilaginous polysaccharide found in the developing cells of two softwoods (14). Also, this method requires a knowledge of the proportions of the sugar units in the wood heteropolysaccharides since the polysaccharide composition of each fraction is calculated from the relative concentrations of the sugars in the hydrolyzate. Coté, et al. (15), for example, point out that the data of Meier and Wilkie (5) were calculated before it was known that some galactose units are a part of the heteropolymer, galactoglucomannan, in softwoods (16).

HEMICELLULOSE DEPOSITION IN THE DEVELOPING CELL WALL

Conclusive evidence exists that lignin is deposited in depth within the developing wall, i.e., by intussusception (17-20), but conflicting reports have appeared about mechanisms of cellulose and hemicellulose deposition. The ability of isotope labeling techniques to differentiate recently synthesized material from previously formed products has been used by a number of investigators to study the patterns of polysaccharide formation and the sites of their incorporation into cell walls. Green (21) used a novel counting method with a tritium precursor to demonstrate incorporation of new wall substance at the inner face of the elongating primary cell wall of the alga, Nitella. Two autoradiography studies of tritium-labeled polysaccharides biosynthesized in the thick primary walls of oat coleoptile epidermal cells yielded conflicting conclusions. One study suggested that deposition of both cellulose and noncellulosic polysaccharides occurs throughout the wall (22); a later investigation concluded that the bulk of the cellulose is deposited appositionally and the other polysaccharides are deposited intussusceptionally (23).

While the first-formed primary cell wall usually grows by increasing its surface area, keeping a relatively constant wall thickness, the secondary wall forms to the inside of the primary wall at the end of cell enlargement, growing only in thickness. The lamellate arrangement of cellulose microfibrils usually observed in walls undergoing secondary thickening is consistent with appositional deposition of cellulose. Such observations led Roelofsen (24) to write: "It seems beyond doubt that at least the main part of the cellulose is not formed within the wall, but by apposition to it. This certainly applies to secondary thickening..." Evidence gained by Dennis and Colvin (25)

and Preston (26) suggests that the outer cytoplasmic membrane is responsible for cellulose synthesis and, therefore, also implies that cellulose is deposited appositionally. Based on electron microscope studies of developing primary and secondary cell walls, Wardrop (27) stated:

> "...it would seem at this stage resonable to postulate that, insofar as the phenomena of vesicular secretion and lamellar apposition are involved in wall synthesis, the former is effective in the incorporation of matrix and incrusting constituents into the wall and the latter in elaborating the cellulose framework."

Thus, although there seems to be some agreement that cellulose and hemicellulose are deposited by different mechanisms, direct evidence conclusively indicating the manner of deposition of these components in the secondary wall is still lacking.

RADIOACTIVE TRACERS AND CELL WALL METABOLISM

Radioactive tracers have found extensive application to the study of biosynthetic reactions leading to cell wall formation. Notwithstanding the possible problems of misinterpretation from the administration of sometimes "unnatural" precursors, tracer techniques have afforded knowledge about metabolic pathways which could not have been obtained by other means. The major limitation in tracer work is that simply demonstrating that a precursor is converted to a certain product does not prove that the precursor is a normal intermediate in the biosynthesis of that component. Of course, if the object is simply to label a specific product, any suitable precursor will suffice, "natural" or not.

The carbohydrate products of photosynthesis are the major source of raw material for cell wall formation. Transported from the leaves and other sites

of photosynthesis, the bulk of the photosynthate is sucrose and other nonreducing sugars (28). Cells undergoing differentiation not only consume these nutrients by catabolic pathways, but also transform them by a complex sequence of enzymatic reactions into the various wall polysaccharides and lignin.

Polysaccharide Synthesis

Free sugars must be activated, i.e., phosphorylated, as a first step toward polysaccharide formation. The sugar phosphates are then converted to higher energy sugar nucleotides which apparently serve as the glycosyl donors for the various polysaccharides. A number of specific enzymes are capable of acting on these phosphates and nucleotides to yield the various nucleotides containing the sugar moieties necessary for synthesizing specific polysaccharides. Current evidence indicates that cellulose is formed from uridine diphosphate (UDP)-D-glucose and/or guanosine diphosphate (GDP)-D-glucose; starch, from adenosine diphosphate (ADP)-D-glucose and/or UDP-D-glucose; polysaccharides containing pentoses and uronic acids, from the appropriate UDP sugars; and polysaccharides containing D-mannose and L-fucose, from GDP-D-mannose and GDP-L-fucose (29,30). The activation of free sugars and their subsequent interconversions as sugar phosphates and sugar nucleotides are consistent with the schemes presented in Fig. 1 and 2 which are based on reported metabolic pathways (29-32).

Figure 1 illustrates how various free sugars can be converted to the UDP sugars. UDP-D-glucose is a major sugar nucleotide and is capable of producing the other UDP sugars in a direct manner, as indicated, by the action of specific enzymes. Alternatively, the uronic acid and pentose nucleotides can be formed through the myo-inositol oxidation pathway. While sucrose and glucose undoubtedly serve as the major source of carbohydrate for the manufacture of

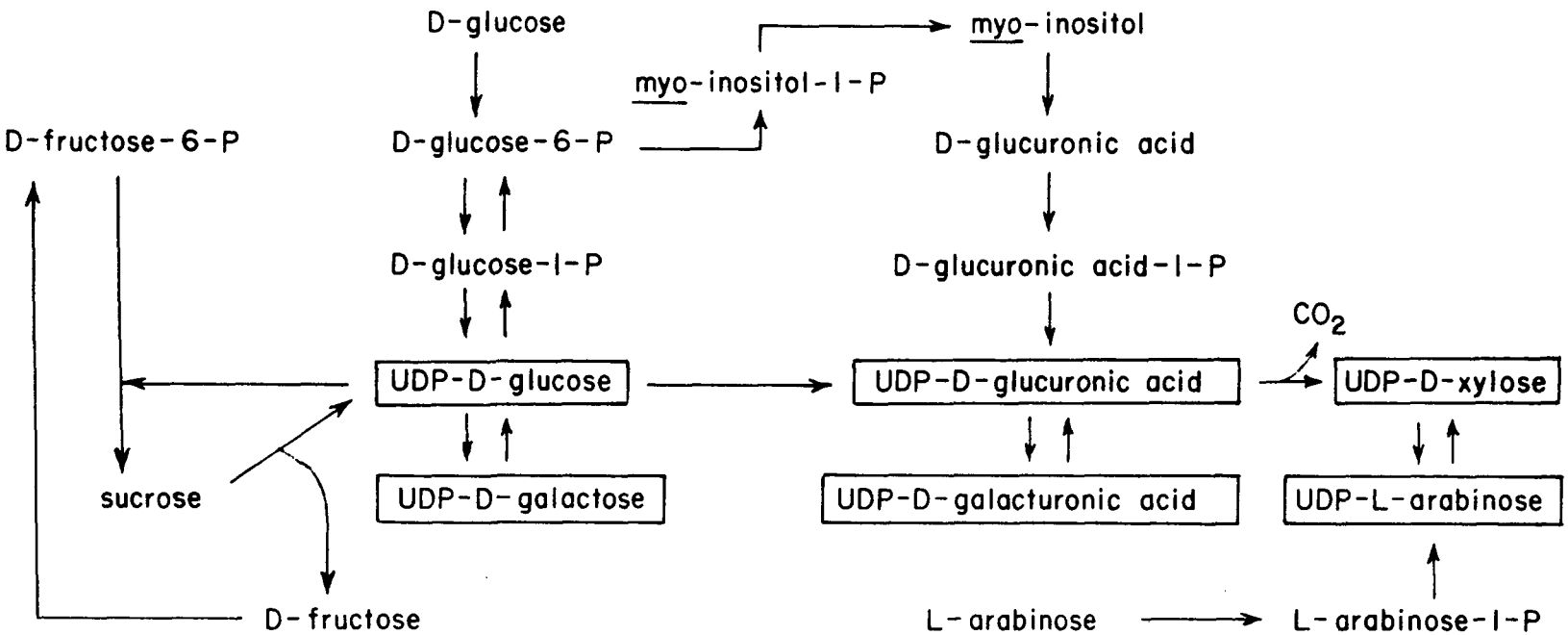

Figure 1. Metabolic Pathways Leading to the Formation of the UDP Sugars.
P = Phosphate; UDP = Uridine Diphosphate

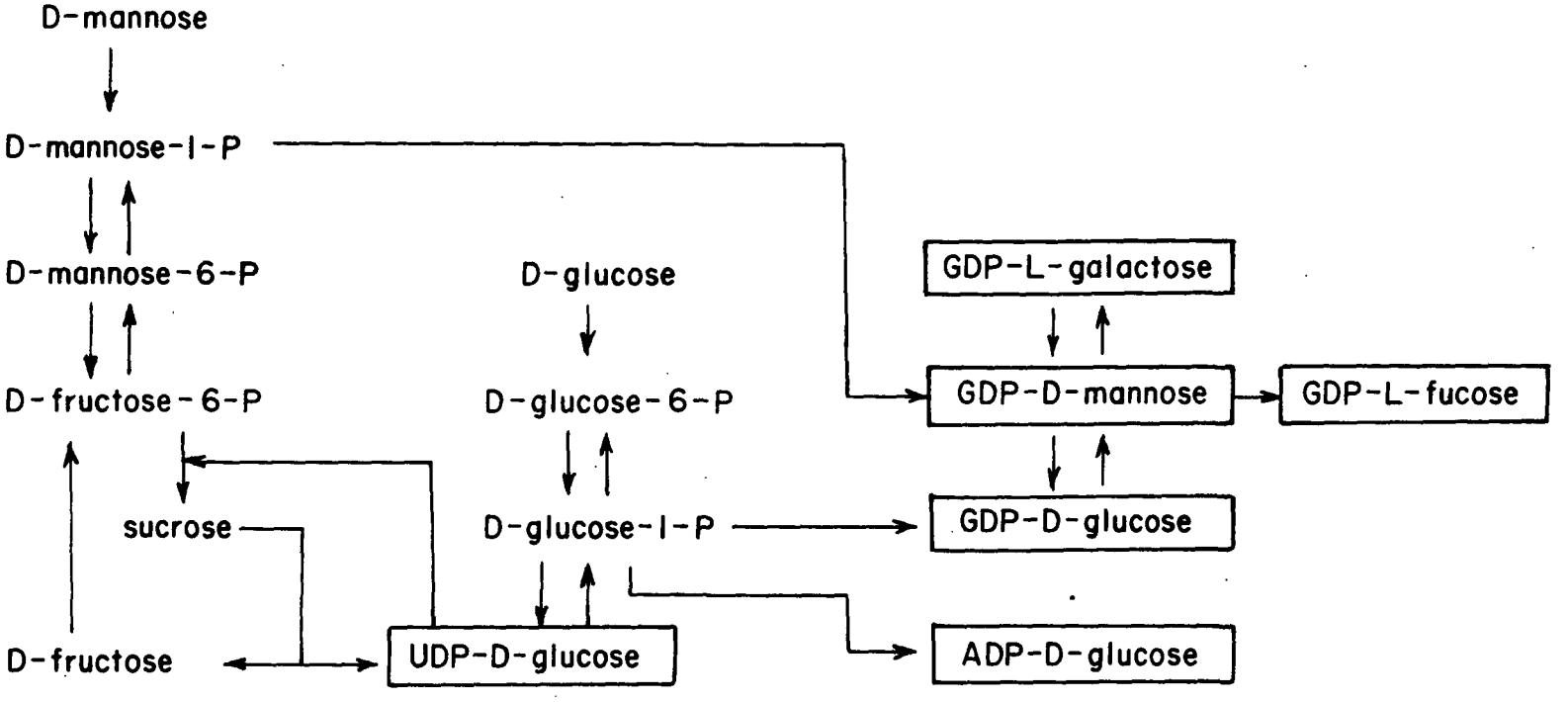

Figure 2. Metabolic Pathways Which Generate the GDP Sugars, ADP-D-Glucose, and UDP-D-Glucose.
GDP = Guanosine Diphosphate; ADP = Adenosine Diphosphate;
UDP = Uridine Diphosphate; P = Phosphate

the sugar nucleotides, free L-arabinose can also serve as a carbon source for the pentose nucleotides. In this case, UDP-L-arabinose is formed from L-arabinose-1-phosphate (33) which is derived from the free sugar (34). UDP-D-xylose can be formed from UDP-L-arabinose by the action of a specific epimerase (35). Since the reaction producing UDP-D-xylose from UDP-D-glucuronic acid is irreversibe, radioactively tagged L-arabinose cannot directly label the hexose and hexuronic acid nucleotides. Also, since the decarboxylation of UDP-D-glucuronic acid involves the removal of C-6, D-glucose specifically labeled at C-6 is a poor precursor for labeling the pentosans (36-38).

Figure 2 shows how the enzymatic reactions leading to the formation of the GDP sugars are external but still related to the group of reactions which produce the various other sugar nucleotides. D-Mannose, although not reported as a free sugar in most plants, has been successfully metabolized into polysaccharides in plant tissue. Roberts (39) found that labeled D-mannose is specifically incorporated into the D-mannosyl, L-galactosyl, and L-fucosyl units of polysaccharides in corn roots. He suggests that D-mannose-1-P is preferentially converted to the GDP sugars (GDP-D-mannose, GDP-L-fucose, and GDP-L-galactose) instead of equilibrating with the other hexose phosphates.

Lignin Synthesis

Existing evidence suggests that lignin, like the other cell wall constituents, is derived from simple carbohydrates. D-Erythrose-4-P and phosphoenol pyruvic acid, intermediates in the two catabolic pathways, apparently provide the carbon skeleton for the sequence of reactions involved in lignin biosynthesis (40). Tracer studies have indicated that both catabolic pathways (glycolysis and the pentose phosphate shunt) act to convert tagged glucose into the carbohydrates which lead to the excellent lignin precursor, shikimic

acid (41). Also, the pentose phosphate pathway appears to offer the means of converting labeled pentoses into lignin (42).

Hemicellulose Precursors

In the course of conducting experiments on cell wall metabolism in plants, evidence has been obtained showing that certain simple carbohydrates can be administered and metabolized specifically into various noncellulosic polysaccharides. In accordance with the schemes presented in Fig. 1 and 2, it has been demonstrated that L-arabinose (36,43-45), D-glucuronic acid (36,46-48), myo-inositol (32,44,48-52), and D-mannose (39) are incorporated specifically into the noncellulosic polysaccharides of primary growth in various tissues.

APPROACH OF THE THESIS

The main goal of this thesis was to examine directly the deposition pattern of a hemicellulose relative to those of cellulose and lignin in the woody cell wall. An experimental approach using radioactive tracers and high resolution autoradiography seemed to offer the means of achieving this goal. For reasons to be explained later in this section, the tritium isotope was selected for this work. In order to accomplish the major goal of this thesis research, the following three minor objectives were established:

1. Demonstrate specific incorporation of a tritium-labeled precursor into a wood hemicellulose.
2. Demonstrate incorporation of a tritium-labeled precursor principally into cellulose and lignin in the same type wood used in step 1.
3. Localize the labeled wall components in the developing woody cells by high resolution autoradiography.

These research objectives differ significantly from earlier work because of the tissue being studied. Prior demonstrations of specific labeling of noncellulosic polysaccharides and comprehensive high-resolution autoradiography experiments have been concerned with tissue containing only primary cell walls. In woody tissue the secondary cell wall accounts for the bulk of the total wood substance. Also, the secondary cell wall hemicelluloses are thought to differ from those in the primary wall (54).

A clonal stock of quaking aspen (Populus tremuloides Michx.) plantlets was selected as the source of wood for this study. This choice was made because of the genetic homogeneity of these individual plantlets, their demonstrated fast growth rate, and their ready availability from The Institute of Paper Chemistry forest genetics group (55,56). In addition, fractions of developing P. tremuloides wood had been chemically examined by other workers (12,57), and their results might be related to this study.

Two commercially available labeled sugars, L-arabinose-1-^{3}H and D-mannose-2-^{3}H, were chosen as potentially specific precursors for noncellulosic wood polysaccharides. It was realized at the outset that time limitations would not allow a complete study of both precursors and that one of these would be chosen, based on initial results, for a more complete study.

Glucose-6-^{3}H was chosen as the labeled precursor for cellulose and lignin. It has been demonstrated in other tracer studies using woody stems that glucose is a good precursor for both cellulose (58) and lignin (58-60). Glucose specifically labeled at C-6 should not significantly label pentosans, thereby making this precursor especially attractive for comparison with L-arabinose-1-^{3}H, which should label only pentosans.

Administration of the labeled sugars by infusion was the method chosen for feeding the precursors to the plantlets. As pointed out by Neish (40), infusion through the cut basal end of a stem allows for the rapid uptake of administered label and movement via the transpiration stream to areas of secondary growth.

Simple methods of wood analysis were used to determine the distribution of tritium label among the cell wall constituents. The degree of specificity of incorporation of the different precursors was established by analysis of the relative radioactivities of the different sugar units of the polysaccharides following hydrolysis and by determination of radioactivity in the Klason lignin.

Liquid emulsion autoradiography was used in conjunction with light and electron microscopy to localize the labeled cell wall components. High-resolution autoradiography has been demonstrated to offer a means to localize tritium-tagged compounds on a scale satisfactory for this research (61).

Basically, autoradiography localizes a source of radioactivity in tissue by image formation in a layer of photographic emulsion applied over a section of the tissue. Figure 3 illustrates the situation existing in a typical autoradiographic preparation. During an exposure period, ionizing radiation emitted by the radioactive material which passes through the emulsion layer can induce the formation of a latent image among the silver halide crystals. After an exposure period (often as long as several months) the latent image is chemically converted to a permanent image composed of silver grains. The size and shape of the developed silver grains are dependent upon the size of the silver halide crystals and the procedure chosen for chemical development.

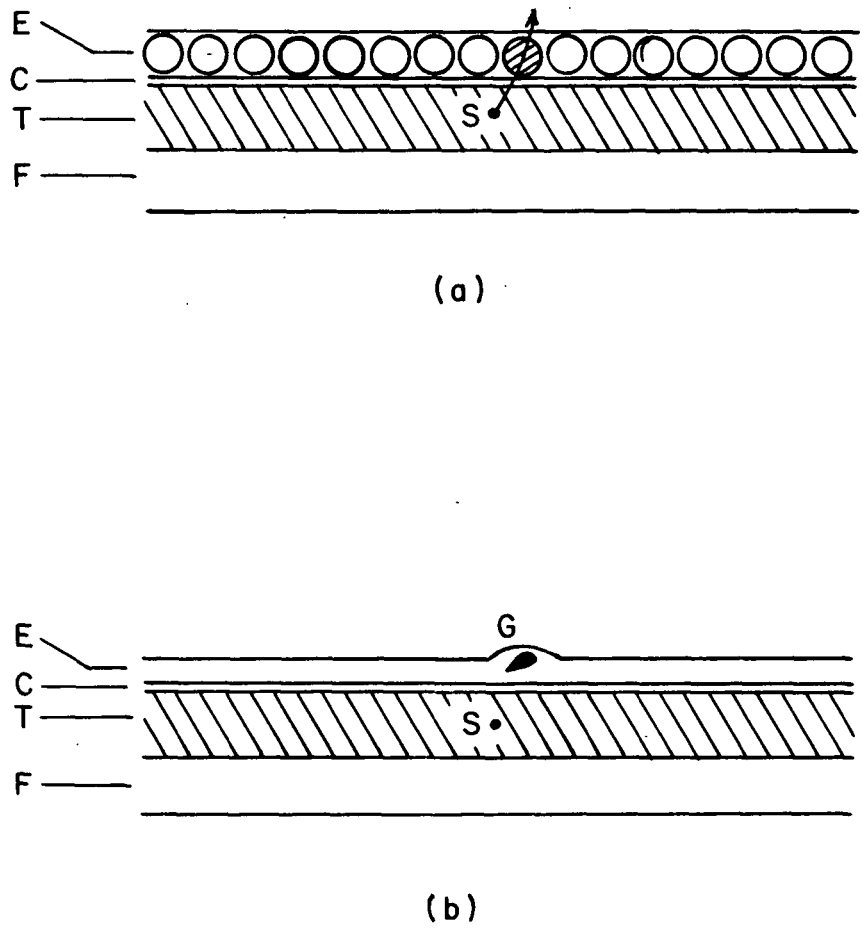

Figure 3. Cross Section of Autoradiograph Preparation:
(a) During Exposure Period
(b) After Development

E = Emulsion Layer; C = Carbon Layer;
T = Tissue Section; F = Support Film;
S = Source of Radioactivity;
G = Developed Silver Grain. Adapted from Juniper, et al. (62)

The main problem in high-resolution autoradiography is to infer the location of the radioactive source from the distribution of developed grains. To maximize grain formation in areas close to the source, it is best to use isotopes which emit the lowest energy radiation. The tritium isotope is ideal in this respect since 80% of its β-particles travel less than 1 μm from their source in an embedded tissue section (61). A number of good reviews have comprehensively surveyed the procedures used and analyses performed in high-resolution autoradiography (61,63-65).

The grain distributions obtained from the electron microscope autoradiographs in this work were analyzed by comparison with predicted distributions derived from equations developed by Salpeter, et al. (66). From geometrical considerations alone, these workers derived the theoretical distribution function, $f = 1/(1 + x^2/\hat{d}^2)$, to describe the distribution of grains over an extended line source of radioactivity. The theoretical distribution from a typical electron microscope autoradiograph of a line source of tritium activity (1000-A section thickness) is presented in Fig. 4. The grain density, f, is at a maximum directly over the source and is arbitrarily set equal to unity at this point, i.e., when the distance, x, from the line source is equal to zero. The d parameter is constant for any particular autoradiograph and is equal to Salpeter's (66) half-distance (HD) value which is a measure of the autoradiographical resolution. HD is defined as the perpendicular distance from a line source within which 50% of the total grains fall (see Fig. 4). HD values vary with the isotope used, section and emulsion layer thickness, emulsion type, and chemical development procedure. HD values have been determined for a number of different experimental conditions from actual grain distributions obtained from biological (67) and artificial (66) line sources.

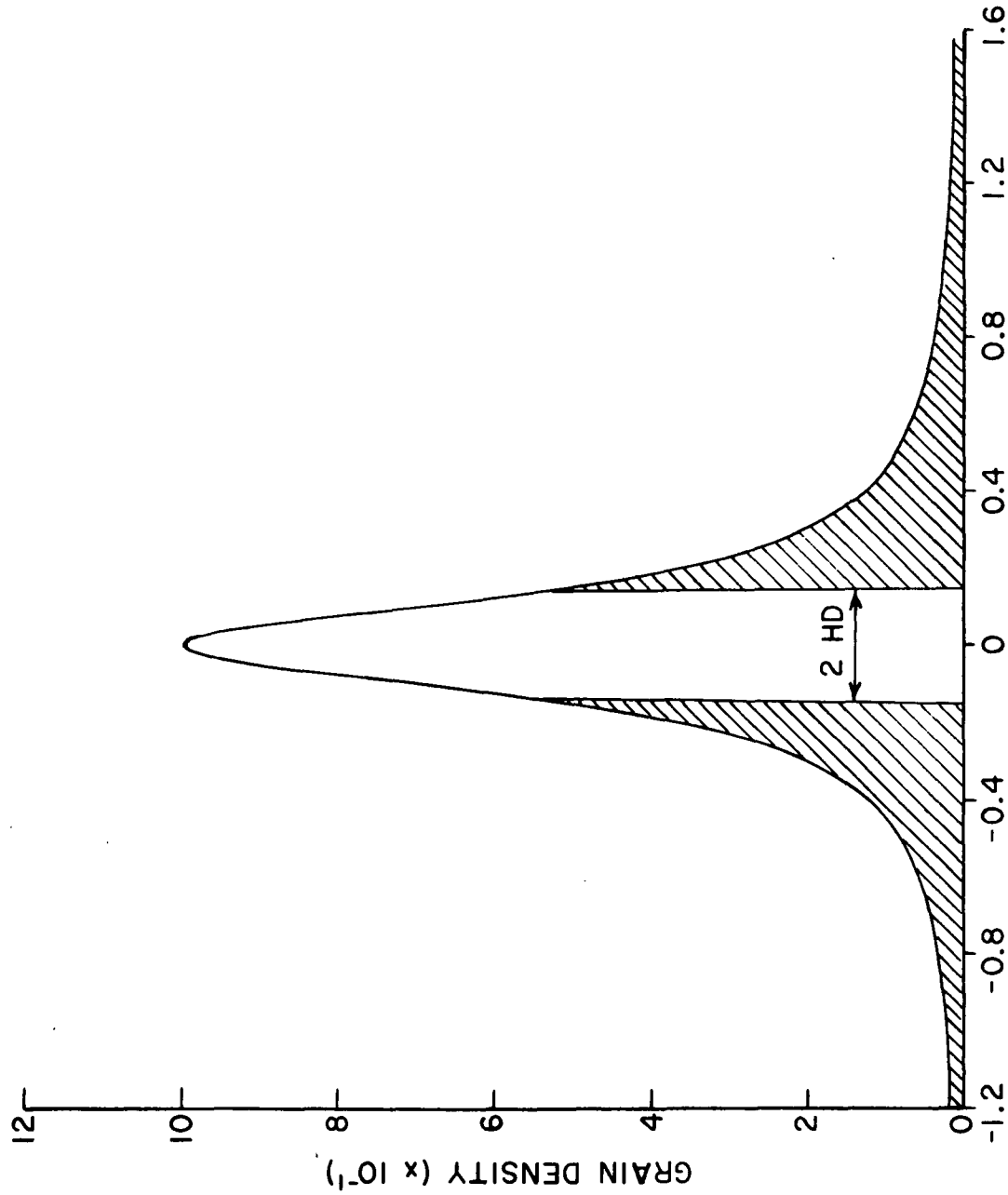

Figure 4. Grain Density Distribution Predicted from a Line Source of Tritium Radioactivity

Salpeter, et al. (66) found that their theoretical function provided a good description of the actual grain distribution for distances up to 2.5 HD from an artificial line source embedded in plastic. Gupta, et al. (67), however, found that the same function described the grain distribution from a biological line source, even at positions beyond the 2.5 HD distance. In this thesis research labeled cell wall components were treated as band sources of radioactivity localized by comparing the actual grain distributions to predicted band source distributions. The latter were obtained by considering a band source to be composed of a number of discrete, evenly spaced line sources — each contributing to the cumulative band distribution in accordance with the line source distribution function.

RESULTS AND DISCUSSION

ADMINISTRATION OF LABELED PRECURSORS

In order to use radioactive tracers for a biosynthetic study, one must have an effective means of feeding the labeled compounds to the growing cells. Most compounds, except basic precursors such as CO_2 and H_2O, must be administered in an unnatural manner. Also, the method selected is determined by the tissue being studied. Water-soluble compounds can be administered to cell suspensions, for example, by simply adding them to the culture medium. Obviously, the developing xylem cells in a tree are not as accessible to such artificially supplied metabolites as cells cultured *in vitro*.

The region of developing woody cells in a young *P. tremuloides* plantlet is illustrated in Fig. 5. The developing xylem can be visualized as a cylinder surrounding the mature xylem and pith with outer sheaths of cambial and phloem tissue. The conductive elements of the mature xylem carry water and associated nutrients upward from the roots in an intact tree. Administration of a water-soluble precursor into this transpiration stream by the infusion technique allows for rapid delivery to all developing xylem cells in the stem.

Preliminary infusion feeding experiments were conducted with stems about 30-cm long cut from actively growing first year plantlets. A dye solution of 0.05% acid fuchsin (68) was administered through the lower end of a cut stem to determine the volume uptake rate and translocation speed. The latter was estimated by timing the appearance of red color at various points from the stem base. Results indicated that, under daylight conditions, one might expect 1 ml of solution to be totally absorbed within 20 minutes and to travel upward at a minimum speed of 40 cm/hour.

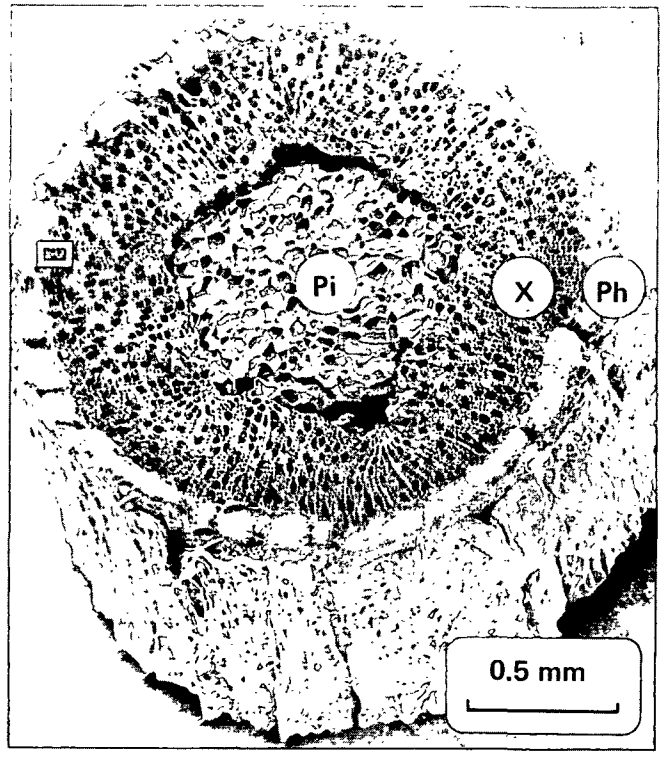

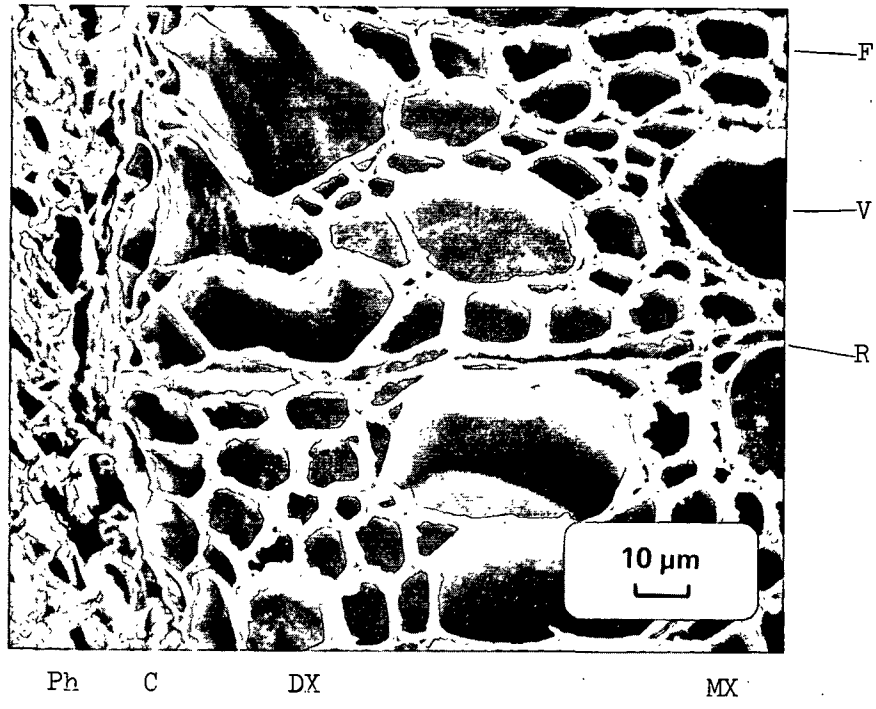

Figure 5. Scanning Electron Micrographs of a First-Year Stem of Populus tremuloides: (a) Transversely Cut Segment of Whole Stem
(b) Enlargement of Region Outlined in (a)

Pi = Pith; X = Xylem; C = Cambium; Ph = Phloem;
F = Libriform Fiber; V = Vessel Element; R = Ray Cell;
DX = Differentiating Xylem; MX = Mature Xylem

Infusion feeding of a radioactive sugar (L-arabinose-1-^{3}H) was conducted next to determine the quantity of radioactive sugar and the incubation conditions required to attain a level of incorporation suitable for subsequent autoradiography. Incorporated activity was monitored by light microscope autoradiography. Stems were incubated in a growth chamber with defined environmental conditions as described in Appendix I. The experiments showed that 100-200 μCi of sugar A provided sufficient labeling of cell wall components, even with as little as 2 hours incubation time. Following the radioactive sugar with a feeding of nonradioactive L-arabinose had no apparent effect on the pattern or amount of incorporation.

The procedure described in Appendix I was used for subsequent infusion feeding experiments. Collecting stem segments after various incubation times from the same seedling afforded a simple and economical use of the radioactive sugars. As results presented later will show, this novel adaptation of the infusion feeding technique proved satisfactory for growth periods of at least 48 hours.

RADIOCHEMICAL STUDIES

In order to justify further autoradiography work, several radiochemical experiments were conducted with the labeled wood. It was hoped, first, that evidence could be obtained to demonstrate that an administered precursor could be metabolized preferentially into a noncellulosic wood polysaccharide. Secondly, it was desired to show that the radioactivity retained in the wood consisted of the labeled polymer products of cell wall biosynthesis and not just the precursor itself or other monomeric intermediates. Finally, it was recognized that the autoradiographs to be obtained would be meaningful only

with a knowledge of the relative amounts of radioactivity in the major cell wall components — cellulose, hemicellulose, and lignin.

RADIOACTIVITY IN COMPONENTS OF WOOD HYDROLYZATE

The relative activities of the various polysaccharides of wood fed labeled sugars were determined indirectly by examination of the simple carbohydrates liberated by acid hydrolysis. Thin layer chromatography (TLC) was used to separate the monosaccharides and other water soluble components in the wood hydrolyzate. The distribution of radioactivity on the chromatogram was established by liquid scintillation counting and fluorography. Details of the procedures used to isolate and hydrolyze the wood and wood polysaccharides are included in Appendix II. TLC procedures and the methods used to detect radioactivity on the chromatogram are listed in Appendix III.

Wood Fed L-Arabinose-1-^{3}H (A)

The hydrolyzate of wood fed sugar A contained three distinct areas of radioactivity when separated by TLC. This is clearly seen in the fluorograph reproduced in Fig. 6. The dark spots on the fluorograph correspond to areas of radioactivity on the chromatogram. Liquid scintillation counting of another chromatogram is presented in Fig. 7. The TLC activity distributions in hydrolyzate from woody tissue covering the range of incubation times, i.e., A-3* to A-72, were essentially the same. The bulk of the total radioactivity was contained in two spots with chromatographic mobilities equal to arabinose and xylose. Since this TLC system separates the pentose sugars especially well, there is little doubt that these two labeled components are indeed xylose and arabinose.

*Samples of radioactive wood are abbreviated by compounding the precursor designation (A,G1,G6, etc.) and the incubation time, in hours. Therefore, A-3 represents woody tissue fed L-arabinose-1-^{3}H and incubated 3 hours. Similarly, "A hydrolyzate" refers to the acid hydrolyzate of wood tissue fed sugar A.

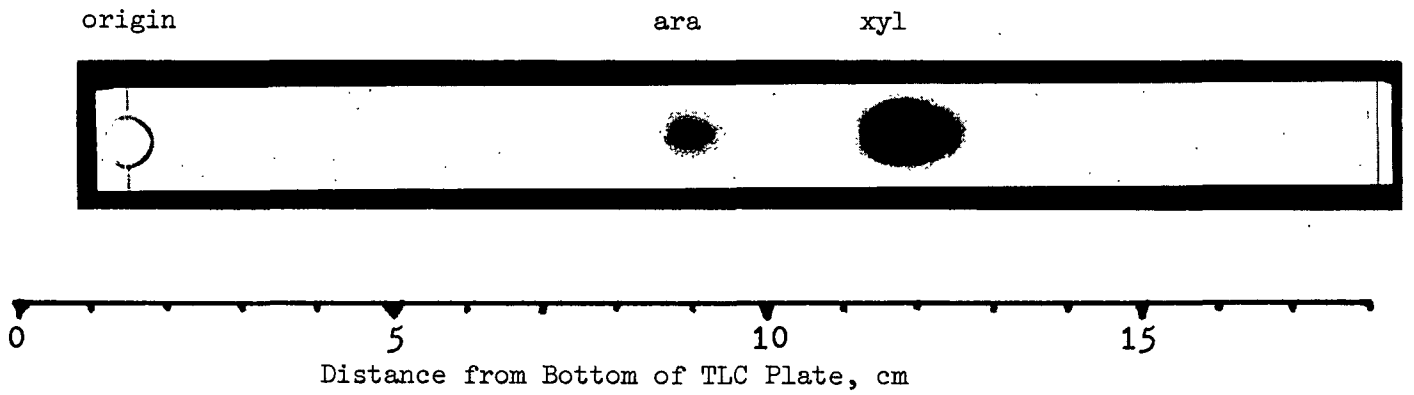

Figure 6. TLC Fluorograph of A-20.5 Hydrolyzate.
ara = Arabinose; xyl = Xylose

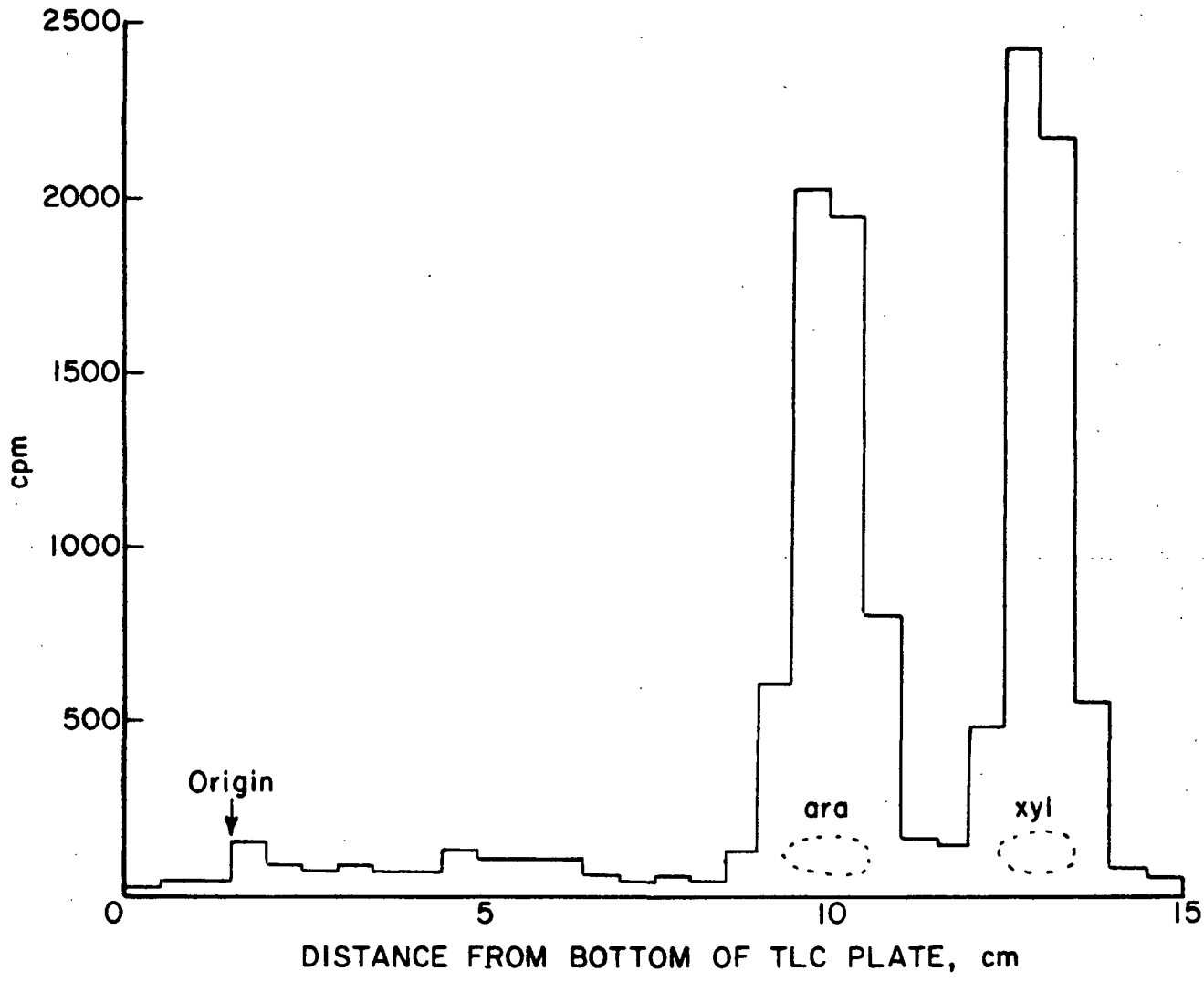

Figure 7. Distribution of Radioactivity from A-48 Hydrolyzate.
ara = Arabinose; xyl = Xylose

The nonmigrating spot of radioactivity shown at the origin position of the TLC fluorograph in Fig. 6 was examined further. The material at this position was eluted from the chromatogram, concentrated, and chromatographed again with an acid TLC system. The results of liquid scintillation counting of this chromatogram are shown in Fig. 8. The single peak of radioacitivity has the same mobility as an aldobiuronic acid, 2-O-(4-O-methyl-D-glucopyranosyluronic acid)-D-xylose, which is an expected hydrolysis product of hardwood xylans (69).

In general, the results of these radiochemical studies indicate that sugar A is metabolized quite specifically into the pentosans in P. tremuloides xylem tissue. These findings not only confirm the results of others (36,43-45) who have experimented with various nonwoody tissues, but also supplement their results since the tissue used here was woody in nature.

Wood Fed D-Glucose-1-^{3}H (G1), D-Glucose-6-^{3}H (G6), and D-Fructose-6-^{3}H (F)

Representative distributions of radioactivity among the components of G1 and G6 hydrolyzates separated by TLC are shown in Fig. 9. The largest amount of activity in both samples appeared among the hexoses, primarily in glucose. The G1 and G6 hydrolyzates, however, showed marked differences in pentose activity. A significant amount of the radioactivity in G1 hydrolyzate appeared to be in xylose while the pentose region in the chromatogram of G6 hydrolyzate appeared almost free of activity. A third region of radioactivity existed near the origin of both chromatograms, possibly due to labeled uronic acids.

Although G6 had been selected as the potentially best precursor for cellulose, the labeling patterns of G1 and F were studied also — mainly to confirm the selection. As Fig. 9 and 10 show, the chromatograms of G1 and F

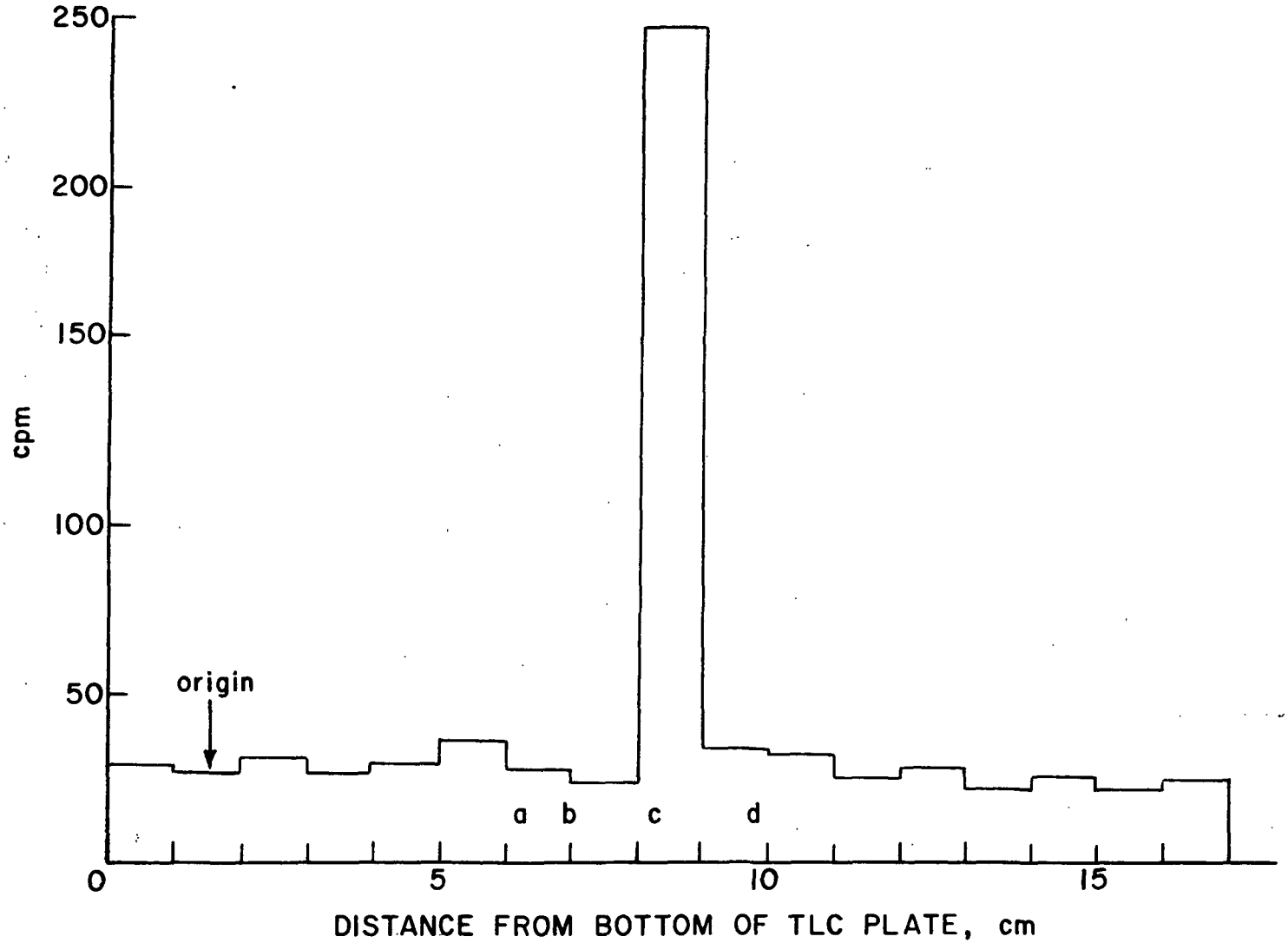

Figure 8. Distribution of Radioactivity Among Acid Components of A-20.5 Hydrolyzate.

a = Aldotriuronic Acid; b = Uronic Acid;
c = Aldobiuronic Acid; d = Xylose

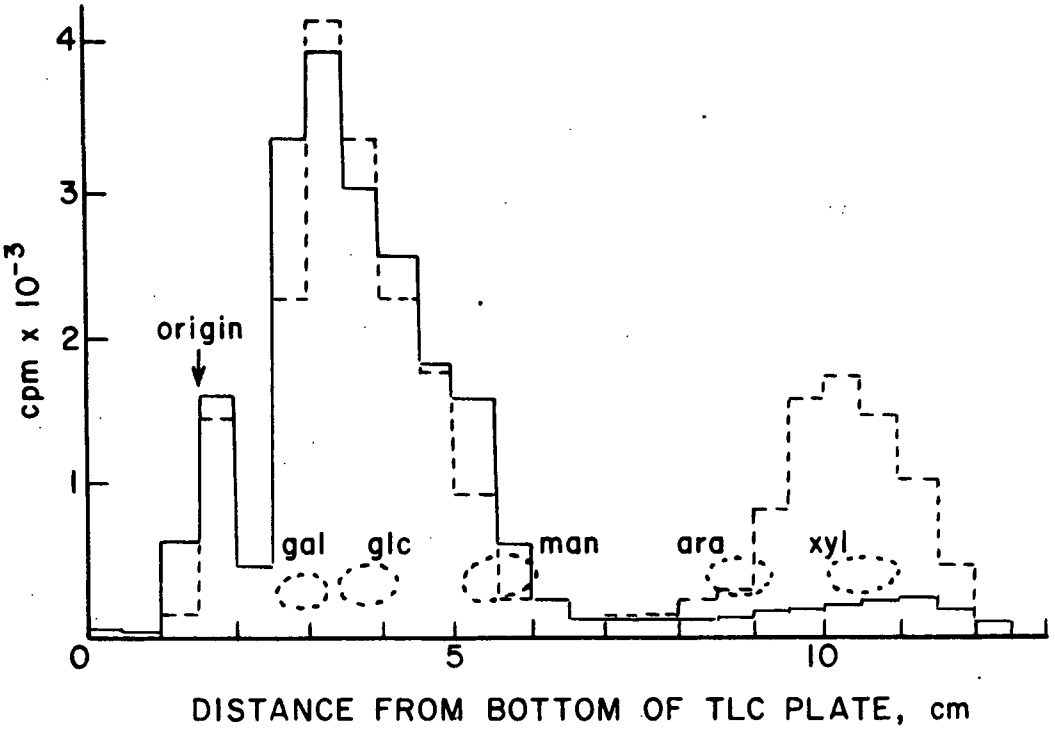

Figure 9. Distribution of Radioactivity from G6-60 (—) and G1-60 (---) Hydrolyzate.

gal = Galactose; glc = Glucose; man = Mannose;
ara = Arabinose; xyl = Xylose

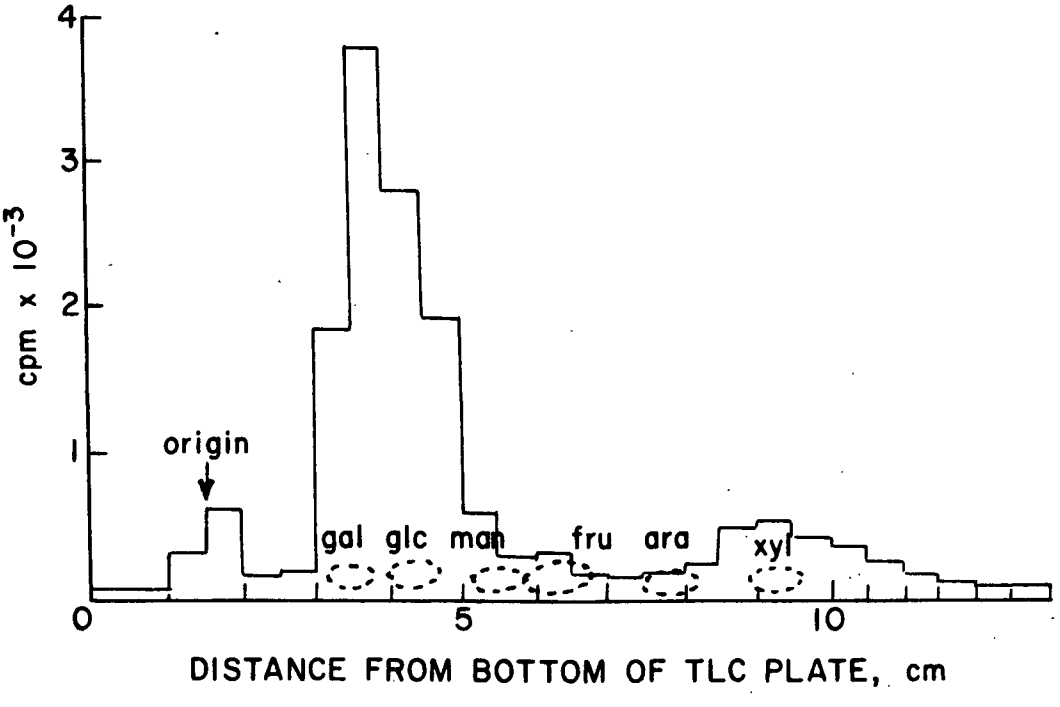

Figure 10. Distribution of Radioactivity in F-72 Hydrolyzate.

fru = Fructose

hydrolyzates contain more radioactivity in the region of the pentoses than the chromatogram of G6 hydrolyzate. The differences observed in pentose labeling are consistent with the C-6 decarboxylation theory as shown in Fig. 1. The slightly greater pentose activity in F hydrolyzate compared to G6 hydrolyzate is probably due to the tritium label in sugar F which was attached to carbon atoms other than C-6. Since sugar F was only nominally labeled at C-6, up to 10% of the label could have been at other positions and, therefore, capable of being carried to the pentoses even with the loss of C-6.

The negligible amount of radioactivity in the area of fructose on the chromatogram of F hydrolyzate is evidence against the simple physical retention of this radioactive monomeric intermediates in the labeled wood. This evidence, therefore, supports the contention that the radioactivity in G1 and F hydrolyzates is indeed due mainly to labeled cellulose and xylan, the two main polysaccharides in P. tremuloides wood. Using the same argument, one might conclude that cellulose is the main carbohydrate labeled in wood fed G6 since glucose appears to be the main labeled product of acid hydrolysis.

While the results presented in Fig. 9 and 10 are from tissue incubated 60 and 72 hours, wood collected from shorter incubations yielded similar distributions of activity. Apparently little or no metabolic recycling of the tritium label occurred among the carbohydrates during the more lengthy incubation periods.

Wood Fed D-Mannose-2-^{3}H (M)

The TLC distribution of activity in the hydrolyzate of wood fed sugar M is shown in Fig. 11. The three peaks of activity in the areas of galactose, mannose, and fucose are consistent with the labeling pattern observed with radioactive D-mannose administered to corn root tips (39). Some differences

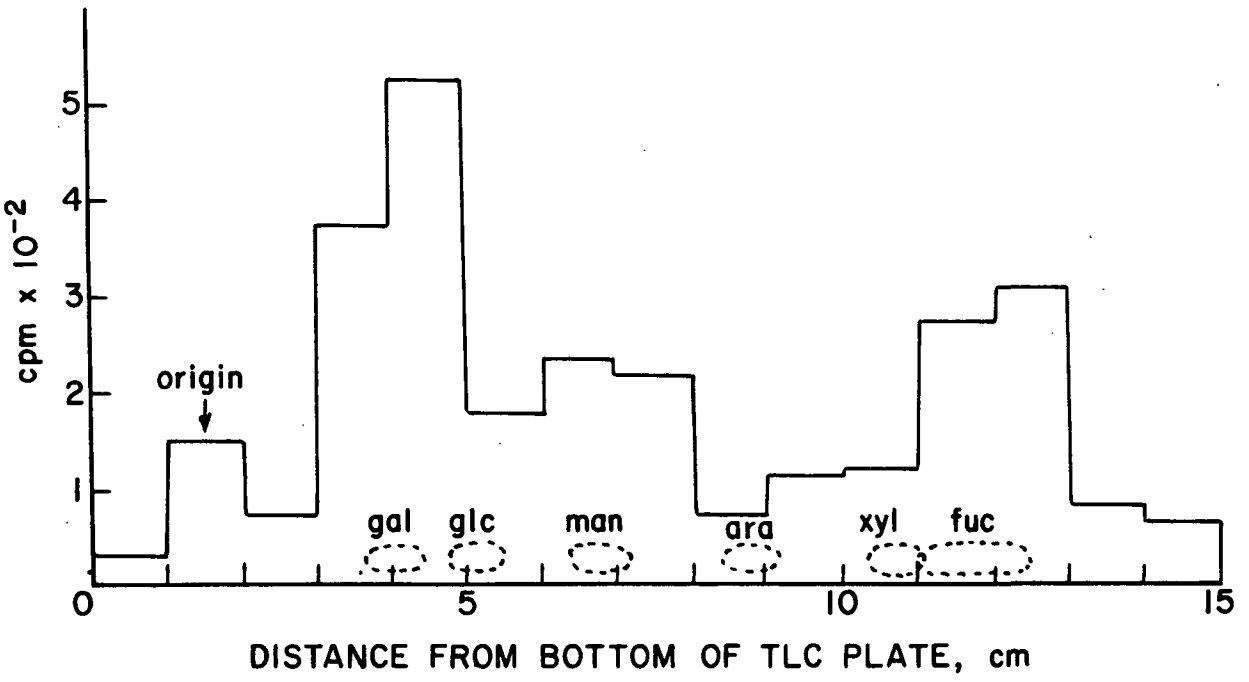

Figure 11. Distribution of Radioactivity in M-72 Hydrolyzate.

gal = Galactose; glc = Glucose; man = Mannose;
ara = Arabinose; xyl = Xylose; fuc = Fucose

were observed in the relative radioactivities of the galactose and mannose peaks in different samples, but all samples consistently displayed activity confined to chromatogram areas corresponding to the galactose, mannose, and fucose positions.

Since glucomannan is the only mannose-containing polysaccharide that has been isolated from hardwood xylem, it seems likely that the radioactive mannose in the hydrolyzate was derived from this polymer. It is more difficult, however, to speculate which polysaccharides might contain the labeled galactose and fucose. Galactans have been found among the pectic polysaccharides of the middle lamella and primary cell wall (12,57) as well as in the secondary cell wall of reaction wood (70,71). Also, a water soluble polymer containing fucose has been detected in the least developed xylem cells of P. tremuloides (72). Albersheim, et al. (73) have recently isolated and determined the structural form of several polymer fragments containing galactose and fucose from a culture of Acer pseudoplatanus cells.

In summary, these radiochemical studies indicated that the label from sugar M is incorporated specifically into sugar units which are probably a part of the noncellulosic polysaccharides of the primary and secondary cell walls of woody cells. These polysaccharides which appear to be labeled, however, are only a small part of the total noncellulosic polysaccharides in aspenwood. The probability that several different minor polysaccharides were labeled by the precursor M, therefore, suggested that sugar A might be a better choice for further radiochemical investigation. Those polysaccharides containing arabinose and xylose, which were specifically labeled by sugar A, constitute the bulk of the noncellulosic polysaccharides in the wood of aspen.

RADIOACTIVITY IN PITH TISSUE OF WOOD FED L-ARABINOSE-1-^{3}H

Pentosans might be classified by their location in the cell wall into two categories: namely, primary and secondary cell wall pentosans. Existing evidence indicates that polymers containing arabinose are confined to the primary wall or middle lamella regions in P. tremuloides xylem (12,57). The recent studies of Acer pseudoplantanus cell cultures (73) indicate that xylose in the primary cell wall may be present only in the form of a xyloglucan with single xylosyl units attached as side chains to a celluloselike polyglucan. The most abundant pentosan in aspenwood, 4-O-methyl glucuronoxylan, apparently is the sole secondary cell wall pentosan (12,57).

The pith tissue in stems fed sugar A could be easily separated from the wood and seemed an ideal subject for the study of labeled pentosan in the primary cell wall of P. tremuloides. As shown in Fig. 5, the pith tissue consists of large diameter, thin-walled cells. With the aid of a stereomicroscope and a scalpel, the softer pith tissue was scraped away from the xylem of longitudinally split stem segments. The pith scrapings and the xylem tissue remaining after debarking were then hydrolyzed and examined radiochemically as described in Appendix II. TLC separation of the labeled hydrolyzate components and subsequent liquid scintillation counting yielded the results shown in Table I.

TABLE I

RADIOACTIVITY IN A-20.5 XYLEM AND PITH HYDROLYZATE

Component	Radioactivity, %	
	Xylem	Pith
Aldobiuronic acid	4.0	2.3
Arabinose	46.0	69.2
Xylose	50.0	28.5

As Table I shows, the relative radioactivities of arabinosyl and xylosyl units in the pith and xylem tissues are consistent with the probable relative contents of primary and secondary cell wall pentosans in these tissues. While the xylem tissue consisted of mature and differentiating cells at all stages of wall growth, the pith scrapings contained only cells with primary cell walls. If arabinose-containing polysaccharides are present only in the primary wall and if the secondary cell wall pentosan is xylan, the greater labeling of arabinosyl units in pith tissue is reasonable.

The results shown in Table I also confirm the assignment given to the nonmigrating component (aldobiuronic acid). The constant aldobiuronic acid: xylose radioactivity (approximately 1:12.5) in the two types of tissue suggests that both hydrolyzate components were derived from the same xylan polymer.

RADIOACTIVITY IN PENTOSAN ISOLATED FROM WOOD FED L-ARABINOSE-1-^{3}H

An alkali-soluble polysaccharide fraction was isolated from wood fed sugar A and then studied using the procedures described in Appendix II. After filtration, precipitation, and thorough washing, the crystalline product was acid-hydrolyzed as done previously with the wood samples. The components of the hydrolyzate were then separated by TLC.

Not unexpectedly, activity on the chromatogram paralleled the distributions of activity on chromatograms obtained from whole wood hydrolyzate, i.e., radioactivity peaks at the origin and positions corresponding to arabinose and xylose. One difference, however, was noted: activity in the area of arabinose was less than that found in the whole wood hydrolyzate. This difference probably reflects a difference in the water solubility of the xylose- and arabinose-containing polysaccharides. Because arabinan is very soluble in water and even

water-alcohol mixtures (74), it is quite probable that the pentosan recovered after washing with 80 and 100% methanol was effectively enriched with labeled xylan.

In summary, the retention of activity in an isolated polysaccharide fraction and the apparent localization of activity in hydrolysis products corresponding to pentosan hydrolysis products indicates that the precursor, sugar A, was incorporated into wood pentosans and not simply retained as unpolymerized precursors containing the labeled sugars.

RADIOACTIVITY IN KLASON LIGNIN

The degree of lignin labeling in woody tissue fed various precursors was determined by measuring the radioactivity in the Klason lignin and whole wood. An oxygen combustion procedure, which is described in Appendix IV, converted the labeled wood components into tritiated water for efficient liquid scintillation counting. The major results of these experiments are presented in Table II. Specific radioactivities of both lignin and whole wood samples are reported on a common basis: radioactivity per unit weight of whole wood.

As Table II shows, a relatively small amount of the radioactivity in woody tissue fed sugar A occurred in the Klason lignin fraction. The tissues fed sugars G6, G1, and F, on the other hand, contained greater percentages of their total activity in the lignin fraction. These results may simply suggest that hexoses are better lignin precursors than L-arabinose. Another possible explanation, however, is that the specific localization of tritium at the C-1 position of L-arabinose somehow limits its potential for incorporation into lignin. Sergeeva and Kreitsberg (42) asserted that pentoses are good precursors for lignin in young seedlings of Populus trichocarpa. Their study,

however, apparently used randomly labeled pentose precursors and they reported no comparable tracer studies employing hexoses.

TABLE II

RADIOACTIVITY IN KLASON LIGNIN AND WHOLE WOOD

Sample	Specific Activity (cpm/mg)		Percent of Total Activity in Lignin
	Lignin	Whole Wood	
A-3	2,110	39,600	5.3
A-12	2,730	46,400	5.9
A-24	3,830	44,800	8.5
A-36	3,870	86,600	4.7
A-48	5,710	164,900	2.9
G6-3	566	4,550	12.4
G6-12	857	5,420	15.8
G6-24	n.d.[a]	14,530	n.d.
G6-36	5,230	33,550	15.6
G6-48	6,920	34,030	20.3
F-24	2,870	15,820	18.1
G1-24	4,450	26,870	16.6

[a]Radioactivity not determined (n.d.).

If pentoses are indeed good precursors of lignin, then the most probable path to lignin would appear to be through the pentose phosphate pathway of metabolism, producing erythrose-4-phosphate, one of the two major carbohydrate precursors of lignin (40,41). Based on the reported reactions of this pathway, only that portion of the pentose carbon skeleton from C-2 to C-5 can be used to form the four-carbon backbone of erythrose-4-phosphate (75). If a pentose is specifically labeled at C-1, the label would then necessarily have to migrate to another carbon before the label could be transferred to erythrose-4-phosphate. Should this event be unlikely to occur during the pentose phosphate interconversion reactions leading to erythrose phosphate formation, then one could

predict, for example, that L-arabinose-1-^{3}H would be a poorer precursor for lignin than L-arabinose randomly labeled with tritium. In any event, the low degree of lignin labeling observed in tissue fed sugar A is significant since it makes an autoradiography study of this tissue especially attractive.

The specific radioactivities of lignin and whole wood from the tissues fed sugar A and G6 increased as the time of incubation lengthened. Differences in the relative quantity of living and nonliving xylem tissue in the various samples undoubtedly contributed to these trends. As the incubation proceeded, samples were collected from successively higher stem locations — each ensuring segment containing a smaller amount of nonliving xylem than the previously collected segment. Therefore, even if each segment contained the same total activity, the specific activity of the topmost segments — which contain the greatest proportion of living xylem tissue — should exceed that of the more massive lower segments. A second cause for increasing specific activities, of course, might be the continued incorporation of soluble label throughout the incubation period. Because of the heterogenous nature of the xylem samples, however, the activity per unit weight of tissue actually incorporating activity could not be determined.

In conclusion, these results, together with the findings of the other radiochemical studies, support the working hypothesis that the supplied precursors were retained as polymeric products of cellular biosynthesis. The specific incorporation of radioactivity from sugar A into pentosans with only a small part of this total activity going into lignin should allow a fairly direct localization of a major hemicellulose by autoradiography of this tissue. In addition, autoradiography of delignified and undelignified tissue fed sugar G6 should provide a means of localizing the recently deposited lignin and cellulose.

AUTORADIOGRAPHY

LIGHT MICROSCOPE (OLM) AUTORADIOGRAPHY

Prior to autoradiography the woody stem tissue was dehydrated and embedded in epoxy resin according to the methods described in Appendix V. Cross sections of tissue (from developing phloem cells to pith cells) were examined by the autoradiography procedures listed in Appendix VI. The tissue examined covered a range of incubation times from 3 to 72 hours. Initial experiments indicated that enough radioactivity had been incorporated into the tissue to make high-resolution (electron microscope) autoradiography feasible. In all tissue examined, the radioactivity appeared to be confined to cells that might be considered as living, i.e., cambial cells, differentiating phloem and xylem cells, and pith parenchyma.

Wood Fed L-Arabinose-1-^{3}H (A)

OLM autoradiographs of woody tissue fed sugar A might be best summarized by Fig. 12. Silver grains appeared in these micrographs either as black specks or orange-gold regions (where they occurred in high concentration). Figure 12a illustrates the disproportionately large incorporation of radioactivity often observed in the walls of ray parenchyma cells near the cambium. These ray parenchyma cells apparently incorporated large amounts of radioactivity into pentosan not only in the course of normal wall development but also during the formation of the special "protective layer" of vessel-associated ray cells (see Fig. 12b). Although the greatest activity occurred in the ray cells, vessels and fibers also contained labeled wall components. As Fig. 12b and 12c show, however, only those vessel elements very close to the cambium incorporated any radioactivity. Fiber cells continued incorporation of label in areas relatively distant from the cambium, apparently because of a slower rate

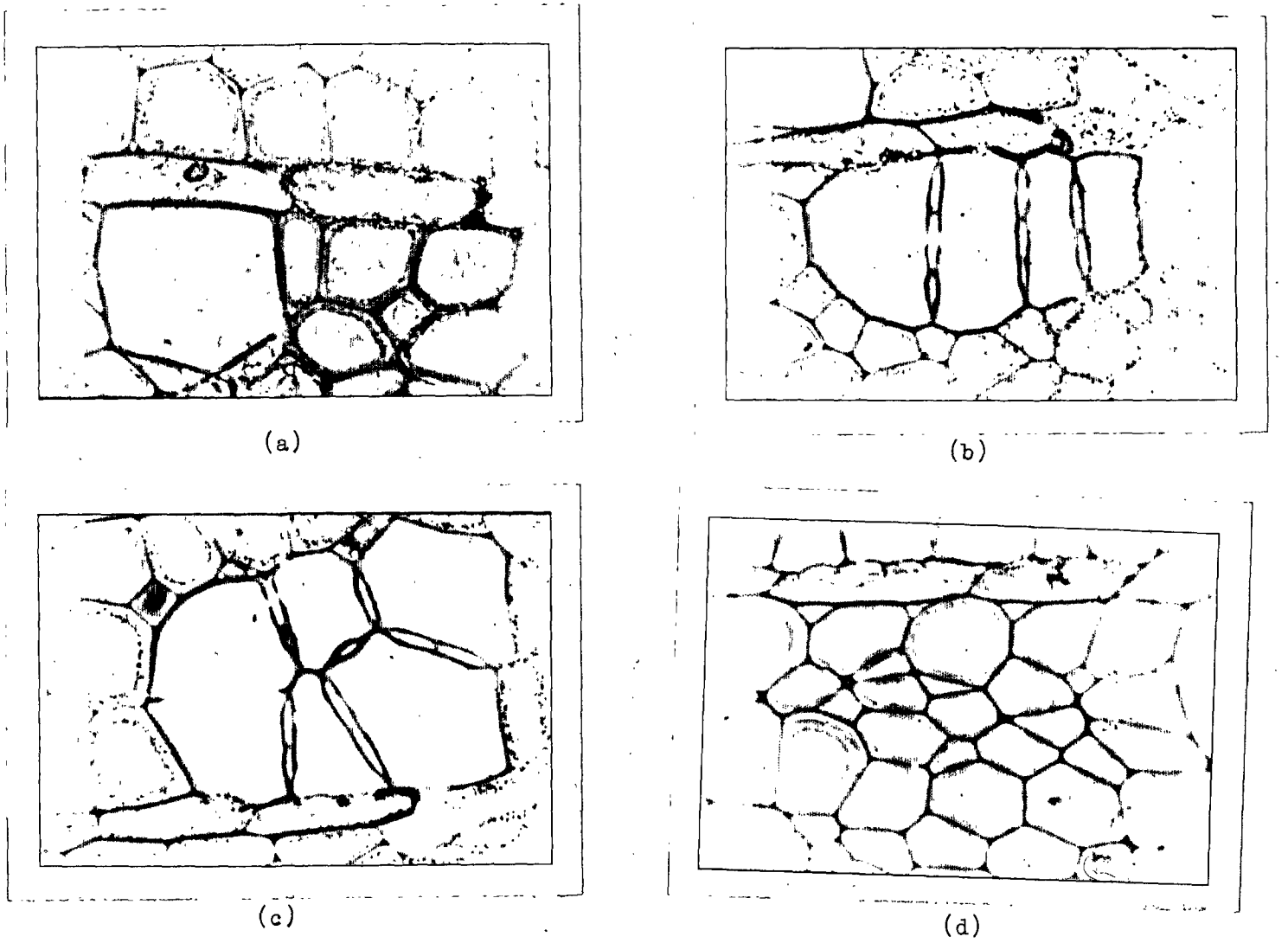

Figure 12. Light Microscope Autoradiographs of A-48 Tissue (1000X).
Cambial Zone Included at the Right of (a), (b), and (c).
Micrograph (d) Shown More Mature Xylem Further to the Left of the Cambial Zone

of differentiation. Ray parenchyma cells, since they continue to live even after adjacent prosenchymatous cells have died, often displayed the pentosan synthesis in protective layers (see Fig. 12d) of vessel-associated cells located as far inward as the primary xylem.

In general, parenchymatous cells of tissue fed sugar A contained the greatest concentration of radioactivity. Both ray parenchyma cells in the xylem and parenchyma cells in the pith contained activity. Except for the protective layer of ray cells, the radioactivity appeared uniformly distributed around the cell wall in all cells incorporating label.

Wood Fed Labeled Hexoses

In contrast to the stem tissue fed sugar A, the wood fed sugars Gl, G6, M, and F showed little or no incorporation of radioactivity into parenchymatous cells. Ray parenchyma occasionally contained radioactivity, but pith parenchyma apparently contained none. Prosenchymatous cells, however, demonstrated patterns of incorporation similar to the tissue fed sugar A. Again, the vessel elements ceased incorporation of activity relatively close to the cambium. Those vessel elements not synthesizing labeled wall components consistently appeared fully lignified and had undergone end wall disintegration, indicating differentiation had been completed (76,77). Those cells incorporating radioactivity appeared to contain a relatively uniform grain density at points around the cell wall.

Wood Fed L-Proline-5-^{3}H (P)

A glycoprotein rich in 4-hydroxy-L-proline, L-arabinose, and D-galactose has been isolated from primary cell walls of higher plants (78,79). Oligosaccharides of L-arabinose, glycosidically linked to 4-hydroxy-L-proline, apparently form the side chains of the network (79,80). Albersheim, et al. (73)

proposed a model structure for the primary cell wall which involves this protein as an integral part of the wall structure. Specific incorporation of the amino acid, proline, into the hydroxyproline of this glycoprotein has been demonstrated in tissue cultures of Acer pseudoplatanus (81,82) with localization of the label throughout the primary cell wall (82). An apparent association of this glycoprotein with unusual wartlike thickenings on the inside of the primary walls of these cells led to the speculation that a proline-rich protein might exist in the secondary wall combined with the hemicelluloses (82). The autoradiography study with labeled proline was added to the present research mainly because the tissue being studied contained cells with secondary walls while earlier investigations had been limited to tissue lacking distinct secondary wall formation. An opportunity existed, therefore, to study the location of this protein in fully differentiated woody cells.

The autoradiography results indicated that the developing xylem cells of P. tremuloides incorporated activity from proline into two regions: cytoplasm and primary wall areas. Cells forming secondary cell walls usually contained activity only in the cytoplasm. The wall activity, when present, appeared to be localized in the primary wall middle lamella regions. Since the cells were plasmolyzed prior to embedding, cytoplasmic material appeared as small, shriveled masses, separated and easily discernible from the cell wall.

Assuming that the labeled proline was incorporated specifically into the hydroxyproline and proline units of protein, one might conclude that this study demonstrates that hydroxyproline rich protein exists in the primary wall of P. tremuloides xylem cells. Since the labeled precursor apparently is able to enter the cytoplasm of cells undergoing secondary wall development, it would

seemingly be available for incorporation into any wall protein formed in these cells. The absence of activity in the secondary cell wall, therefore, may reflect the confinement of protein rich in hydroxyproline to primary wall areas. Of course, it is difficult to build a strong argument on such "negative" evidence, but this experiment apparently points out another difference between primary and secondary cell walls. As discussed in the Historical Review section, chemical studies of young cambial cells and more mature xylem cells have indicated that differences exist in the polysaccharide types and protein contents of cells with and without secondary differentiation (6,12,57).

In summary, the OLM autoradiography results indicated that labeled wall components were synthesized in detectable amounts among the various types of woody cells. Parenchymatous tissue apparently incorporated a relatively large amount of labeled pentosan compared to the prosenchymatous tissue. Finally, radioactive products of wall biosynthesis were apparently formed at all stages of secondary wall development in differentiating fiber cells administered sugars A and G6. This last finding suggests, therefore, that a comparative study of the deposition patterns of the major wall components (cellulose, pentosan, and lignin) by electron microscope autoradiography might indeed be feasible.

ELECTRON MICROSCOPE (EM) AUTORADIOGRAPHY

Ultrathin cross sections of stem tissue were subjected to EM autoradiography according to the procedures described in Appendix VI. As Fig. 13 shows, the silver grains formed by the EM autoradiography procedure were relatively small compared to the grains in OLM autoradiography. This consequence, together with the ability to obtain micrographs with both section and grains in focus allowed for better grain distribution analyses of the EM autoradiographs.

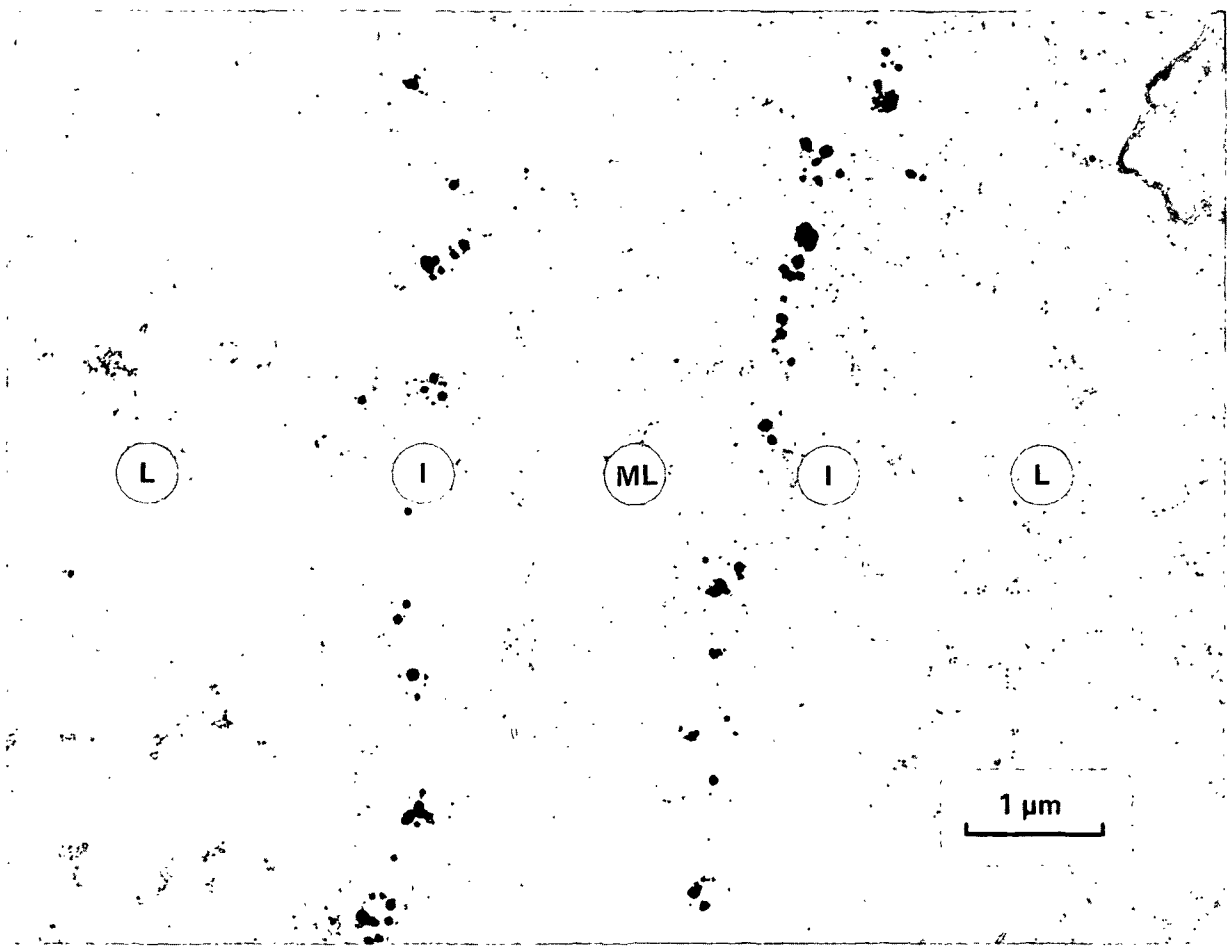

Figure 13. EM Autoradiograph of Two Adjacent A-48 Fiber Cells

L = Cell Lumen; I = Cell Wall/Lumen Interface;
ML = Middle Lamella

The distributions of grains across the walls of individual cells were determined with the aid of a computer program, EMARAN, written especially for this work (see Appendix VII). Input data consisted of grain and wall interface coordinates digitized directly from the electron micrograph with the aid of a microcomparator coupled to a card punch. Points were chosen from the middle lamella and cell wall/lumen interfaces at intervals just far enough apart to allow the lines connecting the points to accurately describe the interfaces.

Figure 14 represents the data as digitized from an autoradiograph of one particular cell. The results of data obtained in this manner from a total of twenty-six cells are reported in this study.

The actual grain density distributions obtained often displayed a rather symmetrical shape as shown by the histograms in Fig. 15. By extending the line source distribution functions to band source distribution functions (as explained in Appendix VIII), it was possible to fit theoretical distributions to the actual distributions and thus describe the location of the band source within the cell wall. The fitted distributions for the actual histogram results are illustrated by the smooth curves in Fig. 15. Another computer program, CRVFIT, was written to allow distributions predicted from up to three different band sources to be fitted to the actual distributions. The model band parameters (width, location, and relative activity) could be varied for each band in order to achieve a "best fit," as described in Appendix VII.

The grain density distributions were computed on two different bases, one expressing the grain density at various distances from the wall/lumen interface, the other yielding a relative-wall-location distribution. Each grain position was computed in two different ways to yield the two types of distributions. For the first case, distances were computed between each grain and the closest point on the wall/lumen interface (the length of a perpendicular line from the interface to the grain). In the second case, distances were also computed between each grain and the closest point on the middle lamella interface: the relative wall location for each grain was then expressed as the distance between grain and lumen interface divided by the local cell wall thickness (the distance between the closest lumen and middle lamella interface points). Thus, a relative wall location of zero designates a position on the

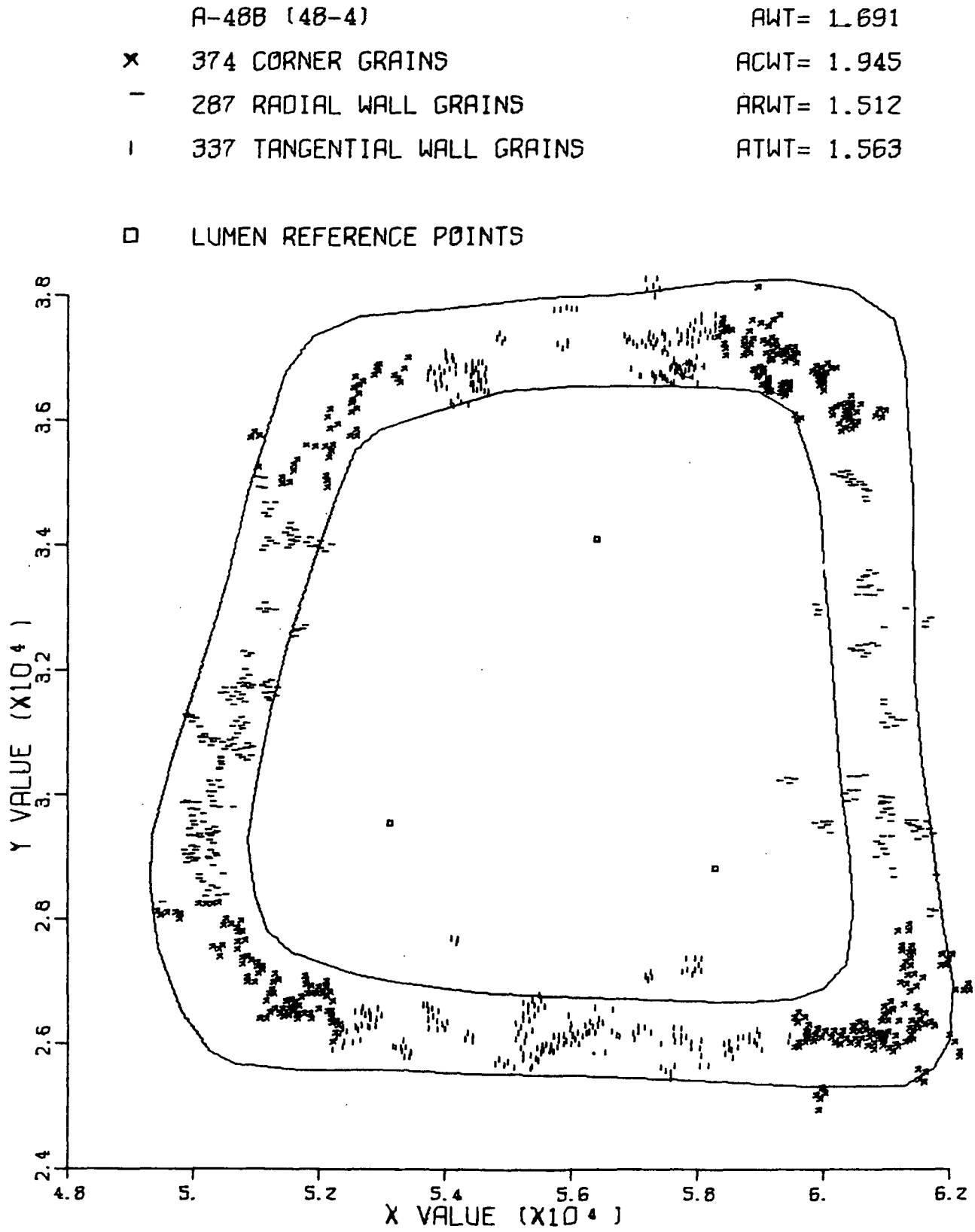

Figure 14. Digitized Autoradiographic Data from A-48B

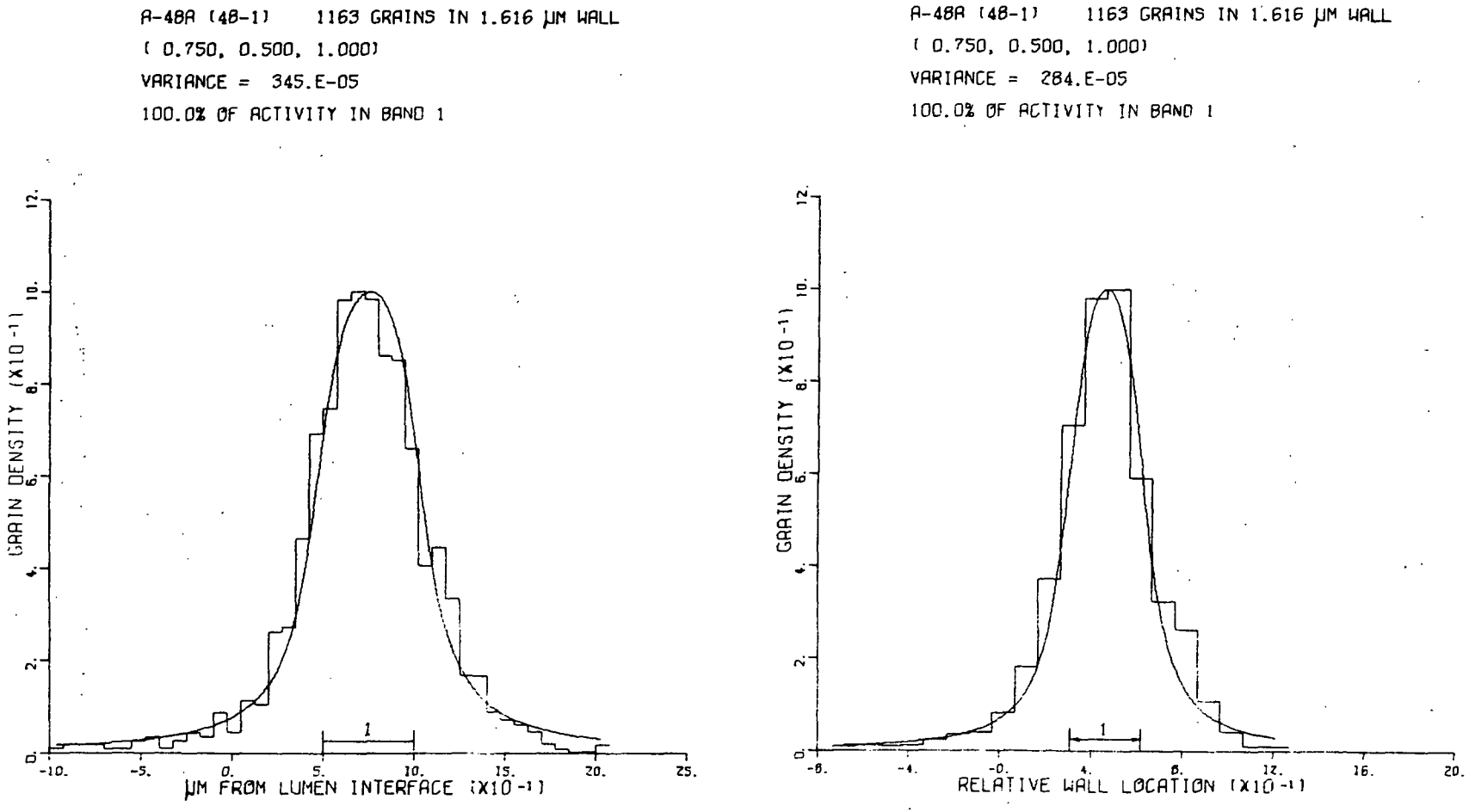

Figure 15. Grain Density Distributions Relative to the Lumen/Cell Wall Interface

lumen interface and value of unity represents a point on the middle lamella interface. For both wall location scales negative values represent points in the lumen.

The relative-wall-location distributions were selected for further analysis with the band source distribution models. This choice was made mainly because the cell walls were nonuniform in thickness — the corner areas being thicker than the tangential and radial walls. Figure 14 illustrates, both graphically and numerically, an example of the differences between the average wall thickness (AWT), average corner wall thickness (ACWT), average radial wall thickness (ARWT), and average tangential wall thickness (ATWT). These average wall thicknesses as indicated in Fig. 14 are in units of μm. Also, as discussed in Appendix VII, these values are averages of thickness determinations made at each grain position. Distributions derived from corner grains* alone were usually very similar to total grain distributions on the relative-wall-location scale but often showed a broader grain density distribution with a maximum further from the lumen interface on absolute-distance scale distributions. This difference, however, is not especially noticeable in the plots shown in Fig. 15 since the actual distributions are almost coincident with predicted distributions based on the same band parameters (0.750, 0.500, 1.000).

Despite the time-saving advantages offered by the computer-assisted analyses of EM autoradiographs, the scope of this particular analysis was necessarily limited. Only fiber cells fed with sugars A and G6 were examined, and then only those from three incubation times (3, 24, and 48 hours). Special

*Silver grains were categorized into three groups according to their location in the cell: tangential wall, radial wall, and corner grains.

emphasis was placed on examining cells lying close to the cambium. Hopefully, these cells were living throughout the incubation period and, therefore, continually depositing cell wall material.

Wood Fed L-Arabinose-1-^{3}H (A)

Prior to conducting the computer-assisted grain analyses, the EM autoradiographs were examined visually and estimates were made of the relative locations of activity in the fiber cell walls. Tissue collected after a 48-hour incubation was inspected first. Examinations of these EM autoradiographs confirmed that activity was indeed localized deep in some fiber walls as had been indicated in the OLM autoradiographs. Tissue from longer-term incubation periods, therefore, was not studied.

In contrast to the grain distributions in A-48 tissue, initial visual examination of A-3 tissue indicated that most of the grains were localized very near the cell lumen in all cells containing activity. Autoradiography of A-24 tissue showed occasional differences in grain distributions over different fiber cell walls — some containing activity deeper in the wall than others. The A-48 autoradiographs confirmed these differences and suggested that a relationship existed between cell maturity and the depth of radioactivity incorporation. The most mature cells, those on the inner fringe of the zone of cells incorporating radioactivity, consistently possessed grain density maxima in wall regions close to the cell lumen. Cells closer to the cambium usually displayed concentrations of grains farther from the lumen interface. The autoradiograph shown earlier in Fig. 13 illustrates a typical difference observed between two adjacent fiber cell walls at different distances from the cambium. In this case, the fiber on the right is closer to the cambium.

More exact descriptions of the location of activity in cell walls of wood fed sugar A are presented in Fig. 16. The band parameters obtained by the grain distribution analysis procedures are represented in this figure by rectangles on a horizontal line positioned according to the location of the bands in the wall. The length of each line indicates the average cell wall thickness and is scaled in 0.5 μm units beginning at the lumen interface. The area enclosed in each rectangle is proportional to the activity in that band relative to the total radioactivity in the wall. The histograms and curves which describe the actual and fitted grain density distributions, respectively, for each of the cells are presented in Appendix IX.

The radioactivity distributions as presented in Fig. 16 represent cells from various locations relative to the cambium. The A-48 group, especially, includes a number of different stages of cell maturity. The cells are arranged from top to bottom in this figure roughly in the order of increasing distance from the cambium.

In general, these results suggest that the bulk of the labeled wall components are deposited very close to the inner face of the cell wall. After three hours incubation, all cells examined showed that most, if not all, radioactivity was localized in a narrow band near the wall/lumen interface. With increasing incubation time, the bands of labeled material were broader and located deeper in the walls of cells closer to the cambium. Cells were selected from each incubation time to represent the extremes of depth of incorporation. Cells A-24A and A-48A, for example, are representative of those cells judged to have radioactivity localized deepest in the wall (relative to the lumen interface). Cell A-48H, on the other hand, is representative of those cells adjacent to the fully mature xylem in which no activity was incorporated. Apparently, the

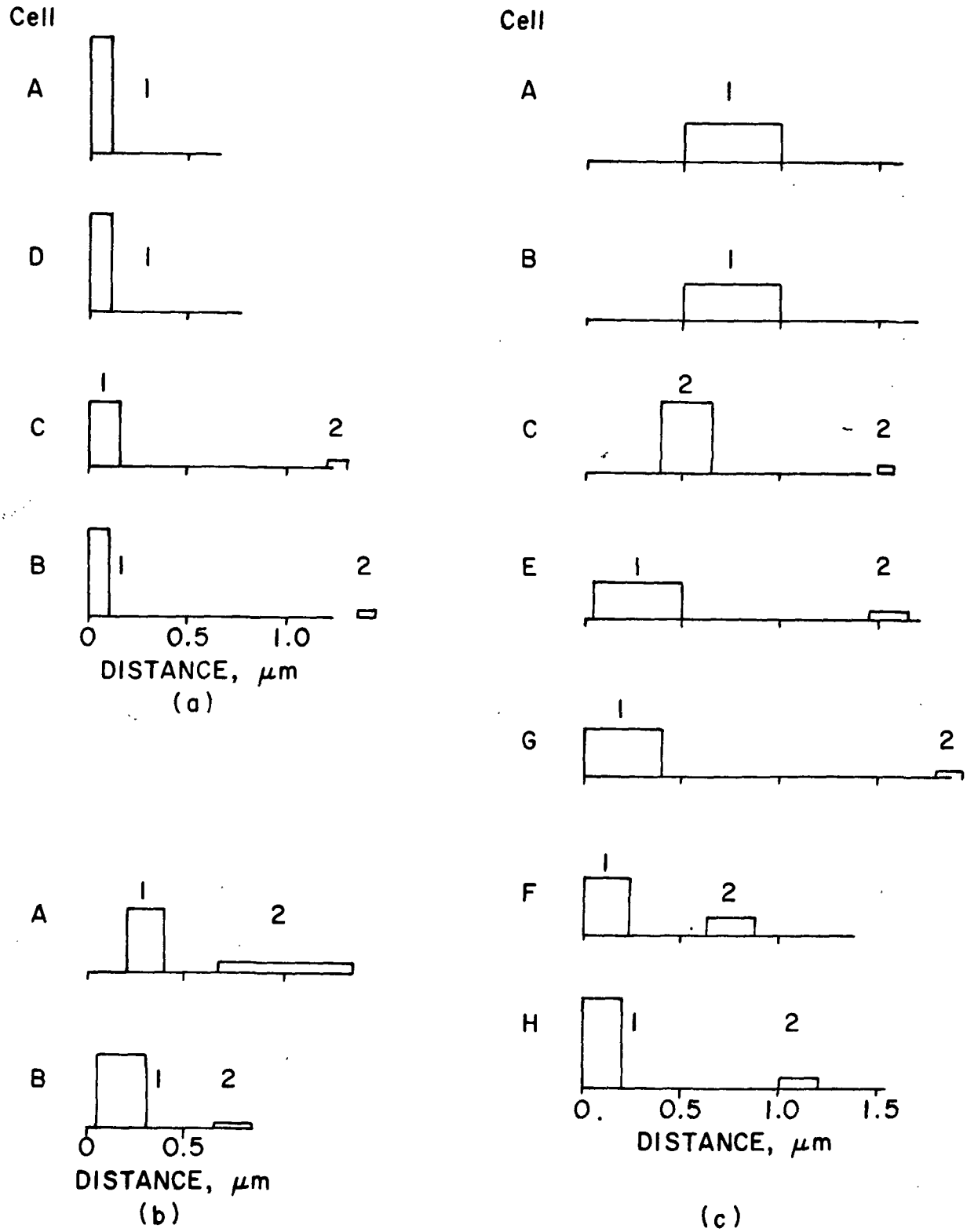

Figure 16. Representation of Radioactivity in Walls of Developing Fiber Cells Fed L-Arabinose-1-^{3}H and Incubated for (a) 3 Hours, (b) 24 Hours, and (c) 48 Hours

infused label is available to cells at all stages of wall development. Cells such as A-48H might very likely have been near the last stages of wall formation when the labeled sugar became available, and, consequently, incorporated labeled components only near the inner surface of the almost completed wall. Cells such as A-48A, A-48B, and A-48C probably were at earlier stages of wall development when the incubation period began. Apparently a pulse of available label was received by these cells, incorporated into wall substance, and followed into the wall by unlabeled wall components formed later in the incubation period.

Wood Fed D-Glucose-6-^{3}H (G6)

The results of the computer analysis of grain distributions in G6-48 fiber cells are presented in Fig. 17 and 18. The actual and fitted curves describing the grain density distributions in each of these cells are included in Appendix IX. Again, the cells are arranged in Fig. 17 and 18 from top to bottom in a sequence of increasing distance from the cambium.

In general, these distributions were more complex than those from the cells examined in the A-48 tissue. Model distributions from as many as three band sources were required to adequately describe the distributions. However, the positions of Band 1 (the band closest to the wall/lumen interface) in the various cells of the G6-48 series could be roughly related to the positions of Band 1 in the cells of the A-48 series. Both G6 and A tissue showed a relationship between the location of Band 1 and the distance of the cell from the cambium. Also, while this band usually contained most of the wall activity, a larger quantity of the activity in the G6 cells — relative to the A cells — existed deeper in the wall (Bands 2 and 3).

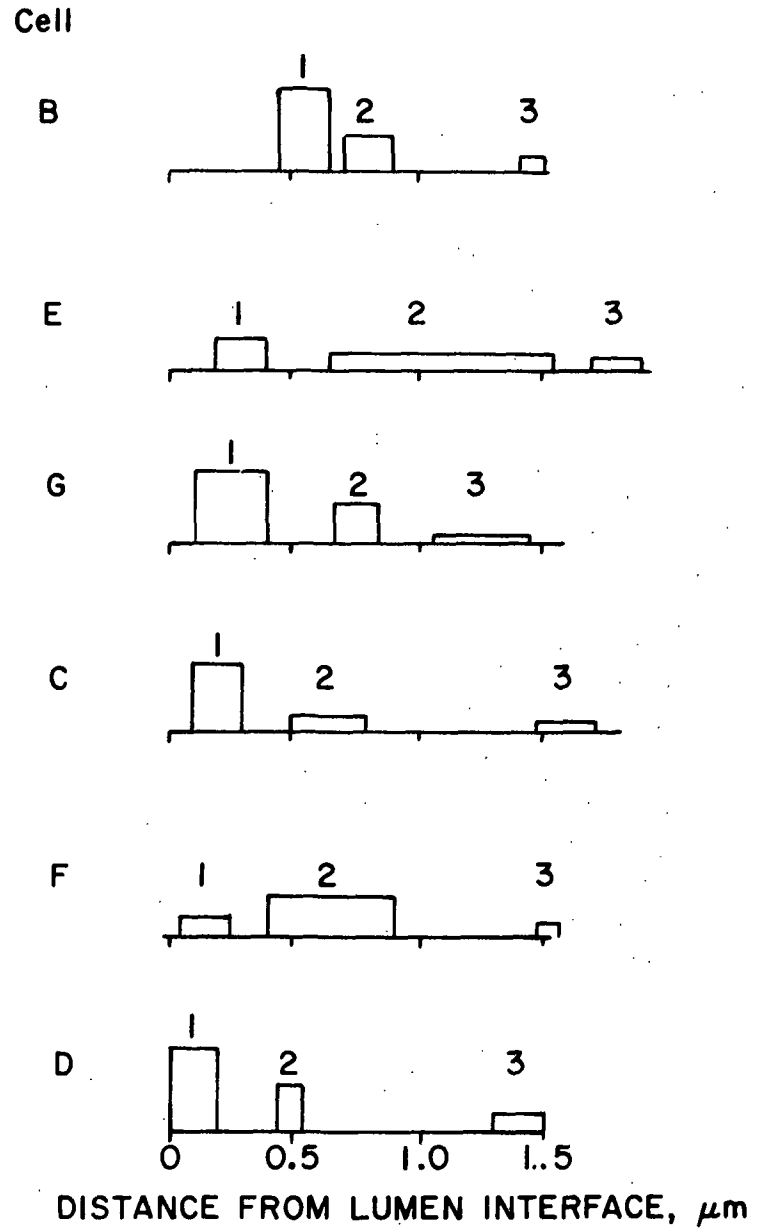

Figure 17. Representation of Radioactivity in Walls of Developing Fiber Cells Fed D-Glucose-6-^{3}H and Incubated for 48 Hours

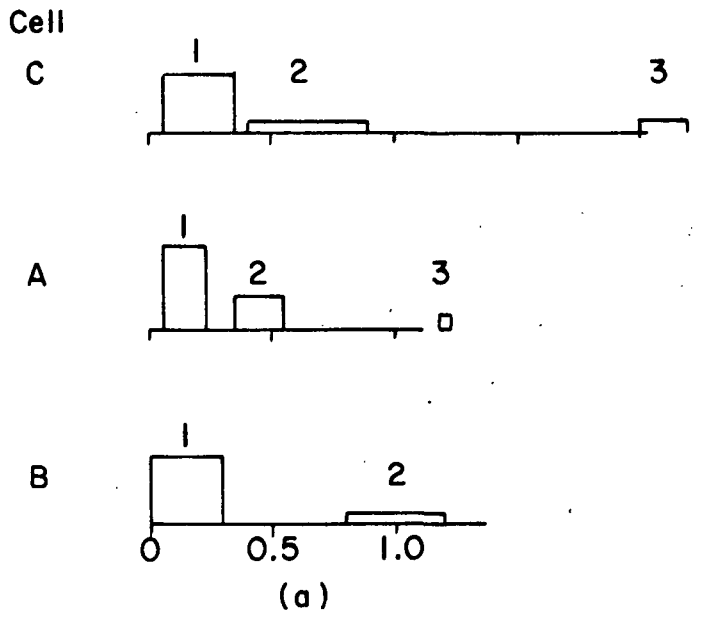

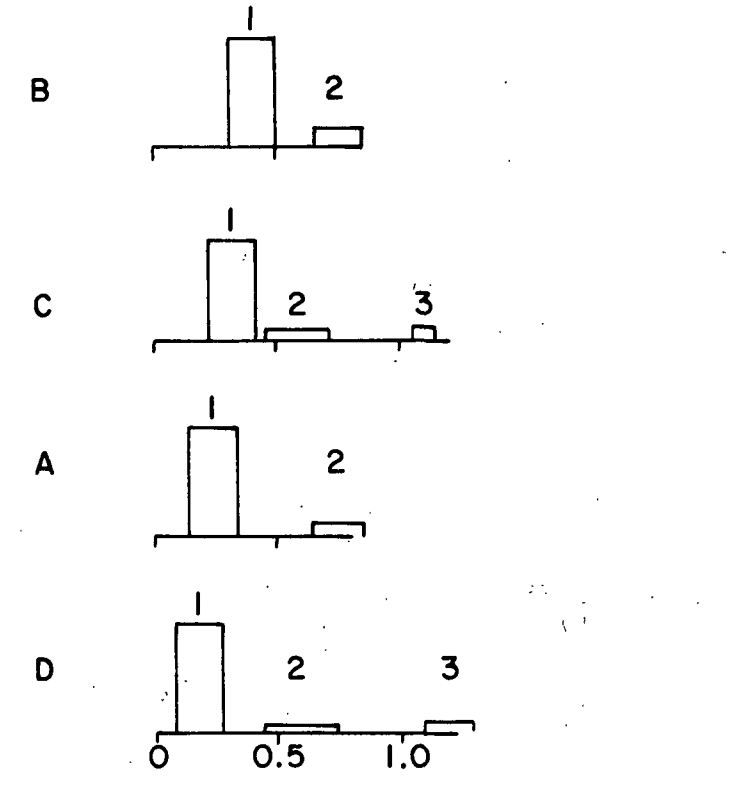

Figure 18. Representation of Radioactivity Remaining After Delignification in Walls of Developing Fiber Cells Fed D-Glucose-6-^{3}H and Incubated for (a) 24 Hours and (b) 48 Hours

Judging only the results shown in Fig. 17, one might speculate that the labeled wall material of Band 1 is cellulose and that Bands 2 and 3 represent labeled lignin. Ultraviolet absorption and specific staining procedures (17-20) have established quite conclusively that lignin is deposited relatively deep in the framework of the developing cell wall.

Tissue fed sugar G6 was examined after delignification in order to confirm these band designations. After an eight-week treatment at room temperature with an acidified (pH 4.5) solution of sodium chlorite (83), the stem tissue was thoroughly washed and subsequently embedded, sectioned, and examined autoradiographically. The autoradiography analyses on cells of this tissue are presented in Fig. 18. Since the radioactivity in Bands 2 and 3 was reduced relative to the radioactivity in Band 1, these results strengthen the band assignments as speculated earlier. According to this hypothesis, Band 1 is labeled cellulose while Bands 2 and 3 are radioactive lignin being deposited in the secondary cell wall and middle lamella regions. The continuing deposition of lignin in the middle lamella region with concurrent lignification of the secondary wall has been indicated elsewhere from ultraviolet absorption studies (84).

Figure 17 indicates that the relative radioactivities in Bands 1 and 2 vary from fiber to fiber in G6-48 tissue. Also, it indicates that the breadth of Band 2 varies considerably among the G6-48 cells. The absence of an evident pattern regarding the two differences of relative band size and radioactivity may be a reflection of the independent nature of lignification within individual cells. Most of the G6-48 cells examined appeared to have incorporated the greater part of the label into Band 1. However, some, such as G6-48F, apparently converted most of the labeled precursor into the wall substance of Band 2.

Therefore, most cells seemed to use the bulk of the supplied label for cellulose synthesis while some apparently converted most of it into lignin. The different stages of wall development existing among the cells when the label became available quite likely played a part in how each cell used the precursor.

DYNAMICS OF SECONDARY WALL FORMATION IN FIBER CELLS

The results of grain analyses of the high-resolution autoradiographs give a good indication of the rate of formation of the secondary wall in developing fiber cells. Assuming appositional deposition of cellulose, the distance between the cell wall/lumen interface and the location of Band 1 in G6 fiber cell walls should represent the thickness of wall material formed during the incubation period. The results shown in Fig. 17 thus indicate that wall substance at least 0.65-μm thick can be added to the inside of a growing cell within 48 hours.

PATTERNS OF CELLULOSE, PENTOSAN, AND LIGNIN DEPOSITION

The apparent proximity of labeled pentosan to the cell wall/lumen interface after a 3-hour incubation period (see Fig. 16a) suggests that pentosan may be deposited in a manner much like cellulose deposition, i.e., appositionally. However, the differences in breadth and location of bands of labeled pentosan and cellulose in developing fiber walls after longer incubation times indicate that the incorporation of label from the sugars A and G6 into these polymers may not be exactly alike. After 48 hours, bands of labeled pentosan appear 0.5 to 1.0 μm from the wall/lumen interface (cells A-48A and A-48B in Fig. 16c) while the deepest band of labeled cellulose appears from 0.45 to 0.65 μm from this interface (cell G6-48B in Fig. 17). Assuming that this observed difference

is real, i.e., that further analyses of other fiber cells incubated 48 hours would confirm these results, two explanations can be offered to account for the observations. First, the differences may reflect different conversion rates of sugars G6 and A into cellulose and pentosan. Second, the observed differences might be the result of an intussusceptional mechanism of pentosan deposition.

Deposition of pentosan by intussusception seems unlikely mainly because of the evidence that indicates that labeled pentosan lies very close to the wall/lumen interface after 3 hours of wall growth. Deposition deeper within the existing wall framework would require either that the polymerized pentosan somehow migrate further into the wall or that a second deposition mechanism operate independently to incorporate pentosan label deeper into the wall than the location of that present after 3 hours.

A more plausible explanation for the apparent locations of the two labeled polysaccharides (pentosan and cellulose) after 48 hours of wall growth takes into account the different features of the pathways postulated for the incorporation of label from the two metabolites, L-arabinose and D-glucose (see Fig. 1). Unlike L-arabinose, D-glucose is commonly found in plant cells (45). Labeled glucose, therefore, is probably subject to the combined effects of isotope dilution and metabolic pooling while enroute to labeling cellulose. Tagged L-arabinose, on the other hand, should be able to label the pentosan donor compounds, UDP-L-arabinose and UDP-D-xylose, with little or no competition from unlabeled arabinose. These metabolic differences might be responsible for a delay in the incorporation of the bulk of the radioactivity from sugar G6 into cellulose relative to the incorporation of radioactivity from sugar A into pentosan. Such a delay could account for the different band locations as

indicated by autoradiography. This scheme could also account for the autoradiography results observed in fiber walls after only 3 hours of growth, since some labeling of cellulose from sugar G6 could occur prior to the main pulse of incorporated radioactivity.

In contrast to cellulose and pentosan, lignin is deposited in depth within the wall by an intussusceptional mechanism. As discussed earlier, Bands 2 and 3 in the cell walls shown in Fig. 17 and 18 represent labeled lignin. The variation in the location, breadth, and relative radioactivity of Band 2 among the different cell walls is consistent with the concept that lignification of the secondary wall is directed on an individual basis by each cell. Furthermore, the continuous and simultaneous deposition of lignin in two discrete bands in cells at all stages of differentiation is evidence that lignification of the middle lamella (Band 3) is independent of that in the secondary wall. This observation may correlate with the evidence that there is a heterogeneous distribution of the two basic lignin groups (syringyl and guaiacyl) with regard to the secondary wall and middle lamella regions of both aspen and birch fibers (85-87).

Abundant evidence in the literature supports the existence of lignin-carbohydrate bonds (88-90). Since the present autoradiography data indicate that the concurrent synthesis of lignin and carbohydrate occurs in separate regions of the cell wall, the formation of lignin-carbohydrate bonds by simple enzymatic combinations of lignin and polysaccharide precursors seems unlikely. The present results, therefore, agree with Freudenberg's hypothesis of lignin formation by a free radical polymerization of lignin monomers (91). Certain intermediates in this polymerization sequence are postulated to react with any available hydroxyl groups (92,93), thereby creating a potential for

lignin to form covalent bonds with polysaccharides already deposited in the cell wall.

DISTRIBUTION OF PENTOSAN ACROSS THE CELL WALL

Sultze (12) and Haas and Kremers (57) have chemically examined fractions of P. tremuloides xylem isolated at different stages of differentiation. Sultze inferred approximate distributions of the carbohydrate constituents across an average fiber wall by correlating the chemical composition and wall development in each fraction. These workers suggested that the minor pentosan, arabinan, was completely deposited prior to the formation of any secondary cell wall. Assuming appositional deposition of xylan, Sultze concluded that this polymer is located throughout the cell wall with a maximum concentration near the middle of the wall. The present autoradiographic results support the above approach insofar as the assumption of appositional deposition of xylan appears to be correct, at least for P. tremuloides.

Because of the heterogeneity of developing woody cells, care should be exercised when attempting to strictly interpret the data derived from their chemical examination, especially a hardwood species. The present autoradiography results, for example, indicate that fiber cells continue to differentiate and incorporate label into pentosan after nearby vessel elements have ceased wall development (see Fig. 12c). In contrast, pentosan deposition apparently continues in the protective layer of ray parenchyma after the fiber cells are completely differentiated (see Fig. 12d). Thus, at least for hardwoods, a fraction of developing xylem collected at a given distance from the cambium can contain not only different cell types but also cells that are at different stages of wall development.

CONCLUSIONS

This research has demonstrated that L-arabinose-1-^{3}H (A) is an excellent precursor for pentosan in the developing wood of Populus tremuloides. Comparative autoradiography studies of the xylem tissue administered sugars A and G6 provided a means of directly examining the depositional patterns of the major cell wall components. Two main conclusions were derived concerning the deposition of pentosan in woody cells.

First, on a macroscale, pentosan synthesis occurs in all types of woody cells — fibers, vessel elements, and parenchyma cells — and at all stages of differentiation, from thin-walled cambial initials to the most mature living cells. Parenchymatous cells, however, apparently incorporate a disproportionately large quantity of pentosan relative to that incorporated by prosenchyma. Also, ray parenchyma cells associated with vessel elements continue to synthesize and incorporate pentosan into the protective layer as it is formed.

Second, on a microscale, pentosan appears to be added to the secondary cell wall of developing fibers by an appositional mechanism. Analyses of EM autoradiographs of cells undergoing secondary wall formation indicate that both pentosan and cellulose are localized soon after their synthesis at the inner face of the wall, but after longer periods of growth, these bands of labeled polysaccharide are located deeper in the wall. The distance from the deepest labeled wall material to the inner face of the wall is thus representative of the thickness of the wall substance formed during the incubation period. Based on the locations of the labeled polysaccharide, fiber cells apparently can increase wall thickness from 0.5 to 1.0 μm during a 48-hour period.

GLOSSARY AND SPECIAL ABBREVIATIONS

Aldobiuronic acid — 2-O-(4-O-methyl-D-glucopyranosyluronic acid)-D-xylose

Lumen — the region of a plant cell interior to the cell wall. As used in this work, it applies to both living and nonliving cells

Middle lamella — the layer of material surrounding each cell wall and separating one cell from another

Parenchymatous tissue — relatively small cells with carbohydrate storage and distribution functions (e.g., ray and pith parenchyma)

Prosenchymatous tissue — cells with conductive and mechanical functions (e.g., fibers and vessel elements)

Protective layer — the layer of wall material in ray parenchyma formed after secondary wall formation that covers the vessel-parenchyma pit membrane and part of the parenchyma wall near the pit.

A* — L-arabinose-1-^{3}H

ADP — adenosine diphosphate

cpm — counts per minute

EM — (transmission) electron microscope

F* — D-fructose-6-^{3}H

Gl* — D-glucose-1-^{3}H

G6* — D-glucose-6-^{3}H

GDP — guanosine diphosphate

M* — D-mannose-2-^{3}H

OLM — optical light microscope

P — L-proline-5-^{3}H

TLC — thin layer chromatography

UDP — uridine diphosphate

---

*These abbreviations (A, F, Gl, G6, and M) are also used to refer to tissues administered these precursors and incubated for various periods of time. For example, G6-48 refers to tissue fed G6 and incubated for 48 hours. In addition, G6-48A refers to a particular cell (designated A) in a G6-48 tissue section. Finally, DG6-48 refers to delignified G6-48 tissue.

SUGGESTED FUTURE WORK

The specific incorporation of L-arabinose-1-^{3}H into P. tremuloides pentosan, as demonstrated in this research, offers an opportunity to autoradiographically examine the cytoplasm of developing cells for the possible involvement of cytoplasmic organelles in pentosan synthesis. Although autoradiography experiments with tritium-labeled glucose, myo-inositol, and methionine have associated the Golgi apparatus (dictyosomes) with synthesis and transport of noncellulosic polysaccharides to the wall (58,94-96), the cytoplasmic localization of label incorporated from L-arabinose has not been reported. Such experiments would necessarily involve shorter incubation periods than those employed in this research. The administration of L-arabinose-1-^{3}H to in vitro cultures of callus tissue from P. tremuloides (97) may offer a more facile approach to such short-term investigations.

The evidence obtained in this research indicating that tritium-tagged D-mannose is capable of specifically labeling various noncellulosic polysaccharides in P. tremuloides provides an inducement for further radiochemical and autoradiographic studies with this precursor. While the polysaccharides containing mannosyl, galactosyl, and fucosyl units are minor components in hardwoods, the glucomannan and galactoglucomannan polymers are the major hemicelluloses in softwoods (98). Further studies of woody tissue administered labeled D-mannose, therefore, could supplement our present knowledge concerning hemicellulose formation and its deposition in the woody cell wall.

ACKNOWLEDGMENTS

The author wishes to express his gratitude to Drs. N. S. Thompson, R. A. Parham, and M. A. Johnson, the members of his thesis advisory committee, for their interest and contributions to this thesis.

The valuable assistance of the following people is also acknowledged: Mrs. Hilkka Kaustinen for her help with the electron microscopy work; Dr. D. W. Einspahr, Dr. L. L. Winton, and their staff for generously providing space and material for conducting some of the experiments; Dr. Julia Stapinski for her aid in translating Russian; and Mrs. Doreen Dimick for her careful typing of the original manuscript.

Other members of the Institute staff who gave unselfishly of their time and talents include Mr. John Bachhuber, Mr. Don Beyer, Mr. John Church, Mr. Marvin "Phat" Filz, Mr. Bob Rae, Mr. Clark Schabo, Mr. Fred Sweeney, and Mr. Paul Van Rossum. Special appreciation is expressed to Drs. Philip Larson and Karl Wolter of the U.S. Forest Service for their helpful discussions at the beginning of this work.

Finally, the financial support of The Institute of Paper Chemistry is gratefully acknowledged.

LITERATURE CITED

1. Perila, O. The chemical composition of carbohydrates of wood cells. J. Polymer Sci. 51:19-56(1961).

2. Meier, H. General chemistry of cell walls and distribution of the chemical constituents across the walls. In Zimmermann's The formation of wood in forest trees. p. 137-51. New York, Academic Press, 1964.

3. Bailey, A. J. Lignin in Douglas-fir: the pentosan content of the middle lamella. Ind. Eng. Chem., Anal. Ed. 8:389-91(1936).

4. Norberg, P. H., and Meier, H. Physical and chemical properties of the gelatinous layer in tension wood fibres of aspen (Populus tremula L.). Holzforschung 20:174-8(1966).

5. Meier, H., and Wilkie, K. C. B. The distribution of polysaccharides in the cell wall of tracheids of pine (Pinus sylvestris L.). Holzforschung 13:177-82(1959).

6. Meier, H. The distribution of polysaccharides in wood fibers. J. Polymer Sci. 51:11-18(1961).

7. Preston, R. D. The physical biology of plant cell walls. London, Chapman and Hall, 1974. 491 p.

8. Katkevich, R. G. Formation and distribution of hemicelluloses in the cell wall. In Sergeeva's Wood cell wall and its alterations during chemical treatments. p. 105-11. Riga, Zinatne, 1972.

9. Timell, T. E. Wood and bark polysaccharides. In Cote's Cellular ultrastructure of woody plants. p. 127-56. Syracuse, N.Y., Syracuse University Press, 1965.

10. Sayner, N., and Chidchester, G. H. Manufacture of wood pulp. In Browning's The chemistry of wood. p. 448. New York, Interscience Publishers, 1963.

11. Rydholm, S. A. Pulping processes. p. 84-7. New York, Interscience Publishers, 1967.

12. Sultze, R. F. A study of the developing tissues of aspenwood. Tappi 40: 985-94(1957).

13. Sultze, R. F. A study of the phenolic and carbohydrate materials in the newly formed tissues of aspenwood. Doctor's Dissertation. Appleton, Wisconsin, The Institute of Paper Chemistry, 1956. 120 p.

14. Thompson, N. S., Kremers, R. E., and Kaustinen, O. A. Effects of alkali on mature and immature jack pine holocellulose. Tappi 51:127-31(1968).

15. Cote, W. A., Kutscha, N. P., Simson, B. W., and Timell, T. E. Studies on compression wood. VI. Distribution of polysaccharides in the cell wall of tracheids from compression wood of balsam fir [Abies balsamea (L.) Mill.]. Tappi 51:33-40(1968).

16. Hamilton, J. K., Partlow, W. V., and Thompson, N. S. The nature of a galactoglucomannan associated with wood cellulose from southern pine. J.A.C.S. 82:451-7(1960).

17. Wardrop, A. B. The phase of lignification in the differentiation of wood fibers. Tappi 40:225-43(1957).

18. Wardrop, A. B. Cellular differentiation in xylem. In Cote's Cellular ultrastructure of woody plants. p. 61-97. Syracuse, N.Y., Syracuse University Press, 1965.

19. Wooding, F. B. P., and Northcote, D. H. The development of the secondary wall of the xylem in Acer pseudoplatanus. J. Cell Biol. 23:327-37(1964).

20. Hepler, P. K., and Fosket, D. E. Lignification during secondary wall formation in Coleus: an electron microscopic study. Am. J. Bot. 57:85-96 (1970).

21. Green, P. B. Concerning the site of the addition of new wall substances to the elongating Nitella cell wall. Am. J. Bot. 45:111-16(1958).

22. Setterfield, G., and Bayley, S. T. Deposition of cell walls in oat coleoptiles. Can. J. Bot. 37:861-70(1958).

23. Ray, P. M. Radioautographic study of cell wall deposition in growing plant cells. J. Cell Biol. 35:659-74(1967).

24. Roelofsen, P. A. The plant cell wall. Encyclopedia of plant anatomy. Vol. III. Part 4. p. 29. Berlin-Nikolassee, Gebruder Borntraeger, 1959.

25. Dennis, D. T., and Colvin, J. R. The relation between cellulose biosynthesis and the structure of the cell envelope in Acetobacter xylinum. In Cote's Cellular ultrastructure of woody plants. p. 199-212. Syracuse, N.Y., Syracuse University Press, 1965.

26. Preston, R. D. Structural and mechanical aspects of plant cell walls with particular reference to synthesis and growth. In Zimmermann's The formation of wood in forest trees. p. 169-88. New York, Academic Press, 1964.

27. Wardrop, A. B. The structure and formation of the cell wall in xylem. In Zimmermann's The formation of wood in forest trees. p. 87-134. New York, Academic Press, 1964.

28. Zimmermann, M. H. Movement of organic substances in trees. Science 133: 73-9(1961).

29. Northcote, D. H. Differentiation in higher plants. In Head's Oxford Biology Readers. No. 44. London, Oxford University Press, 1974.

30. Nikaido, H., and Hassid, W. Z. Biosynthesis of saccharides. Adv. Carbohyd. Chem. 26:381-483(1971).

31. Harris, P. J., and Northcote, D. H. Patterns of polysaccharide biosynthesis in differentiating cells of maize root tips. Biochem. J. 120: 479-91(1970).

32. Loewus, F. A. Metabolism of inositol in higher plants. Ann. N. Y. Acad. Sci. 165:577-98(1969).

33. Neufeld, E. F., Ginsburg, V., Putman, W. E., Fanshier, D., and Hassid, W. Z. Formation and interconversion of sugar nucleotides by plant extracts. Arch. Biochem. 69:602-26(1957).

34. Neufeld, E. F., Feingold, D. S., and Hassid, W. Z. Phosphorylation of D-galactose and L-arabinose by extracts from Phaseolus aureus seedlings. J. Biol. Chem. 235:906-9(1960).

35. Fan, D. F., and Feingold, D. S. Nucleoside diphosphate sugar 4-epimerases. II. Uridine diphosphate arabinose 4-epimerase of wheat germ. Plant Physiol. 46:592-5(1970).

36. Neish, A. C. The biosynthesis of cell wall carbohydrates. IV. Further studies of cellulose and xylan in wheat. Can. J. Biochem. and Physiol. 36:187-93(1958).

37. Neish, A. C. Biosynthesis of hemicelluloses. In Kratzl and Billek's Biochemistry of wood. p. 82-91. London, Pergamon Press, 1958.

38. Slater, W. G., and Beevers, H. Utilization of D-glucuronate by corn coleoptiles. Plant Physiol. 33:146-51(1958).

39. Roberts, R. M. The metabolism of D-mannose-^{14}C to polysaccharide in corn roots. Specific labeling of L-galactose, D-mannose, and L-fucose. Arch. Biochem. 145:685-92(1971).

40. Neish, A. C. Monomeric intermediates in the biosynthesis of lignin. In Freudenberg and Neish's Constitution and biosynthesis of lignin. p. 3-43. New York, Springer-Verlag, 1968.

41. Sarkanen, K. V. Dehydrogenative polymerization and structure of lignins: precursors and their polymerization. In Sarkanen and Ludwig's Lignins. p. 95-163. New York, Wiley-Interscience, 1971.

42. Sergeeva, V. M., and Kreitsberg, Z. N. The role of pentoses and α-D-methylglucoside in lignin biosynthesis. Trudy, Inst. Lesokhoz. Problem, Akad. Nauk. Latv. SSR, Voprosy Lesokhim. i Khim. Drevesiny 12:245-9(1957).

43. Loewus, F., and Jang, R. The conversion of C^{14}-labeled sugars to L-ascorbic acid in ripening strawberries. III. Labeling patterns from berries administered pentose-1-C^{14}. J. Biol. Chem. 232:521-32(1958).

44. Roberts, R. M., Shah, R. H., and Loewus, F. Inositol metabolism in plants. IV. Biosynthesis of apiose in Lemna and Petroselinum. Plant Physiol. 42: 659-66(1967).

45. Roberts, R. M., and Butt, V. S. Incorporation of (1-^{14}C)-L-arabinose into polysaccharides of maize root tips. Planta 94:175-83(1970).

46. Roberts, R. M. The incorporation of ^{14}C-labeled D-glucuronate and D-galactose into segments of the root tips of corn. Phytochem. 6:525-33(1967).

47. Roberts, R. M., and Butt, V. S. Patterns of incorporation of pentose and uronic acid into the cell walls of maize root tips. Expt. Cell Res. 51: 519-30(1968).

48. Loewus, F., and Kelly, S. Inositol metabolism in plants. I. Labeling patterns in cell wall polysaccharides from detached plants given myo-inositol-2-t or -2-^{14}C. Arch. Biochem. 102:96-105(1963).

49. Roberts, R. M., Shah, R. H., and Loewus, F. Conversion of myo-inositol to labeled 4-O-methyl-glucuronic acid in the cell wall of maize root tips. Arch. Biochem. 119:590-3(1967).

50. Loewus, F. Inositol metabolism and cell wall formation in plants. Federation Proc. 24:855-62(1965).

51. Roberts, R. M., and Loewus, F. Inositol metabolism in plants. III. Conversion of myo-inositol-2-^{3}H to cell wall polysaccharides in sycamore (Acer pseudoplatanus L.) cell culture. Plant Physiol. 41:1489-98(1966).

52. Roberts, R. M., Deshusses, J., and Loewus, F. Inositol metabolism in plants. V. Conversion of myo-inositol to uronic acid and pentose units of acidic polysaccharides in root tips of Zea mays. Plant Physiol. 43:979-89(1968).

53. Kroh, M., Miki-Hirosige, H., Rosen, W., and Loewus, F. Inositol metabolism in plants. VII. Distribution and utilization of label from myo-inositol-U-^{14}C and -2-^{3}H by detached flowers and pistils of Lilium longiflorum. Plant Physiol. 45:86-91(1970).

54. Aspinall, G. O. Carbohydrate polymers of plant cell walls. In Loewus' Biogenesis of plant cell walls. p. 95-115. New York, Academic Press, 1973.

55. van Buijtenen, J. P., Joranson, P. N., and Einspahr, D. W. Naturally occurring triploid quaking aspen in the United States. In Proceedings, Soc. of American Foresters Meeting. p. 62-4. Syracuse, New York, 1957.

56. Einspahr, D. W., van Buijtenen, J. P., and Peckham, J. R. Natural variation and heritability in triploid aspen. Silvae Genet. 12:51-6(1963).

57. Haas, B. R., and Kremers, R. E. The pectic substances as an index to the chemistry of wood formation. Tappi 47:568-73(1964).

58. Wooding, F. B. P. Radioautographic and chemical studies of incorporation into sycamore vascular tissue walls. J. Cell Sci. 3:71-80(1968).

59. Acerbo, S. N., Schubert, W. J., and Nord, F. F. Investigations of lignins and lignification. XXII. The conversion of D-glucose into lignin in Norway spruce. J.A.C.S. 82:735-9(1960).

60. Kratzl, K. Lignin — its biochemistry and structure. In Cote's Cellular ultrastructure of woody plants. p. 157-80. Syracuse, N.Y., Syracuse University Press, 1965.

61. Caro, L. G. High resolution autoradiography. In Prescott's Methods in cell physiology. p. 327-63. Vol. I. New York, Academic Press, 1964.

62. Juniper, B. E., Gilchrist, A. J., Cox, G. C., and Williams, P. R. Techniques for plant electron microscopy. p. 78. Oxford, Blackwell Scientific Publications, 1970.

63. Rogers, A. W. Techniques of autoradiography. 2nd ed. New York, Elsevier Scientific Publishing Company, 1973. 372 p.

64. Budd, G. C. Recent developments in light and electron microscope radioautography. Int. Rev. Cytol. 31:21-56(1971).

65. Salpeter, M. M., and Bachmann, L. Autoradiography. In Hayat's Principles and techniques of electron microscopy. Biological applications. Vol. 2. p. 221-78. New York, Von Nostrand Reinhold Co., 1972.

66. Salpeter, M. M., Bachmann, L., and Salpeter, E. E. Resolution in electron microscope radioautography. J. Cell Biol. 41:1-20(1969).

67. Gupta, B. L., Moreton, R. B., and Cooper, N. C. Reconsideration of resolution in EM autoradiography using a biological line source. J. Microscopy 99:1-25(1973).

68. Greenridge, K. M. H. Rates and patterns of moisture movement in trees. In Thimann's The physiology of trees. p. 19-42. New York, Ronald Press, 1958.

69. Timell, T. E. Wood hemicelluloses: Part I. Adv. Carbohyd. Chem. 19: 247-302(1964).

70. Bouveng, H. O., and Meier, H. Studies on a galactan from Norwegian spruce compression wood (Picea abies Karst.). Acta Chem. Scand. 13:1884-9(1959).

71. Meier, H. Studies on a galactan from tension wood of birch (Fagus silvatica L.). Acta Chem. Scand. 16:2275-83(1962).

72. Quick, R. H. A study of the hemicellulose removed during a neutral sulphite semichemical cook of aspenwood. Tappi 39:357-66(1956).

73. Albersheim, P., Bauer, W. D., Keestra, K., and Talmadge, K. W. The structure of the wall of suspension-cultured sycamore cells. In Loewus' Biogenesis of plant cell walls. p. 117-47. New York, Academic Press, 1973.

74. Roudier, A. J., and Eberhard, L. Hemicelluloses of maritime pine from Landes. IV. Polysaccharide extracts from the wood by boiling water. Constitution of an arabinan component. Bull. Soc. Chim. France 2:460-4 (1965).

75. Axelrod, B. The pentose phosphate pathway. In Greenberg's Metabolic pathways. Vol. I. p. 207-22. New York, Academic Press, 1960.

76. Yata, S., Itoh, T., and Kishima, T. Formation of perforation plates and bordered pits in differentiating vessel elements. Wood Res. (Kyoto) 50: 1-11(1970).

77. Meylan, B. A., and Butterfield, B. G. Perforation plate development in Knightia excelsa R. Br.: a scanning electron microscope study. Austral. J. Bot. 20:79-86(1972).

78. Lamport, D. T. A. Cell wall metabolism. Ann. Rev. Plant Physiol. 21: 235-70(1970).

79. Lamport, D. T. A. The isolation and partial characterization of hydroxyproline-rich glycopeptides obtained by enzymatic degradation of primary cell walls. Biochemistry 8:1155-63(1969).

80. Heath, H. F., and Northcote, D. H. Glycoprotein of sycamore tissue-culture cells. Biochem. J. 125:953-61(1971).

81. Dashek, W. V. Synthesis and transport of hydroxyproline-rich components in suspension cultures of sycamore-maple cells. Plant Physiol. 46:831-8 (1970).

82. Roberts, K., and Northcote, D. H. Hydroxyproline: observations on its chemical and autoradiographic localization in plant cell wall protein. Planta 107:43-51(1972).

83. Thompson, N. S., and Kaustinen, O. A. Some chemical and physical properties of pulps prepared by mild oxidative action. Tappi 47:157-62(1964).

84. Wardrop, A. B., and Bland, D. E. The process of lignification in woody plants. In Kratzl and Billek's Biochemistry of wood. p. 102. New York, Pergamon Press, 1958.

85. Stone, J. E. A study of the lignin removed during a neutral sulphite cook of aspen. Tappi 38:610-12(1955).

86. Marth, D. E. Studies on the lignin fraction of aspenwood pulps produced by sulphite-bisulphite cooking liquor systems. Tappi 42:301-8(1959).

87. Fergus, B. J., and Goring, D. A. I. The location of guaiacyl and syringyl lignins in birch xylem tissue. Holzforschung 24:113-24(1970).

88. Pearl, I. A. Annual review of lignin chemistry. Appleton, Wisconsin, The Institute of Paper Chemistry, March, 1974. 90 p.

89. Lai, Y. Z., and Sarkanen, K. V. Isolated lignin-carbohydrate complexes. In Sarkanen's Lignins. p. 220-4. New York, Wiley-Interscience, 1971.

90. Pearl, I. A. The chemistry of lignin. p. 284-91. New York, Marcel Dekker Inc., 1967.

91. Freudenberg, K. Biosynthesis and constitution of lignin. Nature 183: 1152-5(1959).

92. Freudenberg, K., and Grion, G. Contribution to the mechanism of formation of lignin and the lignin-carbohydrate bond. Chem. Ber. 92:1355-63(1959).

93. Freudenberg, K., and Harkin, J. M. Models for the bonding of lignin to carbohydrates. Chem. Ber. 93:2814-19(1960).

94. Northcote, D. H., and Pickett-Heaps, J. D. A function of the golgi apparatus in polysaccharide synthesis and transport in the root-cap cells of wheat. Biochem. J. 98:159-67(1966).

95. Pickett-Heaps, J. D. Incorporation of radioactivity into wheat xylem walls. Planta 71:1-14(1966).

96. Dashek, W. V., and Rosen, W. G. Electron microscope localization of chemical components in the growth zone of lily pollen tubes. Protoplasma 61:192-204(1966). Biol. Abstr. 48:99111.

97. Winton, L. L., and Mathes, M. C. Aspen callus. In Kruse and Patterson's Tissue culture. Methods and applications. p. 161-5. New York, Academic Press, 1973.

98. Timell, T. E. Wood hemicelluloses. Part II. Adv. Carbohyd. Chem. 20: 409-83(1965).

99. Benson, M. K., and Schwalbach, D. E. Techniques for rooting aspen root sprouts. Tree Planters' Notes 21:12-14(1970).

100. Thompson, N. S., and Springer, A. M. A mathematical model for the rate of extraction of xylan from wood chips. Paperi Puu 53:499-510(1971).

101. Saemen, J. F., Moore, W. E., Mitchell, R. L., and Millett, M. A. Techniques for the determination of pulp constituents by quantitative paper chromatography. Tappi 37:336-43(1954).

102. Stahl, E., and Kaltenbach, U. Thin-layer chromatography. VI. Trace analysis of sugar mixtures on kieselguhr G layers. J. Chromat. 5:351-5 (1961).

103. Waldi, D. Spray reagents for thin-layer chromatography. In Stahl's Thin-layer chromatography. p. 483-502. New York, Academic Press, 1965.

104. Timell, T. E. Enzymatic hydrolysis of a 4-O-methyl-glucuronoxylan from the wood of white birch (Betula papyrifera Marsh.). Svensk Papperstid. 65:435-47(1962).

105. Dickey, E. E. Unpublished work, 1969.

106. Hamilton, J. K., and Thompson, N. S. Graded acid hydrolysis studies of a xylan polyuronide associated with wood cellulose from western hemlock. J.A.C.S. 79:6464-9(1957).

107. Trevelyan, W. E., Procter, D. P., and Harrison, J. S. Detection of sugars on paper chromatograms. Nature 166:444-5(1950).

108. Wadman, W. H. Quantitative analysis of mixtures of sugars by the method of partition chromatography. Part V. Improved methods for the separation and detection of the sugars and their methylated derivatives on the paper chromatogram. J. Chem. Soc. 1950:1702-6.

109. Randerath, K. Film detection of weak β-emitters, particularly tritium. Anal. Biochem. 34:188-205(1970).

110. Gupta, G. N. A new approach of combustion in plastic bags for radioassay of H^3, C^{14}, and S^{35} in biological, biochemical and organic materials. Microchem. J. 13:4-19(1968).

111. Lewis, J. D. A modified plastic bag combustion technique for the radioassay of the ^{14}C and ^{3}H in biological tissues. International J. of Applied Radiation and Isotopes 23:39-40(1972).

112. Mollenhauer, H. H. Plastic embedding mixtures for use in electron microscopy. Stain Technol. 39:111-14(1964).

113. Crefeld, W. H. On some improvements in the preparation of high-resolution radioautographs by the flat substrate method. Histochemie 32:281-4(1972).

114. Kopriwa, B. M. A semiautomatic instrument for the radioautographic coating technique. J. Histochem. Cytochem. 14:923-8(1967).

115. Richter, C. B., and King, C. S. Formalin as a hardener of photographic emulsions to facilitate staining of epon sections after autoradiography. Stain Technol. 47:268-9(1972).

116. O'Brien, T. P., Feder, N., and McCully, M. E. Polychromatic staining of plant cell walls by toluidine blue O. Protoplasma 59:368-73(1964).

117. Hiraoka, J. A holder for mass treatment of grids, adapted especially to electron staining and autoradiography. Stain Technol. 47:297-301(1972).

APPENDIX I

PRECURSOR ADMINISTRATION AND TISSUE INCUBATION PROCEDURES

Plantlets of a natural triploid clone of P. tremuloides (55,56) were grown from root sprouts in a greenhouse using the techniques described by Benson and Schwalbach (99). Actively growing plantlets 30-35 cm in height were severed from their roots 5-10 cm above the soil surface. These detached stems were quickly placed into a 0.1% sodium hypochlorite solution and trimmed under water to heights of 23.0 ± 1.5 cm. The bottom two leaves of each stem were excised at the petiole and the stem base immediately inserted into a sterile 10 mm × 75 mm test tube containing the labeled precursor in solution. The test tube had been sealed with Saran wrap when empty, autoclaved, and 0.5 ml of precursor solution added by injection with a sterile 1-cc syringe just before insertion of the stem. A small slit in the Saran wrap was made with a razor blade to allow the stem to fit into the tube without uncovering the tube completely.

The tritium precursors were obtained as sterile aqueous solutions from the supplier*. 150 μCi each of G1 (5.3 Ci/mM), G6 (6.66 Ci/mM), F (650 mCi/mM), M (611 mCi/mM), and P (10 Ci/mM), and 200 μCi of A (12 Ci/mM) were fed to individual stems. After each stem had absorbed the radioactive solution (15-20 minutes), its base was rinsed with sterile distilled water and inserted into another sterile 10 mm × 75 mm test tube containing distilled water. Sterile water was added at intervals to allow the stem base to remain immersed throughout the incubation period.

*Specific activities and radiochemical purities were accepted as stated by the supplier, Amersham/Searle Corporation, 2636 S. Clearbrook Drive, Arlington Heights, IL 60005.

Incubations were conducted in a growth chamber at constant conditions of temperature and humidity (55% RH and 80°F ± 2°F). Lighting was constant at 2200-ft candles during the long-day conditions (16 hours of light per day). The administrations were begun 3 hours into the 16-hour period of illumination.

One segment was collected from the base of each stem after 3, 12, 24, 36, 48, 60, and 72 hours of incubation. Each excision was made under 0.1% sodium hypochlorite in a petri dish. The stem was quickly returned to its incubation vessel after each segment excision and the 2-cm segment subdivided into 3 pieces as shown in Fig. 19. The top and bottom 0.5-cm pieces were designated for radiochemical study while the 1-cm middle piece was used for autoradiography. The 1-cm segment was further cut into two 0.5-cm pieces which were quartered by two radial-longitudinal slices. Immediately after segmenting, all pieces were put into ice-cold 30% MeOH and stored in the dark at 0°C.

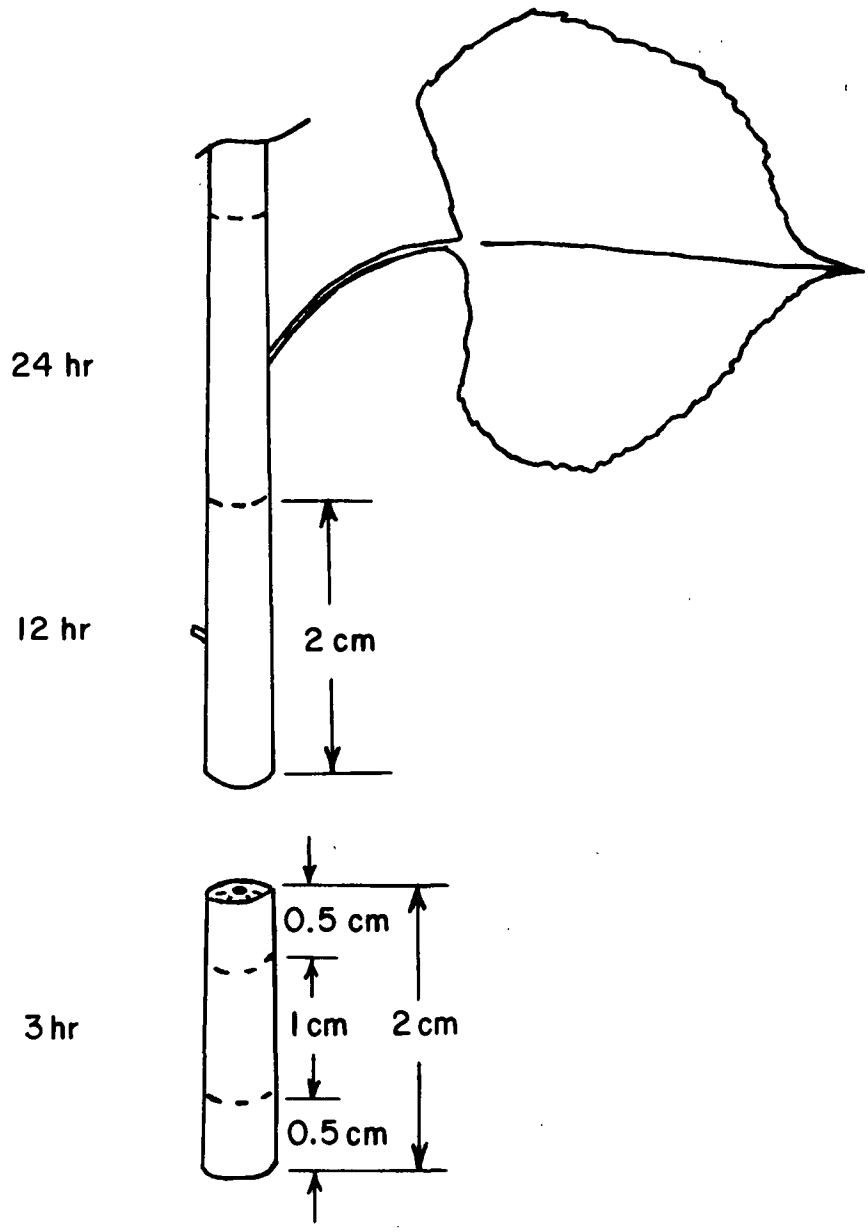

Figure 19. Stem Incubation and Segment Collection Scheme. Segments were Collected as Indicated After Various Periods of Incubation (3 Hours, 12 Hours, 24 Hours, etc.)

APPENDIX II

PROCEDURES USED TO ISOLATE AND HYDROLYZE LABELED POLYSACCHARIDES

ISOLATION OF MATERIALS

After incubation, the collected woody stem segments were stored at 0°C in 30% methanol in the absence of light for 12-24 hours. The segments were then washed twice (4-hr periods) with an ice-cold solution of the unlabeled precursor (1 g/liter) in 30% ethanol and carried through a room-temperature dehydration sequence similar to the procedure used with the tissue examined by autoradiography. The dehydration schedule described in Appendix V was followed except that after total dehydration in 100% ethanol the segments were returned to 95% ethanol for storage until needed.

Xylem and pith tissues were manually isolated from the stem segments. After soaking in distilled water for 30 minutes the segments were easily debarked with a razor blade under a stereomicroscope. The bark separated cleanly in one piece from the xylem cylinder at the cambium after a longitudinal incision was made through the bark. The debarked stem segment was then halved by a radial-longitudinal razor cut exposing the pith. Pith and xylem fractions were then isolated by scraping the core of exposed pith tissue away from the xylem.

A fraction rich in pentosan was further isolated from the xylem tissue by a room-temperature treatment with alkali (100). The xylem was diced transversely with a razor blade into pieces less than 0.5 mm in length. These small pieces were then mixed with similar but nonradioactive wood from other first-year aspen seedlings. This mixture (0.4 g) was treated with 4 ml of 12% sodium hydroxide for 28 hours. The filtered extract was added with stirring to 50 ml of methanol containing 0.83 ml of glacial acetic acid. The precipitated polymer

was recovered by centrifugation and washed successively with 100-ml volumes of 80 and 100% methanol.

ACID HYDROLYSIS PROCEDURE

All samples were hydrolyzed by a scaled-down version of the procedure of Saemen, et al. (101) using a 0.003-g sample. The wood was placed in 3-ml centrifuge tubes with 0.03 ml of 72% sulfuric acid. This prehydrolysis step was conducted at 30°C with occasional stirring. After one hour, 0.84 ml of distilled water was added to each centrifuge tube, a glass marble placed over the rim of each tube, and the vessels kept in a pressure cooker at 237°F for one hour. The hydrolyzate was then neutralized with a saturated solution of barium hydroxide — added dropwise with stirring — to a final pH of 5.5. After neutralization, the tubes were centrifuged and the supernatant liquid pipetted into vials containing Amberlite IR-120 cation exchange resin. After a few minutes of agitation, the liquid was pipetted into clean vials for concentration in a vacuum oven at 35°C. The concentrated hydrolyzate was finally diluted with 20 µl of 50% ethanol prior to chromatography.

APPENDIX III

DETERMINATION OF RADIOACTIVITY AMONG THE HYDROLYZATE COMPONENTS

THIN LAYER CHROMATOGRAPHY (TLC) PROCEDURES

Neutral sugars were separated on a kieselguhr TLC system (Brinkman precoated kieselguhr-on-aluminum sheets buffered with 0.05M sodium acetate) with multiple development (4X) in ethyl acetate-isopropanol-water (100:25:12.5, v/v) (102). Separated sugars were located by comparison with the positions of reference sugars chromatographed adjacent to the radioactive hydrolyzate. Anisaldehyde reagent (103) was used for detecting these reference sugars.

A cellulose TLC system (Machery-Nagel MN Polygram Cel) was used to separate the components that did not migrate in the kieselguhr system. The developer used was ethyl acetate-acetic acid-water (18:7:8, v/v) (104). Samples of aldotriuronic acid, aldobiuronic acid, glucuronic acid, galacturonic acid, cellobiose, and xylose were chromatographed for reference alongside the unknowns. The aldotriuronic acid used in this work was obtained from Dickey (105). Aldobiuronic acid was produced from the aldotriuronic acid by a hydrolysis procedure described by Hamilton and Thompson (106). A 10-mg sample was hydrolyzed for 3 hours with 2.0 ml of 2.5N H_2SO_4 at 100°C. The hydrolyzate was neutralized with barium hydroxide to pH 2.8, centrifuged, and pipetted into a clean vial. After concentration, the hydrolyzate components were separated by paper chromatography with the same acid developer used with cellulose TLC. The aldobiuronic acid was eluted from the chromatogram with water and concentrated. Reference compounds were detected on chromatograms by alkaline silver nitrate (107) and p-anisidine hydrochloride (108).

MEASUREMENT OF ACTIVITY ON CHROMATOGRAMS

The TLC fluorographic method of Randerath (109) provided a straightforward means of localizing and gauging relative distributions of radioactivity on the chromatograms. A 15-ml solution of scintillant (0.7 g of 2,5-diphenyloxazole per 10-ml ether) was poured evenly over each 20 cm × 20 cm TLC plate and dried. A sheet of Kodak RP/R2 x-ray film was placed adjacent to the coated TLC plate, sandwiched between glass plates, wrapped with black paper and foil, and stored at -78°C (in a freezer with solid CO_2). After an exposure period of 10-20 days, the film was allowed to warm to room temperature and was then developed at 68°F according to the schedule below:

Solution	Time, min
Kodak D-19 (diluted 1:2)	8 (with agitation)
Kodak Rapid Fixer	5
Water (running)	20

Liquid scintillation counting of these same TLC plates showed quantitative measurement of radioactivity on different areas of the chromatogram. Strips of the chromatogram 0.5 inch in width were cut along the direction of component migration and then cut transversely into 0.5 or 1.0-cm pieces. These pieces were placed individually into glass counting vials. After adding 20 µl of distilled water followed by 5 ml of Beckman's cocktail D, radioactivities were measured on a Beckman DPM-100 liquid scintillation counter.

APPENDIX IV

DETERMINATION OF RADIOACTIVITY IN KLASON LIGNIN AND WHOLE WOOD SAMPLES

Samples of Klason lignin and whole wood were derived from debarked stem segments which had been diced transversely into pieces less than 0.5-mm thick. The debarked and diced wood samples were weighed after conditioning for 24 hours at 50% RH and 73°F. Klason lignin was obtained from the same hydrolysis procedure as described in Appendix II. The lignin was collected before neutralization, however, on 8-μm Millipore filters and thoroughly washed with distilled water.

The radioactivities of wood and lignin samples were measured by liquid scintillation counting of their combustion products. Samples were combusted by the technique of Gupta (110) using oxygen-filled plastic bags and a modified combustion assembly as suggested by Lewis (111). Wood samples to be combusted were dispersed with cotton inside a rolled envelope of lens tissue. Lignin samples were combusted with the filters upon which they were collected.

The combustion apparatus was basically the same as that used by Gupta (110), consisting of three main parts (plastic bags, sample support coil, and combustion assembly) with various accessories. Kapak*, heat-sealable polyester pouches (6 1/2 inches × 8 inches) served as disposable combustion vessels. Two beads of silicone rubber (Dow Corning Silicone Rubber Sealer) were applied to each pouch, one near the center and one in a lower corner, setting overnight. Platinum-20% iridium wire (0.025 inch) was wound into coils (10 mm × 5 mm diameter) for sample supports. A combustion assembly was fabricated from two watch glasses

*Kapak Ind., Bloomington, Minn. 55431.

(75-mm diameter) held together by two glass rods (50 mm in length) in a design similar to that of Lewis (111). Silicone rubber bonded the glass rods to the watch glasses.

The procedure for the combustion of one sample was as follows:

1. Apply India ink to both tips of the lens tissue covering the sample and allow to dry.
2. Place the covered sample in the coil and put the combustion assembly into the plastic bag.
3. Seal the top to the bag with a hot iron.
4. Partially evacuate the bag via a syringe needle inserted through the center bead of silicone rubber.
5. Add oxygen to the bag in a similar manner until the bag is full.
6. Repeat Step 4.
7. Repeat Step 5, except stop inflating the bag about 20% short of its full capacity.
8. Suspend the bag from a clip attached to a ring stand over a sink.
9. Ignite sample by focusing a light beam from a projection lamp* on the inked spots of the lens tissue.
10. Run a stream of cold water over the suspended bag until it is cooled.
11. Inject 10 ml of p-dioxane into the bag (through a silicone rubber bead).
12. Shake the bag at intervals during a 15 to 30-minute equilibration period.
13. Withdraw two 2.5-ml aliquots from the bag with a disposable syringe and add to counting vials with 10-ml liquid scintillant (Beckman's cocktail D) for counting.

*150 w/125 v General Electric type DFN lamp.

APPENDIX V

DEHYDRATION AND EMBEDMENT PROCEDURES

Segments of stem tissue to be examined by autoradiography were first washed in solutions of the unlabeled precursor as described in Appendix II. These segments were then dehydrated according to the following sequence:

Solution	Minimum Time
15% Ethanol	30 min
30% Ethanol	30 min
50% Ethanol Aspiration under 5-10 in Hg vacuum	30 min
70% Ethanol	30 min
95% Ethanol	30 min
100% Ethanol	30 min
100% Ethanol	Overnight
100% Ethanol	30 min
Ethanol:propylene oxide (1:1, v/v)	3 hr
100% Propylene oxide	3 hr
100% Propylene oxide	Overnight

Dehydrated segments were embedded in Epon-Araldite (112) resin containing the following components:

12.5 g Epon 812

7.5 g Araldite 502

27.5 g DDSA (dodecynylsuccinic anhydride)

1.5 g Dibutylphthalate

1.0 g DMP-30 (2,4,6-dimethylamino-methylphenol)

The schedule for infiltration and embedment was as follows:

1. Propylene oxide:Epon-Araldite (2:1), 4 hr at room temperature.
2. Propylene oxide:Epon-Araldite (1:2), 4 hr at room temperature.
3. Epon-Araldite, overnight at room temperature.
4. Epon-Araldite, 4 hr at room temperature.
5. Transfer segments to filter paper for draining, then to fresh Epon-Araldite in embedding mold. Aspirate to remove air bubbles.
6. Polymerize at 60°C, overnight, and allow to cool at least 12 hr before sectioning.

APPENDIX VI

AUTORADIOGRAPHY PROCEDURES

LIGHT MICROSCOPY

Sections for light microscopy were cut approximately 0.4-μm thick using a Sorvall MT2-B ultramicrotome equipped with a diamond knife. Ribbons of sections were transferred to collodion-coated glass microscope slides with a 4-mm loop of nichrome wire. During this operation the slide was placed on a slide-holding device similar to that described by Crefeld (113). Because this device was mounted on the microtome knife stage, it allowed the transfer of sections from the knife boat to the slide under continuous microscopic observation. After drying, the sections were coated with a layer of carbon approximately 5-10-nm thick using a Denton DV-502 vacuum evaporator.

A layer of Ilford L-4 liquid emulsion* was applied in the dark (see below), to the above slides with the dipping apparatus shown in Fig. 20. By withdrawing a slide from the emulsion at constant speed, this apparatus coated the slides with a reproducible, uniform layer of constant thickness in the same manner as the semiautomatic instrument of Kopriwa (114). A constant speed of withdrawal was accomplished by a one-third rpm synchronous motor turning a drum, D1. The latter pulled a cable (by friction) directly linked to the slide as shown in the figure. The two drums, D1 and D2, provided two different withdrawal speeds, 49 and 67 mm/sec, respectively.

Because of its photosensitivity, the emulsion was handled in a darkroom illuminated by a Wratten OC safelight kept at least 3 feet from the area of

*Ilford Ltd., Ilford, Essex, England.

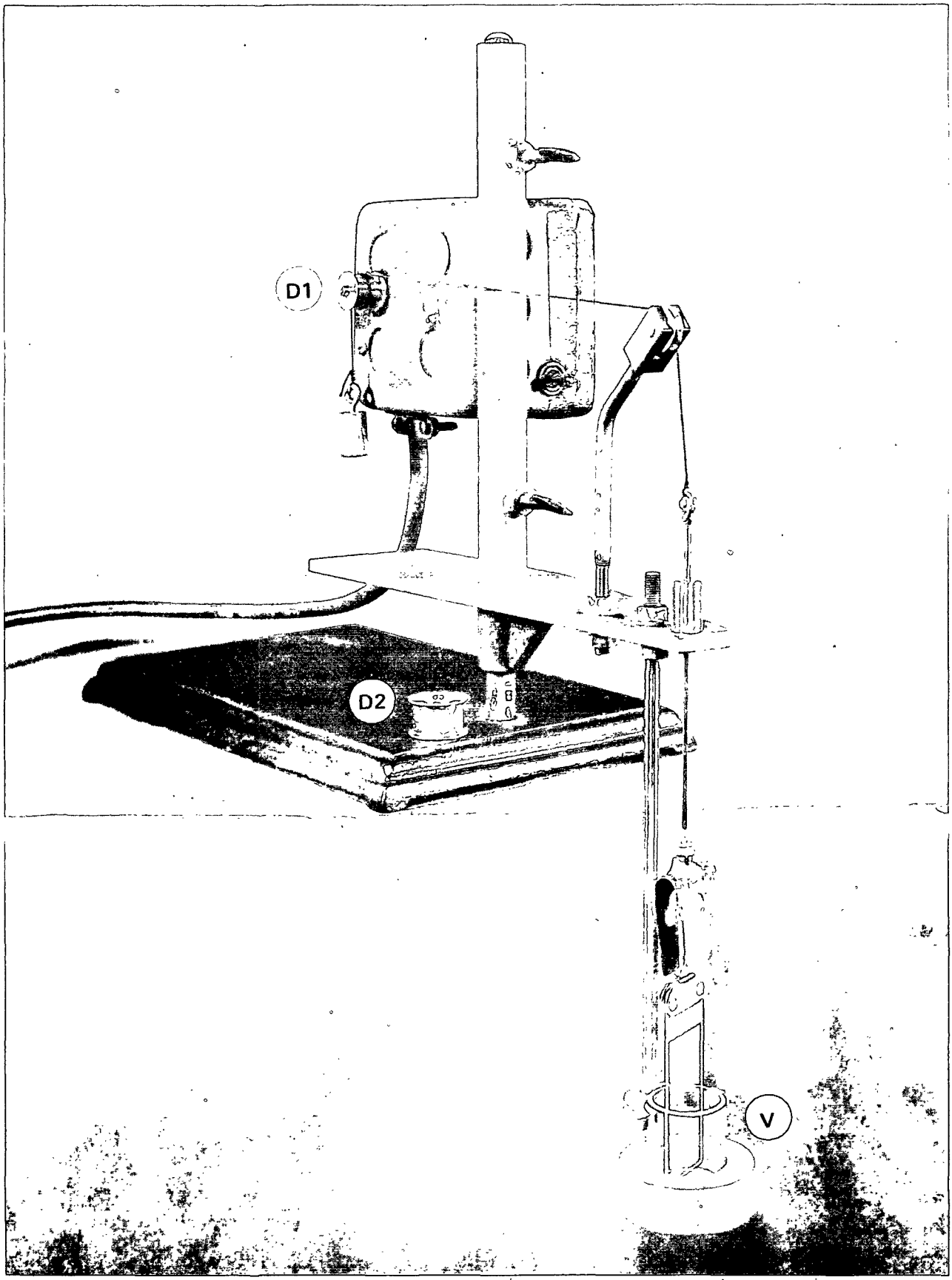

Figure 20. Slide Dipping Apparatus

operation. The humidity of the darkroom was maintained above 50% RH. The operations involved in applying the emulsion to the slides are outlined below:

1. Remove about 3 g of emulsion from the stock bottle with a porcelain spatula and melt it in a 15-ml centrifuge tube in a 40-45°C water bath.
2. Gauge the volume of melted emulsion and add approximately three times this volume of 1% glycerol (also at 40-45°C).
3. Stir very slowly with a glass rod until mixed (2-3 min).
4. Pour the diluted emulsion slowly into the glass dipping vessel (V in Fig. 20), which is partially submerged in a constant temperature bath (35°C).
5. After allowing the emulsion to reach thermal equilibrium with the water bath, place a slide into the dipping vessel and grip it with the metal clips (as shown in Fig. 20).
6. Switch on the power to the motor.
7. When the slide has cleared the top of the dipping vessel, remove it from the clips.

The thickness of the emulsion coating was estimated by determining the interference color of the dry emulsion under normal illumination. As suggested by Salpeter and Bachmann (65), a slightly overlapping monolayer of silver halide crystals about 1700-A thick (purple interference color) was selected as the best thickness. Test slides were dipped until a correct emulsion thickness was obtained. If the color of the test slide indicated that the layer was a different thickness, one or more corrective actions could be taken. If the layer was too thick, distilled water was added dropwise with a syringe to the dipping vessel. If the layer was too thin, the withdrawal speed was increased by changing from the smaller diameter drum, D1, to the larger diameter drum, D2, and/or lowering the temperature of the water bath. Normally, the water bath was maintained at 35°C.

Dipped slides were placed upright to dry in a neoprene-coated wire rack inside a lightproof, constant humidity (45% RH) chamber. After drying (usually 2 hours) the slides were placed in black slide boxes with a small package of Drierite wrapped in tissue paper. The boxes were filled with an atmosphere of CO_2 prior to their being sealed with black masking tape. The sealed boxes were then stored inside a refrigerator at 4°C for the duration of the exposure period.

After approximately 10 days, the slides were processed in the following solutions at 20°C:

Solution	Time
Kodak D-19 (diluted 1:2)	4 min
1% Acetic acid	10 sec
Kodak Rapid Fixer	5 min
Water (running)	5 min
Distilled water	1 min
5% Formaldehyde	10 min

The formaldehyde treatment hardened the emulsion layer, thus allowing staining of the sections at high temperature without damage to the autoradiograph (115). Staining was accomplished with toluidine blue (0.05% in 0.1M phosphate buffer, pH 6.8) for 2 minutes at 70-80°C (116). This temperature was achieved by placing the slide flat in a petri dish floating on a water bath at 80°C. The autoradiographs were observed with a Zeiss photomicroscope using a phase-contrast, oil-immersion optical system.

ELECTRON MICROSCOPY

Sections for electron microscopy were cut approximately 1000-A thick (pale gold interference color) on the same ultramicrotome used for light microscopy. Two different techniques were used for applying the layer of liquid emulsion over the sections and subsequently processing the autoradiographs.

GLASS SUBSTRATE TECHNIQUES

This method was an extension of the procedure used with light microscope autoradiographs. With the exception of the slide dipping apparatus, it was the same as the procedure described by Salpeter and Bachmann (65). Some modifications in technique were made, however, as suggested by Crefeld (113). Slides were coated with collodion by dipping into a 0.7% solution of collodion in amyl acetate, then reinforced at the bottom edge with a second dip (after drying) in 5% collodion to a depth of about 2 mm. The transfer of sections to the collodion-coated slides was conducted as before for light microscopy. Also, the slides were coated with a 50-A layer of carbon and a 1700-A layer of Ilford L-4 emulsion as described before. The dried slides were stored at 4°C in dry, lightproof slide boxes containing a CO_2 atmosphere.

After exposure periods of 6-10 weeks, the slides were processed in a development procedure which yielded small, punctate silver grains. The gold thiocyanate, Elon-ascorbic acid, and fixer solutions were prepared by the formulae described by Salpeter and Bachmann (65) and used the same day (1-8 hr after mixing) at 20°C. The processing schedule was as follows:

Solution	Time
Gold thiocyanate	5 min
Distilled water	10 sec
Elon-ascorbic acid	8 min
Nonhardening fixer	1 min
Distilled water	30 sec
Distilled water	30 sec
Distilled water	30 sec

After processing, the collodion layer containing the sections was carefully stripped from the glass slide by the procedure detailed by Salpeter and Bachmann (65). Formvar-coated nickel grids were placed over the ribbons of sections on the collodion layer and the floating membrane picked up onto filter paper by suction. After drying, the collodion layer was dissolved by a 4-minute immersion in amyl acetate. The specimen grids were then poststained with 2% potassium permanganate according to the following schedule:

1. Put drops of stain (drawn from below surface of solution) onto wax bottom petri dish.
2. Float grids on the drops, section side down, for 10 minutes in the covered dish.
3. Rinse successively in three vessels of distilled water, 20 rapid dips in each vessel.
4. Dry grids by blotting edge with lens paper.

The finished autoradiograph preparations were examined in an RCA model EMU-3F transmission electron microscope operated at 50 kv.

GRID SUBSTRATE TECHNIQUE

In this procedure the liquid emulsion was applied directly to specimen grids containing the tissue sections. The ribbons of sections were picked up from the knife trough of the ultramicrotome onto collodion-coated nickel grids and stained with 2% potassium permanganate as described before.

The grids were first coated with carbon (5-10 nm) and then coated with Ilford L-4 emulsion by the procedure described by Hiraoka (117). The stained grids were inserted into the opened slots of flexible plastic Hiraoka Supporting Plates* under a stereomicroscope. When the plate was lying flat, the slots firmly gripped the edges of the grids and held them in a position perpendicular to the plane of the plate. Up to 16 grids could be held on each plate during the various autoradiography steps from carbon coating through chemical processing. The diluted emulsion at 35°C was applied (in the darkroom) to the specimen side of the grids with a fine pipet while the supporting plate was held vertically. Excess emulsion was removed by moving the grids into a vertical position and touching strips of filter paper to the lower edges of the grids.

The emulsion-coated grids were then dried on the supporting plates and placed in slide boxes for storage in a manner similar to that used with the glass slides. Each box contained a bag of Drierite and a CO_2 atmosphere. After the exposure period, the grids were processed by the gold thiocyanate and Elon-ascorbic acid sequence described earlier. After drying, the grids were ready for examination in the electron microscope.

*Polysciences, Inc., Warrington, PA 18976.

APPENDIX VII

COMPUTER PROGRAMS FOR GRAIN DISTRIBUTION ANALYSIS

This appendix contains the user instructions and listings for the computer programs employed in the analysis of electron microscope autoradiographs. The programs were written especially for use with data obtained in this thesis research. Therefore, they are most applicable for analysis of grain distributions relative to the boundaries of band-shaped structures such as cell walls. Both programs* are coded in basic FORTRAN IV. The programs were used in this research with the IBM 360/44 OS and RAX operating systems.

EMARAN

The directions for use of the EMARAN program are contained in Table III. A listing of EMARAN and its subroutines (GRNDIS, PLTDAT, and GRAF) are included in Table IV. Graphical output was accomplished by a Calcomp model 565 plotter. The unlisted subroutines associated with this plotting function and used in subroutine GRAF (e.g., PLOT, SCALE, etc.) were written by staff of The Institute of Paper Chemistry computer center.*

CRVFIT

The directions for using the CRVFIT program are presented in Table V. A listing of the program is contained in Table VI. The GRAF subroutine used with CRVFIT is not included in this listing since it is the same subroutine used with EMARAN (see Table IV).

*The program package is available at copying costs from The Institute of Paper Chemistry computer center (File Number IPC-TH-005).

TABLE III

USER INSTRUCTIONS FOR EMARAN

PROGRAM EMARAN--FOR ANALYSIS OF ELECTRON MICROSCOPE AUTORADIOGRAPHS

DIRECTIONS FOR USE

POINTS FROM GRAINS AND WALL INTERFACES ARE DIGITIZED FROM THE MICROGRAPH VIA A MICROCOMPARATOR. GRAIN POINTS REPRESENT MIDPOINTS OF IDENTIFIABLE SILVER GRAINS. INTERFACE POINTS ARE SELECTED FROM VARIOUS POINTS ALONG THE CELL WALL-LUMEN INTERFACE AND, SIMILARLY, FROM POINTS ALONG THE WALL-MIDDLE LAMELLA INTERFACE. INTERFACE POINTS ARE SPACED CLOSE ENOUGH SO THAT THE CURVATURE OF THE INTERFACE IS DESCRIBED BY STRAIGHT LINES JOINING THE DESIGNATED POINTS. INTERFACE POINT COORDINATES SHOULD BE INPUT SEQUENTIALLY, BY MOVING ALONG THE INTERFACE AND AROUND THE CELL TO A STOPPING POINT SHORT OF THE POINT FIRST INPUT. THE FIRST TWO INTERFACE POINTS SHOULD BE SELECTED SO THAT THE LINE SEGEMENT CONNECTING THEM SHOULD NOT BE PERPENDICULAR TO ANY SILVER GRAINS IN THE VICINITY. GRAIN DISTANCES ARE COMPUTED WITH RESPECT TO THE WALL-LUMEN INTERFACE AND THE LOCAL THICKNESS OF THE WALL. THUS EACH GRAIN IS DESCRIBED IN TERMS OF ABSOLUTE DISTANCE FROM THE WALL-LUMEN INTERFACE AS WELL AS FRACTION-OF-LOCAL-WALL-THICKNESS DISPLACEMENT FROM THE INTERFACE. REFERENCE POINTS IN THE LUMEN ARE INPUT TO ALLOW ASSIGNMENT OF POSITIVE OR NEGATIVE VALUES TO THE GRAIN DISTANCES DEPENDING ON WHICH SIDE OF THE LUMEN INTERFACE THEY LIE (POSITIVE IF ON THE WALL SIDE). REFERENCE POINTS SHOULD BE CHOSEN FROM TWO LUMEN REGIONS-- NEAR THE LUMEN CENTER AND TOWARD ANY ACUTE ANGLE CELL CORNERS.

TWO POINTS DEFINING A LINE IN THE TANGENTIAL DIRECTION ARE INPUT TO ALLOW RADIAL AND TANGENTIAL WALL ASSIGNMENTS TO BE MADE. EACH GRAIN IS CLASSIFIED INTO ONE OF THREE TYPES--RADIAL WALL, TANGENTIAL WALL, OR WALL CORNER. THE DESIGNATION DEPENDS ON THE ANGLE OF THE LUMEN INTERFACE SEGMENT CLOSEST TO THE GRAIN AND THE ANGLE OF THIS SEGMENT RELATIVE TO THE SEGMENTS ON EITHER SIDE (INTERFACE CURVATURE).

FREQUENCY DISTRIBUTIONS OF GRAIN DISTANCES MAY BE COMPUTED FROM ANY NUMBER OF DATA SETS (WITHIN THE LIMITS OF THE DIMENSIONED ARRAYS AND, THEREFORE, THE STORAGE CAPACITY OF THE COMPUTER). DATA SETS FOR CUMULATIVE ANALYSIS MAY BE DERIVED EITHER FROM DIFFERENT MICROGRAPHS, E.G., DIFFERENT MICROTOME SECTIONS OF THE SAME CELL, OR FROM DIFFERENT PARTS OF THE SAME MICROGRAPH, E.G., DIFFERENT CELL AREAS OF THE SAME MICROTOME SECTION. DATA IS INPUT ON IBM CARDS IN THE FOLLOWING FORMAT AND SEQUENCE--

CARD NAME	COLUMNS	FORMAT	VAR. NAME	MEANING
OPTION CARD	1-2	I2	NDATA	OPTION FOR NUMBER OF DATA SETS TO READ AND FOR WHICH TO COMPUTE GRAIN DISTANCES BEFORE CALCULATING THE CUMULATIVE DISTRIBUTIONS.
	3-4	I2	NPTS	OPTION TO PLOT GRAIN DENSITY DISTRIBUTIONS FOR ALL WALL AREAS--CORNERS, RADIAL WALLS, TANGENTIAL WALLS--(NPTS=0) OR TO PLOT DISTRIBUTION ONLY FOR TOTAL WALL GRAINS (NPTS=NONZERO NUMBER).
ID CARD	1-16	4A4	ID1	IDENTIFICATION FOR DATA SET
DATA CARD	1-3	I3	N1	NO. OF LUMEN INTERFACE PTS.
	4-6	I3	N2	NO. OF MIDDLE LAMELLA PTS.
	7-9	I3	N3	NO. OF GRAIN PTS.
MAGNIF. CARD	1-5	F5.0	TEMMAG	MAGNIFICATION OF MICROGRAPH FROM WHICH DATA SET DERIVED
DATA CARD	1-10	2F5.0	XSL1,YSL2	1ST COORD PR. OF TANG. LINE
	11-20	2F5.0	XSL2,YSL2	2ND COORD PR. OF TANG. LINE
DATA CARD(S)	1-80	16F5.0	XW(),YW()	N1 PAIRS OF COORDINATES FOR LUMEN INTERFACE POINTS
DATA CARD(S)	1-80	16F5.0	XML(),YML()	N2 PAIRS OF COORDINATES FOR MIDDLE LAMELLA INTERFACE POINTS
DATA CARD	1-2	I2	NLUM	NO. OF LUMEN REFERENCE POINTS (MAXIMUM OF FIVE)
DATA CARD	1-80	16F5.0	XLUM(),YLUM()	PAIRS OF COORDINATES WHICH DEFINE LUMEN REFERENCE POINT
DATA CARD(S)	1-80	16F5.0	XG(),YG()	N3 PAIRS OF GRAIN COORDINATES

SUPPLEMENTARY INFORMATION

(1) THE TABLE SHOWN ABOVE IS CORRECT FOR THE CASE OF ONE DATA SET. IF MORE THAN ONE DATA SET IN INPUT, EACH SUCCEEDING SET (WITH THE SAME FORMAT AS IN THE TABLE BEGINNING WITH THE ID CARD) IS SIMPLY ADDED AFTER THE LAST DATA CARD OF THE PRECEDING SET.

(2) SALPETER'S HALF DISTANCE (HD), THE PREDICTED DISTANCE FROM A LINE SOURCE WITHIN WHICH HALF OF ALL GRAINS SHOULD LIE, IS CONSTANT FOR THE CONDITIONS USED BY THE AUTHOR (150 NM) AND THEREFORE IT IS NOT READ INTO THE PROGRAM BUT DEFINED NEAR ITS BEGINNING (HD=150.). THE HD VALUE IS USED IN THE PROGRAM FOR ESTABLISHING THE UNIT DISTANCE OF THE HISTOGRAM 'BIN' USED IN COMPUTING THE GRAIN DENSITY DISTRIBUTION ON AN ABSOLUTE DISTANCE SCALE. FWTSP2 IS THE ANALOG OF HD WHEN COMPUTING THE GRAIN DENSITY DISTRIBUTION ON THE FRACTIONAL WALL THICKNESS SCALE. IT IS DEFINED AT THE BEGINNING OF THE PROGRAM JUST AFTER HD.

(3) THE COMPUTED CELL WALL THICKNESS, AVGWT, IS AN AVERAGE OF THE WALL THICKNESSES CALCULATED FROM ALL WALL POSITIONS WHICH INCLUDE A SILVER GRAIN. THE VALUE OF AVGWT, THEREFORE, IS A WEIGHTED AVERAGE AND MAY BE BIASED TOWARD CERTAIN WALL AREAS IF THEY CONTAIN A DISPROPORTIONATE NUMBER OF GRAINS.

(4) THE VALUE OF THE ANGLE (ARAD) DIFFERENTIATING RADIAL FROM TANGENTIAL WALL SEGMENTS IS DEFINED AT THE BEGINNING OF THE PROGRAM. SIMILARLY, THE ANGLE DEFINING CORNER REGIONS (ALNR) IS STATED AT THE BEGINNING OF THE PROGRAM.

TABLE IV

LISTING OF EMARAN AND ITS SUBROUTINES

```
C*************************************************************************
C  PROGRAM EMARAN--MAINLINE FOR ANALYSIS OF EM AUTORADIOGRAPHY
C  TO BE USED WITH SUBROUTINES GRNDIS, PLTDAT, AND GRAF
      DIMENSION GDIST(1225),FWT(1225),XW(85),YW(85),XG(1225),YG(1225),
     * XML(85),YML(85),GRNARR(1225),FWTARR(1225),ID1(4),LDIST(7),LFWT(7)
     * ,XLUM(5),YLUM(5),ISEG(85),IDW(3),IDC(3),IDR(3),IDT(3),
     * CDIST(400),RDIST(800),TDIST(800),CFWT(400),RFWT(800),TFWT(800)
      COMMON LX(7),LY(7),ID(13),SVAL(4)
      WRITE (1,106)
      END FILE 1
      REWIND 1
      READ (1,105) LDIST,LFWT
      REWIND 1
      HD=150.
      FWTSP2=0.2
C  FWTSP2 = TWICE THE STEP LENGTH USED IN COMPUTING THE DISTRIBUTION DATA
C  IN SUBROUTINE PLTDAT FOR FRACTION-OF-WALL THICKNESS PLOT
      ID=2
      ACNR=0.380
      ARAD=0.500
      IEQL=0
      LTL=0
      IEQML=0
      LTML=0
C 'ID' IS USED TO DEFINE OUTPUT FORM, I.E., PRINTOUT, CARDS, TAPE, DISK.
C  ARAD IS THE ANGLE (IN RADIANS) RELATIVE TO THE TANGENTIAL LINE WHICH
C  AN INTERFACE SEGMENT MUST EXCEED IN ORDER TO BECOME 'RADIAL'
C  ACNR IS THE ANGLE (IN RADIANS) BETWEEN INTERFACE SEGMENTS ON EITHER
C  SIDE OF AN INCLUDED SEGMENT WHICH MUST BE EXCEEDED IN ORDER FOR THE
C  SEGMENT TO BECOME A 'CORNER'
C  IEQL AND IEQML DEFINE PLOTTING SYMBOLS FOR THE LUMEN AND MIDDLE LAMELLA
C  INTERFACES, RESPECTIVELY. (0=NO SYMBOLS, 4=SQUARES)
C  LTL AND LTML DEFINE THE LINE TYPE (0=LINE ONLY, 1=LINE AND SYMBOLS)
    1 READ (5,100) NDATA,NPTS
      NSET = 1
      CAVWT = 0.
      CACWT=0.
      CARWT=0.
      CATWT=0.
      WRITE (6,118) ACNR,ARAD
    2 READ (5,101) ID1
      WRITE (6,201) ID1
      READ (5,102) N1,N2,N3
      READ (5,103) TEMMAG
      READ (5,103) XSL1,YSL1,XSL2,YSL2
      READ (5,103) (XW(L),YW(L),L=1,N1)
      READ (5,103) (XML(J),YML(J),J=1,N2)
      READ (5,100) NLUM
      READ (5,103) (XLUM(IJK),YLUM(IJK),IJK=1,NLUM)
      READ (5,103) (XG(JJ),YG(JJ),JJ=1,N3)
C   LOOPS 79 AND 99 CHECK FOR AND CORRECT DUPLICATE INTERFACE POINTS
      N1L=N1-1
      DO 79 I=1,N1L
      IF (XW(I)-XW(I+1)) 79,71,79
   71 XW(I+1)=XW(I+1)+1.
      IF (YW(I)-YW(I+1)) 79,72,79
   72 XW(I+1)=XW(I+2)
      YW(I+1)=YW(I+2)
      N1=N1-1
   79 CONTINUE
      N2L=N2-1
      DO 99 J=1,N2L
      IF (XML(J)-XML(J+1)) 99,91,99
   91 XML(J+1)=XML(J+1)+1.
      IF (YML(J)-YML(J+1)) 99,92,99
   92 XML(J+1)=XML(J+2)
      YML(J+1)=YML(J+2)
      N2=N2-1
   99 CONTINUE
      FACTOR = 1000C./(1.2*3.937*TEMMAG)
      NSEG=N1-1
   29 CUMWT=0.
      CUMCWT=0.
      CUMRWT=0.
      CUMTWT=0.
      NC=0
      NR=0
      NT=0
      WRITE (6,108)
      WRITE (6,109)
      ANGTAN=ABS(ATAN((YSL2-YSL1)/(XSL2-XSL1)))
C  LOOP 30 ASSIGNS EACH LUMEN INTERFACE SEGMENT A DESIGNATION (C,R,T)
C  1ST AND LAST SEGMENTS ARE NOT IN CORNER (C) AREAS
      DO 30 I=1,NSEG
   55 X2D=XW(I+1)-XW(I)
      Y2D=YW(I+1)-YW(I)
      IF (X2D) 32,56,32
   32 IF (Y2D) 33,57,33
   56 XW(I)=XW(I)+1.
      GO TO 55
   57 YW(I)=YW(I)+1.
      GO TO 55
   33 IF (I-1) 35,35,34
   34 IF (I-NSEG) 36,35,35
   35 T2=Y2D/X2D
      ANGT2=ATAN(T2)
      AVASEG=ABS(ANGT2-ANGTAN)
      IF (AVASEG-ARAD) 54,54,53
   36 X1D =  XW(I)-XW(I-1)
      Y1D =  YW(I)-YW(I-1)
      X3D =  XW(I+2)-XW(I+1)
      Y3D =  YW(I+2)-YW(I+1)
      T1=Y1D/X1D
      T3=Y3D/X3D
      IF (T1) 61,64,62
   61 IF (T3) 64,64,63
   62 IF (T3) 63,64,64
   63 CHSLP=ABS(ATAN(T1)+ATAN(T3))
      GO TO 65
   64 CHSLP=ABS(ATAN(T1)-ATAN(T3))
   65 IF (CHSLP-ACNR) 35,35,52
   52 ISEG(I)=1
C  SEGMENT DESIGNATED A CORNER (C) SEGMENT
      GO TO 59
   53 ISEG(I)=2
C  SEGMENT DESIGNATED A RADIAL WALL (R) SEGMENT
      GO TO 59
   54 ISEG(I)=3
C  SEGMENT DESIGNATED A TANGENTIAL WALL (T) SEGMENT
```

TABLE IV (Continued)

LISTING OF EMARAN AND ITS SUBROUTINES

```
   59  WRITE (6,300) I,CHSLP,AVASEG,ISEG(I)
   30  CONTINUE
       WRITE (6,107)
       DO 10 K=1,N3
       GX = XG(K)
       GY = YG(K)
       CALL GRNDIS (XW,YW,N1,GX,GY,XPP,YPP,DISTL,XLUM,YLUM,NLUM,N1S)
       CALL GRNDIS (XML,YML,N2,GX,GY,XPP2,YPP2,DISTML,XLUM,YLUM,NLUM,NS)
       WALLT1=(SQRT(ABS((XPP-XPP2)**2+(YPP-YPP2)**2)))*FACTOR
       GDIST(K)=DISTL*FACTOR
       WALLT2 = ABS(DISTL-DISTML)*FACTOR
       DIFFWT = ABS(WALLT1-WALLT2)
       IF (DIFFWT-10) 4,3,3
    3  WRITE (6,104) K,GX,GY,XPP,YPP,XPP2,YPP2,WALLT1,WALLT2,DIFFWT
    4  FWT(K)  = GDIST(K)/WALLT1
       CUMWT = CUMWT + WALLT1
C GRAIN ASSIGNED 'C','R', OR 'T' BY VALUE OF ISEG(N1S)
       IF (ISEG(N1S)-2) 38,39,40
   38  NC=NC+1
       WRITE (3,202) XG(K),YG(K)
       CDIST(NC)=GDIST(K)
       CFWT(NC)=FWT(K)
       CUMCWT=CUMCWT+WALLT1
       GO TO 10
   39  NR=NR+1
       WRITE (4,202) XG(K),YG(K)
       RDIST(NR)=GDIST(K)
       RFWT(NR)=FWT(K)
       CUMRWT=CUMRWT+WALLT1
       GO TO 10
   40  NT=NT+1
       WRITE (11,202) XG(K),YG(K)
       TDIST(NT)=GDIST(K)
       TFWT(NT)=FWT(K)
       CUMTWT=CUMTWT+WALLT1
   10  CONTINUE
       END FILE 3
       REWIND 3
       END FILE 4
       REWIND 4
       END FILE 11
       REWIND 11
       AVWT = CUMWT/(N3*1000)
       WRITE (6,210) NC,NR,NT,AVWT
       IF (NC) 42,42,41
   41  ACWT=CUMCWT/(NC*1000)
   42  IF (NR) 44,44,43
   43  ARWT=CUMRWT/(NR*1000)
   44  IF (NT) 46,46,45
   45  ATWT=CUMTWT/(NT*1000)
   46  CAVWT = CAVWT + AVWT
       CACWT=CACWT+ACWT
       CARWT=CARWT+ARWT
       CATWT=CATWT+ATWT
       WRITE (1,122) ID1,AVWT
       WRITE (1,110)
       END FILE 1
       REWIND 1
       READ (1,111) (ID(I),I=1,12)
       READ (1,113) LX,LY
       REWIND 1
       CALL GRAF  (XML,YML,1,1,N2,LTML,IECML)
       DO 80 I5=1,3
       IF (I5-2) 81,82,83
   81  IF (NC) 181,80,181
  181  WRITE (1,115) NC,ACWT
       READ (3,202) (XG(I),YG(I),I=1,NC)
       REWIND 3
       GO TO 88
   82  IF (NR) 182,80,182
  182  WRITE (1,116) NR,ARWT
       READ (4,202) (XG(I),YG(I),I=1,NR)
       REWIND 4
       GO TO 88
   83  IF (NT) 183,80,183
  183  WRITE (1,117) NT,ATWT
       READ (11,202) (XG(I),YG(I),I=1,NT)
       REWIND 11
   88  END FILE 1
       REWIND 1
       READ (1,111) (ID(I),I=1,12)
       REWIND 1
       IF (I5-2) 84,85,86
   84  CALL GRAF (XG,YG,-1,1,NC,-1,3)
       GO TO 80
   85  CALL GRAF (XG,YG,-1,1,NR,-1,1)
       GO TO 80
   86  CALL GRAF (XG,YG,-1,1,NT,-1,2)
   80  CONTINUE
       WRITE (1,112) ACNR,ARAD
       END FILE 1
       REWIND 1
       READ (1,111) (ID(I),I=1,12)
       REWIND 1
       CALL GRAF  (XW,YW,-1,1,N1,LTL,IECL)
       WRITE (1,119)
       END FILE 1
       REWIND 1
       READ (1,111) (ID(I),I=1,12)
       REWIND 1
       CALL GRAF  (XLUM,YLUM,-1,1,NLUM,-1,4)
       CALL PLOT (0.,3.7,3)
       CALL PLOT (0.,0.,3)
       IF (NSET -1) 5,5,6
    5  NCUM = 0
       NCCUM=0
       NRCUM=0
       NTCUM=0
    6  DO 20 IJ=1,N3
       NCUM = NCUM + 1
       GRNARR(NCUM) = GDIST(IJ)
       FWTARR(NCUM) = FWT (IJ)
   20  CONTINUE
       DO 50 I2=1,NC
       NCCUM=NCCUM+1
       WRITE(12,202) CDIST(I2),CFWT(I2)
   50  CONTINUE
       DO 60 I3=1,NR
       NRCUM=NRCUM+1
       WRITE(13,202) RDIST(I3),RFWT(I3)
```

TABLE IV (Continued)

LISTING OF EMARAN AND ITS SUBROUTINES

```
 60  CONTINUE
     DO 70 I4=1,NT
     NTCUM=NTCUM+1
     WRITE (14,202)TDIST(I4),TFWT(I4)
 70  CONTINUE
     IF (NDATA-NSET)7,7,89
 89  NSET=NSET+1
     GO TO 2
  7  END FILE 12
     REWIND 12
     END FILE 13
     REWIND 13
     END FILE 14
     REWIND 14
     AVWT = CAVWT/NSET
     ACWT = CACWT/NSET
     ARWT = CARWT/NSET
     ATWT = CATWT/NSET
     WRITE (1,120)
     END FILE 1
     REWIND 1
     READ (1,121) IDW,IDC,IDR,IDT
     REWIND 1
     KKK=0
     CALL PLTDAT(GRNARR,AVWT,NCUM,ID1,IDW,HD,LDIST,IO,KKK)
     IF (NPTS) 94,93,94
 93  READ(12,203) (GRNARR(IC),IC=1,NCCUM)
     REWIND 12
     CALL PLTDAT(GRNARR,ACWT,NCCUM,ID1,IDC,HD,LDIST,IO,KKK)
     READ(13,203) (GRNARR(IR),IR=1,NRCUM)
     REWIND 13
     CALL PLTDAT(GRNARR,ARWT,NRCUM,ID1,IDR,HD,LDIST,IO,KKK)
     READ (14,203)(GRNARR(IT),IT=1,NTCUM)
     REWIND 14
     CALL PLTDAT(GRNARR,ATWT,NTCUM,ID1,IDT,HD,LDIST,IO,KKK)
 94  KKK=1
     CALL PLTDAT(FWTARR,AVWT,NCUM,ID1,IDW,FWTSP2,LFWT,IO,KKK)
     IF (NPTS) 1,95,1
 95  READ(12,204) (FWTARR(IFC),IFC=1,NCCUM)
     REWIND 12
     CALL PLTDAT(FWTARR,ACWT,NCCUM,ID1,IDC,FWTSP2,LFWT,IO,KKK)
     READ(13,204) (FWTARR(IFR),IFR=1,NRCUM)
     REWIND 13
     CALL PLTDAT(FWTARR,ARWT,NRCUM,ID1,IDR,FWTSP2,LFWT,IO,KKK)
     READ (14,204)(FWTARR(IFT),IFT=1,NTCUM)
     REWIND 14
     CALL PLTDAT(FWTARR,ATWT,NTCUM,ID1,IDT,FWTSP2,LFWT,IO,KKK)
     GO TO 1
100  FORMAT (2I2)
101  FORMAT (4A4)
102  FORMAT (2I3,I4)
103  FORMAT (16F5.0)
104  FORMAT(1H ,I4,3(4X,F6.0,1X,F6.0),3(4X,F6.0))
105  FORMAT (2(7A4))
106  FORMAT('UM FROM LUMEN INTERFACE 23. RELATIVE WALL LOCATION  22')
107  FORMAT (1H1,'GRAIN      XG,YG       XPP,YPP(LUMEN)      XPP,YPP(ML
    *)     WALLT1    WALLT2    DIFFWT'/)
108 FORMAT(1HC,'SEGMENT CURVATURE  ABS(SEGMENT ANGLE)  ASSIGNMENT')
109 FORMAT(1H ,'NUMBER  (RADIANS)       (RADIANS)      (C=1,R=2,T=3)'/)
110  FORMAT ('X VALUE                  7Y VALUE                  7')
111  FORMAT (12A4)
112  FORMAT ('(ACNR=',F6.3,', ARAD=',F6.3,')')
113  FORMAT (2(6A4,I2))
115  FORMAT (I3,' CORNER GRAINS                    ACWT=',F6.3)
116  FORMAT (I3,' RADIAL WALL GRAINS               ARWT=',F6.3)
117  FORMAT (I3,' TANGENTIAL WALL GRAINS           ATWT=',F6.3)
118 FORMAT(1H1,'ACNR=',F6.3,', ARAD=',F6.3)
119  FORMAT ('LUMEN REFERENCE POINTS')
120  FORMAT(' UM WALL      UM CORNERS  UM R WALLS  UM T WALLS ')
121  FORMAT(4(3A4))
122  FORMAT (4A4,'                        AWT=',F6.3)
201 FORMAT(1H ,4A4)
202 FORMAT(2F20.8)
203 FORMAT(F20.8)
204 FORMAT(20X,F20.8)
210 FORMAT(1HO,'NC= ',I3,' NR= ',I3,' NT= ',I3,', AVWT=',F8.3/)
300 FORMAT(1H ,2X,I2,6X,F5.3,11X,F5.3,14X,I2)
    END
```

TABLE IV (Continued)

LISTING OF EMARAN AND ITS SUBROUTINES

```
**************************************************************************
      SUBROUTINE GRNDIS(XW,YW,NL,XG,YG,XPP,YPP,GDIST,XLUM,YLUM,NL,NS)
C     TO BE USED WITH MAINLINE PROGRAM EMARAN
C  THIS SUBROUTINE CALCULATES AND TRANSFERS TO MAINLINE PROGRAM
C       (1) DISTANCE FROM GRAIN TO WALL INTERFACE (GDIST)
C       (2) POINT ON INTERFACE PERPENDICULAR TO GRAIN (XPP,YPP)
C       (3) NO. OF INTERFACE SEGMENT CONTAINING XPP,YPP (NS)
      DIMENSION  XW(75),YW(75),XLUM(5),YLUM(5)
      L = 1
      M = 0
C THE FOLLOWING COMPUTES PAIRS OF DISTANCES FROM A PARTICULAR GRAIN TO
C WALL POINTS TO FIND THE FIRST (AND PERHAPS ONLY) MINIMUM DISTANCE.
C THIS DISTANCE IS SAVED AS DMIN.
    6 DIST1 = SQRT(ABS((XG   -XW(L))**2+(YG   -YW(L))**2))
      DIST2 = SQRT(ABS((XG   -XW(L+1))**2+(YG   -YW(L+1))**2))
      IF (DIST2 - DIST1) 7,8,8
    7 L = L + 1
      GO TO 6
    8 M = L
      DMIN = DIST1
      IF (L- N1)   9, 10, 10
C THE FOLLOWING COMPUTES DISTANCES FROM GRAIN TO WALL POINTS BEYOND THE
C FIRST MINIMUM COMPARING EACH TO DMIN.  ANY DISTANCE SMALLER BECOMES THE
C NEW DMIN.
    9 DIST3 = SQRT(ABS((XG   -XW(L+2))**2+(YG   -YW(L+2))**2))
      L = L + 1
      IF (DMIN-DIST3) 12,12,11
   11 M = L
      DMIN = DIST3
   12 IF (L- N1)  9,10,10
C THE FOLLOWING GEOMETRICALLY FINDS THE LINE SEGMENT BETWEEN WALL POINTS
C TO WHICH A PERPINDICULAR CAN BE DRAWN FROM THE GRAIN.  ALSO BY GEOMETRY
C THE POINT OF INTERSECTION OF THE TWO LINES IS FOUND (XPP,YPP).
   10 CLOSE1 = SQRT(ABS((XG   -XW(M-1))**2+(YG   -YW(M-1))**2))
      CLOSE2 = SQRT(ABS((XG   -XW(M))  **2+(YG   -YW(M))  **2))
      SEGDIS = SQRT(ABS((XW(M)-XW(M-1))**2+(YW(M)-YW(M-1))**2))
      COSINE =-(CLOSE1**2-CLOSE2**2-SEGDIS**2)/(2.*CLOSE2*SEGDIS)
      IF (COSINE) 13,14,15
   13 M = M+1
      GO TO 10
   14 XPP = XW(M)
      YPP = YW(M)
      GO TO 16
   15 COSIN2=-(CLOSE2**2-CLOSE1**2-SEGDIS**2)/(2.*CLOSE1*SEGDIS)
      IF (COSIN2) 116,114,115
  114 XPP = XW(M-1)
      YPP = YW(M-1)
      GO TO 16
  116 NBTWN = M-1
      XPP = XW (NBTWN)
      YPP = YW (NBTWN)
      GO TO 16
  115 XDIFF = XW(M) - XW(M-1)
      YDIFF = YW(M) - YW(M-1)
      IF (XDIFF) 16,17,18
   17 XPP = XW(M)
      YPP = YG
      GDIST     = ABS( XW(M) - XG)
      GO TO 81
   18 IF (YDIFF) 80,82,80
   82 YPP = YW (M)
      XPP = XG
      GDIST     = ABS (YW(M) - YG)
      GO TO 81
   80 SLS = YDIFF/XDIFF
      YPP = (YW(M)+(SLS**2)*YG   +SLS*(XG   -XW(M)))/(1.+SLS**2)
      XPP = SLS*(YG   -YPP) + XG
C THE FOLLOWING COMPUTES THE DISTANCE FROM THE GRAIN POINT TO THE PERPEN-
C DICULAR POINT.  THIS DISTANCE (GDIST) IS ASSIGNED TO BE NEGATIVE IF ON
C THE LUMEN SIDE OF THE INTERFACE.
   16 GDIST   = SQRT(ABS((XG   -XPP)**2+(YG   -YPP)**2))
   81 NS=M-1
      DO 20 I=1,NL
      REFD1 = SQRT(ABS((XPP-XLUM(I))**2+(YPP-YLUM(I))**2))
      REFD2 = SQRT(ABS((XG- XLUM(I))**2+(YG- YLUM(I))**2))
      IF (REFD1-REFD2) 19,19,20
   20 CONTINUE
      GDIST = -GDIST
   19 RETURN
      END
**************************************************************************
```

TABLE IV (Continued)

LISTING OF EMARAN AND ITS SUBROUTINES

```
************************************************************************
      SUBROUTINE PLTDAT(ARR,AVGWT,NCUM,IDPLCT,IC2,HD,LXS,IO,KKK)
C     TO BE USED WITH MAINLINE PROGRAM EMARAN
C THIS SUBROUTINE CALCULATES AND WRITES DATA FOR GRAIN DISTRIBUTION PLOT
      DIMENSION DMIDPT(75),ARR(1),GNO(75),IDPLCT(4),LXS(7),FGNO(75)
     *,BIN1(75),BIN2(75),ID2(3),X(150),Y(150)
      COMMON LX(7),LY(7),ID(13),SVAL(4)
      ID(13)=0
      STEPL = HD / 2.
      CALL SHELL (ARR,1,NCUM)
C  SHELL SUBROUTINE SORTS NUMBERS INTO ARRAY OF ASCENDING ORDER
      I3 = 1
      NSTEP=((   ARR(NCUM)-   ARR(1))/STEPL)+1
      IF (NSTEP - 100) 901,901,900
  901 DO 75 I1 = 1, NSTEP
      STEPN = I1
      DMIDPT (I1) =(ARR (1) + (STEPN * STEPL) - STEPL/2.)
      BIN1 (I1) = DMIDPT (I1) - STEPL/2.
      BIN2 (I1) = BIN1 (I1) + STEPL
      IF (KKK) 80,80,81
   80 DMIDPT (I1) = DMIDPT (I1)/1000.
      BIN1 (I1) = BIN1 (I1)/1000.
      BIN2 (I1) = BIN2 (I1)/1000.
   81 I2 = 0
      GO TO 76
   72 I3 = I3 + 1
      I2 = I2 + 1
      IF ((I3-(NCUM+1))76,73,74
   76 IF (   ARR(I3) - (   ARR(1) + STEPN * STEPL))   72,73,73
   73 GNO (I1)  = I2
      GO TO 75
   74 GNO(I1)= 0.
   75 CONTINUE
      GNOMAX=-999999999.
      DO 98 IL1 = 1, NSTEP
      GNOMAX = AMAX1(GNO(IL1),GNOMAX)
   98 CONTINUE
      IF (KKK) 1,1,2
    1 WRITE (IO,107)
      GO TO 3
    2 WRITE (IO,108) AVGWT
    3 WRITE (IO,100) IDPLOT,NCUM,AVGWT,ID2
      WRITE (1,100) IDPLOT,NCUM,AVGWT,ID2
      WRITE (IO,104)  LXS
      WRITE (1,104)  LXS
      WRITE (IO,105)
      WRITE (1,105)
      END FILE 1
      REWIND 1
      READ (1,104) (ID(I),I=1,12)
      READ (1,106)  LX
      READ (1,106)  LY
      REWIND 1
      WRITE (IO,101) NSTEP
      DO 500 IL3 = 1,NSTEP
      FGNO(IL3)=GNO(IL3)/GNOMAX
      WRITE (IO,102) DMIDPT(IL3),BIN1(IL3),BIN2(IL3),FGNO(IL3),FGNO
     * (IL3),IL3
      IDT1=IL3+(IL3-1)
      IDT2=IL3+IL3
      X(IDT1)=BIN1(IL3)
      X(IDT2)=BIN2(IL3)
      Y(IDT1)=FGNO(IL3)
      Y(IDT2)=FGNO(IL3)
  500 CONTINUE
      N2STEP=2*NSTEP
      CALL GRAF  (X,Y,1,1,N2STEP,0,0)
      CALL PLOT(0.,3.7,3)
      CALL PLOT(0.,C.,3)
      GO TO 1000
  900 WRITE (6,103) NSET
 1000 WRITE (6,110) AVGWT,ID2,KKK
      RETURN
  100 FORMAT(4A4,I4,' GRAINS IN',F6.3,3A4)
  101 FORMAT (I3)
  102 FORMAT(5(2X,F8.3),27X,I3)
  103 FORMAT (1H0,'MORE THAN 100 BINS IN DATA SET ',I3)
  104 FORMAT (12A4)
  105 FORMAT('GRAIN FREQUENCY          15')
  106 FORMAT (6A4,I2)
  107 FORMAT (' 1.0')
  108 FORMAT (F6.3)
  109 FORMAT (5(2X,F8.3))
  110 FORMAT (1H0,' HISTOGRAPH DATA FROM ',F6.3,3A4,' NOW ON TAPE (KKK=
     *',I2,')')
      END
      SUBROUTINE SHELL(LIST,ISTRT,L)
      DIMENSION LIST(1)
      REAL LIST,B
      M = L - ISTRT + 1
  200 M = M/2
      IF (M) 300,40,300
  300 K = L-M
      J = ISTRT
   41 I = J
   49 LL = I+M
      IF(LIST(I) - LIST(LL)) 60,60,50
   50 B = LIST(I)
      LIST(I) = LIST(LL)
      LIST(LL) = B
      I = I-M
      IF (I - ISTRT) 60,49,49
   60 J = J+1
      IF (J-K) 41,41,200
   40 RETURN
      END
************************************************************************
```

TABLE IV (Continued)

LISTING OF EMARAN AND ITS SUBROUTINES

```
************************************************************************
      SUBROUTINE GRAF (X,Y,NX,NY,N,LT,IEQ)
C       TO BE USED WITH MAINLINE PROGRAMS EMARAN AND CRVFIT
C  THIS SUBROUTINE SCALES, DRAWS AND LABELS AXES, AND PLOTS AN ARRAY OF
C  POINTS (X(N),Y(N)).  NX=NY=1 IF ARRAY IS FIRST TO BE PLOTTED ON THE
C  SCALED GRAPH.  IF SUBSEQUENT ARRAYS ARE TO BE PLOTTED ON THE SAME
C  GRAPH, LET NX=-1.  LT DEFINES THE LINE TYPE (-1=SYMBOLS ONLY, 0=LINE,
C  +1=LINE AND SYMBOLS).  IEQ DEFINES THE SYMBOL TYPE (1=.,2=I,3=X,4=O).
      DIMENSION X(1),Y(1)
      COMMON LX(7),LY(7),ID(13),SVAL(4)
      INTEGER CHAR(4)
      CHAR (1)= 109
      CHAR (2)= 184
      CHAR (3)= 170
      CHAR (4)= 175
      IF(ID(13))100,1,2
    1 CALL ITLZ
      CALL DPT(1,4)
      CALL PLOT(0.0,-11.0,-3)
      CALL PLOT(0.0,1.5,-3)
    2 IF(NX)4,100,3
    3 ID(13)=1
      CALL PLOT(7.75,-1.5,3)
      CALL PLOT(7.75,9.0,2)
      CALL PLOT(8.5,0.0,-3)
      CALL SCALE(X,7.0,N,1)
      CALL AXIS(0.0,0.0,LX,-LX(7),7.0,0.0,X(N+1),X(N+2))
      CALL SCALE(Y,7.0,N,1)
      CALL AXIS(0.0,0.0,LY,LY(7),7.0,90.0,Y(N+1),Y(N+2))
      SVAL(1)=X(N+1)
      SVAL(2)=X(N+2)
      SVAL(3)=Y(N+1)
      SVAL(4)=Y(N+2)
    4 YPAGE=9.5-(ID(13)*0.35)
      IF(LT)5,9,5
    5 IF (IEQ-1) 6,6,7
    6 HTS=0.18
      GO TO 8
    7 HTS=0.35
    8 CALL DRAW(0.5,YPAGE+0.08,0.0,CHAR(IEQ),1.0,0.0,HTS)
    9 CALL SYMBOL(1.0,YPAGE,0.14,ID,0.0,48)
      ID(13)=ID(13)+1
      X(N+1)=SVAL(1)
      X(N+2)=SVAL(2)
      Y(N+1)=SVAL(3)
      Y(N+2)=SVAL(4)
      NMIN=N+1
      ND=NMIN+1
      XMIN=X(NMIN)
      DX=X(ND)
      YMIN=Y(NMIN)
      DY=Y(ND)
      II = LT
      KK = LT
      IPEN = 4
      J = 1
      DO 20 I=1,N
      XX = (X(J)-XMIN)/DX
      YY = (Y(J)-YMIN)/DY
      IF(KK)13,11,11
   11 CALL PLOT(XX,YY,IPEN)
      IPEN = 2
      IF(KK) 17,17,12
   12 IF(NI-KK) 17,13,13
   13 IF (IEQ-1) 14,14,15
   14 HT = 0.07
      GO TO 16
   15 HT = 0.14
   16 CALL DRAW (XX,YY,0.0,CHAR(IEQ),1.0,0.0,HT)
      NI = 0
      CALL PLOT (XX,YY,3)
   17 J = J + 1
      NI = NI + 1
   20 CONTINUE
      CALL PLOT (XX,YY,3)
  100 RETURN
      END
************************************************************************

/END CARD READ, JOB TERMINATED
```

TABLE V

USER INSTRUCTIONS FOR CRVFIT

****

PROGRAM CRVFIT--FOR FITTING A CURVE TO OUTPUT FROM PROGRAM EMARAN

DIRECTIONS FOR USE

THIS PROGRAM ALLOWS THE OPERATOR TO JUDGE, BY TRIAL AND ERROR, THE BEST SET OF PARAMETERS FROM WHICH ONE CAN APPROXIMATE THE LOCATION AND RELATIVE ACTIVITY OF LABELED COMPONENTS IN THE CELL WALL. INITIAL VALUES FOR THE BAND SOURCE PARAMETERS (NBAND, XDSPL, BNDW, AMPL) ARE ESTIMATED BY A VISUAL FITTING OF THE GRAPHICAL OUTPUT FROM PROGRAM EMARAN TO REFERENCE CURVES REPRESENTING THE GRAIN DENSITY DISTRIBUTIONS TO BE EXPECTED FROM BANDS OF DEFINED WIDTH. THE LINE SOURCE GRAIN FREQUENCY FUNCTION OBTAINED BY SALPETER ET AL. (J. CELL BIOLOGY, VOL.41, PAGES 1-20 (1969)) IS THE BASIS FOR THE DEVELOPMENT OF THE COMPUTATIONS. EACH BAND SOURCE IS DEFINED BY THE FOLLOWING PARAMETERS-- (1) DISTANCE OF BAND MIDPOINT FROM WALL-LUMEN INTERFACE IN MICROMETERS, (2) BAND WIDTH IN MICROMETERS AND (3) RELATIVE BAND ACTIVITY.

THE PROGRAM PLOTS A GRAIN FREQUENCY HISTOGRAPH FROM A SET OF HISTOGRAPH DATA OUTPUT FROM PROGRAM EMARAN. THEN IT COMPUTES AND PLOTS THE PREDICTED FREQUENCY DISTRIBUTION FROM UNIFORMLY LABELED BAND SOURCES OF ACTIVITY (MAXIMUM OF THREE). A MEASURE OF THE DEGREE OF DEVIATION OF THE HISTOGRAPH DATA POINTS FROM THE PREDICTED DISTRIBUTION CURVE (DEFINED HERE AS 'VARIANCE') IS COMPUTED FROM THE FOLLOWING RELATION --

$$\text{VARIANCE} = \frac{\text{SUM OF SQUARES OF DIFFERENCES (BETWEEN GRAIN DENSITY VALUES)}}{\text{(NUMBER OF DATA POINTS)} - 1}$$

DATA IS INPUT IN THE FOLLOWING FORMAT AND SEQUENCE --

DATA	COLUMNS	FORMAT	NAME	MEANING
DATA CARD	1-6	F6.3	AVWT	AVERAGE WALL THICKNESS IN MICRONS. (1.0 IF DATA SET IS ON 'UM FROM LUMEN INTERFACE' SCALE)
ID CARD	1-48	12A4	ID()	IDENTIFICATION OF HISTOGRAPH DATA SET (ALL 48 CHAR DRAWN)
LABEL CARD	1-24	6A4	LX(1-6)	LABEL FOR X AXIS
	25-26	I2	LX(7)	NO. OF CHARACTERS IN LX DRAWN
LABEL CARD	1-24	6A4	LY(1-6)	LABEL FOR Y AXIS
	25-26	I2	LY(7)	NO. OF CHARACTERS IN LY DRAWN
DATA CARD	1-3	I3	N	NO. HISTOGRAPH POINTS TO READ
DATA CARD(S)	1-10	2X,F8.3	XMIDPT()	LOCATION OF BIN CENTER
	11-20	2X,F8.3	XDAT()	LEFT BOUNDARY OF BIN
	21-30	2X,F8.3	XDAT()	RIGHT BOUNDARY OF BIN
	31-40	2X,F8.3	YDAT()	GRAIN DENSITY IN BIN
	41-50	2X,F8.3	YDAT()	GRAIN DENSITY IN BIN
TERMINAL INPUT	1-2	I2	KAHEAD	OPTION TO SKIP THIS DATA SET
TERMINAL INPUT	1-2	I2	NBAND	NUMBER OF BAND SOURCES
TERMINAL INPUT(S) (INPUT ONCE FOR EACH BAND)	1-5	F5.0	XDSPL	DISPLACEMENT OF BAND CENTER FROM WALL-LUMEN INTERFACE IN MICROMETERS
	6-10	F5.0	BNDW	BAND WIDTH IN MICROMETERS
	11-15	F5.0	AMPL	RELATIVE BAND ACTIVITY PARAMETER (APPROX. RANGE-- 0-2)
TERMINAL INPUT	1-5	F5.0	AMPLF	CUMULATIVE AMPLITUDE FACTOR
TERMINAL INPUT	1-2	I2	N5	OPTION TO TERMINATE PROGRAM (N5≠0) OR TO REPEAT WITH NEW INPUT FROM TERMINAL (N5 0)

THE PROGRAM HAS THE OPTION OF READING IN DIFFERENT BAND SOURCE INFORMATION (NUMBER, WIDTH, AND LOCATION) FROM THE TERMINAL. THIS INPUT MAY BE REPEATED (IN THE ORDER SHOWN IN THE ABOVE TABLE) ANY NUMBER OF TIMES BEFORE TERMINATING THE JOB. THE DECISION WOULD BE BASED ON THE GRAPHICAL OUTPUT (VISUAL CLOSENESS OF FIT) AND THE COMPUTED VARIANCE VALUE.

****

TABLE VI

LISTING OF CRVFIT

```
*************************************************************************
/JOB GO,TIME=30
/FILE DISK=(1,NREC=9C,IDENT),RSIZ=48,VOL=SYSFL1,DISP=(NEW,DELETE)
/FILE DISK=(2,NREC=9C,LABEL),RSIZ=48,VOL=SYSFL1,DISP=(NEW,DELETE)
/FILE DISK=(3,NREC=9C,LABEL3),RSIZ=48,VOL=SYSFL1,DISP=(NEW,DELETE)
/FILE DISK=(4,JL23A),VOL=SYSFL1,DISP=(OLD,KEEP)
C  PROGRAM CRVFIT
C  TO BE USED WITH SUBROUTINE GRAF (SAME ONE USED WITH PROGRAM EMARAN).
C  DISK FILE 4 IS USED ONLY IF THIS FILE CONTAINS THE DATA TO BE INPUT.
C  THE VARIABLE, IO, IS USED TO SPECIFY THE SOURCE OF THE DATA (DISK,
C  TAPE, CARDS, ETC.).
      DIMENSION XDAT(150),YDAT(150),X(205),Y(205),XMIDPT(75),
     9 Y1(205),Y2(205),Y3(205),XS(25),YS(25),WTFCTR(3),LACF(12)
     *,LYY(7)
      COMMON LX(7),LY(7),ID(13),SVAL(4)
      ID(13)=0
      IO=4
   41 READ(IO,109) AVWT
C  AVWT = 1.0 IF HISTOGRAPH DATA IS ON ABSOLUTE DISTANCE SCALE
C  AVWT = AVG. WALL THICKNESS IF DATA SET IS OF 'RELATIVE WALL LOCATION'
      READ(IO,100) (ID(I1),I1=1,12)
      WRITE (1,100) (ID(I1),I1=1,12)
      END FILE 1
      REWIND 1
      READ(IO,101) LX,LYY
      READ(IO,110) N
      NX2=N*2
      DO 19 I=1,N
      IDT1=I+(I-1)
      IDT2=I+I
      READ(IO,103)XMIDPT(I),XDAT(IDT1),XDAT(IDT2),YDAT(IDT1),YDAT(IDT2)
   19 CONTINUE
   90 WRITE (6,100) (ID(I1),I1=1,12)
      WRITE (6,204)
  204 FORMAT ('NEXT INPUT IS KAHEAD. IF GREATER THAN 0,SKIPS THIS DATA
     9 SET AND READS NEXT SET')
      READ (9,102) KAHEAD
      IF (KAHEAD) 42,42,41
   42 STEPL=(XMIDPT(N)*AVWT-XMIDPT(1)*AVWT)/200.
      DO 60 J=1,200
      X(J)=0.
      Y(J)=0.
      Y1(J)=0.
      Y2(J)=0.
      Y3(J)=0.
   60 CONTINUE
      M2=1
      WRITE (6,200)
  200 FORMAT ('NEXT INPUT IS NBANDS')
      READ (9,102) NBANDS
      YMAX=0.
      TOTWT=0.
      DO 50 K=1,NBANDS
      WRITE (6,201) K
  201 FORMAT ('NEXT INPUT IS PARAMETERS FOR BAND ',I2)
      READ (9,104) XDSPL,BNDW,FRACT
      WTFCTR(K)=FRACT
      TOTWT=TOTWT+WTFCTR(K)
      IF (K-2) 92,92,93
   92 IFILE=2
      IFORMT=100
      GO TO 94
   93 IFILE=3
      IFORMT=107
   94 WRITE (IFILE,106) XDSPL,BNDW,FRACT
      BNDSTP=BNDW/99.
      XLINE=XDSPL-(BNDW/2.)
C  LOOPS 30 AND 40 CREATE A BAND SOURCE DISTRIBUTION FROM 100 LINE SOURCES
C  EQUALLY SPACED WITHIN THE BAND
      DO 40 J1=1,100
      DO 30 J2=1,200
      IF (J2-1) 31,31,32
   31 X(J2)=XMIDPT(1)*AVWT
      GO TO 33
   32 X(J2)=X(J2-1)+STEPL
   33 XMICRN=(X(J2)-XLINE)/0.15
      XPWR=XMICRN**2
      YO=1/(1+XPWR)
      Y(J2)=Y(J2)+YO
   30 CONTINUE
      XLINE=XLINE+BNDSTP
   40 CONTINUE
C LOOPS 70 & 80 CREATE ARRAYS (XS,YS) WHICH DESCRIBE THE BAND POSITIONS
      DO 70 N2=1,3
      XS(M2)=(XDSPL-BNDW/2.)/AVWT
      IF (N2-2) 71,72,73
   71 YS(M2)=0.
      GO TO 74
   72 YS(M2)=0.05
      GO TO 74
   73 YS(M2)=0.025
   74 M2=M2+1
   70 CONTINUE
      DO 80 N3=1,3
      XS(M2)=(XDSPL+BNDW/2.)/AVWT
      IF (N3-2) 81,82,83
   81 YS(M2)=0.025
      GO TO 84
   82 YS(M2)=0.05
      GO TO 84
   83 YS(M2)=0.
   84 M2=M2+1
   80 CONTINUE
C LOOP 20 CREATES A DISTRIBUTION ARRAY FOR EACH BAND (Y1(),ETC.) AND THE
C CUMULATIVE DISTRIBUTION ARRAY (Y1()+Y2()+Y3()).
      DO 20 K1=1,200
      X(K1)=X(K1)/AVWT
      IF (K-2) 21,22,23
   21 Y1(K1)= Y(K1)*FRACT
      Y(K1)=0.
      GO TO 25
   22 Y2(K1)= Y(K1)*FRACT
      Y(K1)=0.
      GO TO 25
   23 Y3(K1)= Y(K1)*FRACT
      Y(K1)=0.
   25 IF (K-NBANDS) 20,26,20
   26 Y(K1)= Y1(K1)+Y2(K1)+Y3(K1)
      YMAX=AMAX1(Y(K1),YMAX)
```

TABLE VI (Continued)

LISTING OF CRVFIT

```
   20  CONTINUE
   50  CONTINUE
       WRITE (6,203)
  203  FORMAT ('NEXT INPUT IS CUMULATIVE AMPLITUCE FACTOR')
       READ (9,104) AMPLF
       DO 55 K2=1,200
       Y(K2)=(Y(K2)/YMAX)*AMPLF
   55  CONTINUE
       REWIND 1
       READ(01,100) (ID(I1),I1=1,12)
       REWIND 1
       CALL GRAF  (XDAT,YDAT,1,1,NX2,0,0)
       END FILE 2
       REWIND 2
       IF (NBANDS-1) 96,96,97
   96  READ (2,100) (ID(I1),I1=1,12)
       GO TO 98
   97  READ (2,107) (ID(I1),I1=1,12)
   98  REWIND 2
       CALL GRAF  (X,Y,-1,1,200,0,0)
       SSQYD=0.
C  LOOP 10 COMPUTES THE SUM OF SQUARES OF THE Y DISPLACEMENT OF THE DATA
C  POINTS FROM THE FITTED CURVE
       DO 10 II=1,N
       IF(II-1) 2,2,1
    1  IF(II-N) 3,2,2
    2  YCURV=Y(II)
       GO TO 8
    3  KK=2
    4  IF (XMIDPT(II)-X(KK)) 6,7,5
    5  KK=KK+1
       GO TO 4
    6  XDELTA=XMIDPT(II)-X(KK)
       XDIFF=X(KK)-X(KK-1)
       YDIFF=Y(KK)-Y(KK-1)
       YCURV=Y(KK-1)+YDIFF*(XDELTA/XDIFF)
       GO TO 8
    7  YCURV=Y(KK-1)
    8  II2=II*2
       SQYDIF=(YDAT(II2)-YCURV)**2
       SSQYD=SSQYD+SQYDIF
   10  CONTINUE
       VAR=SSQYD/(N-1)
       WRITE (3,105) VAR
       END FILE 3
       REWIND 3
       IF (IFORMT-100) 11,11,12
   11  READ (3,100) (ID(I1),I1=1,12)
       GO TO 13
   12  READ (3,107)  (ID(I1),I1=1,12)
   13  REWIND 3
       M2=M2-1
       CALL GRAF  (XS,YS,-1,1,M2,0,0)
C LOOP 65 COMPUTES AND WRITES (ON GRAPH) THE PERCENT ACTIVITY IN EACH BAND
       YPAGE=8.45
       DO 65 K3=1,NBANDS
       WTFCTR(K3)=(WTFCTR(K3)/TOTWT)*100.
       WRITE (3,108) WTFCTR(K3),K3
       END FILE 3
       REWIND 3
       READ (3,100) LACT
       CALL INIT (LACT,6,6,108)
       REWIND 3
       YPAGE=YPAGE-0.35
       CALL SYMBOL (1.0,YPAGE,0.14,LACT,0.0,28)
   65  CONTINUE
       WRITE (6,202)
  202  FORMAT ('NEXT INPUT IS N5. IF GREATER THAN ZERO, RECYCLES')
       READ (9,102) N5
       IF (N5) 91,91,90
   91  CALL FINAL
       CALL EXIT
  100  FORMAT (12A4)
  101  FORMAT (6A4,I2)
  102  FORMAT (I2)
  103  FORMAT (5(2X,F8.3))
  104  FORMAT (3F5.0)
  105  FORMAT ('VARIANCE =',3PE10.0)
  106  FORMAT ('(',F6.3,',',F6.3,',',F6.3,')')
  107  FORMAT (6A4)
  108  FORMAT (F5.1,'  OF ACTIVITY IN BAND',I2)
  109  FORMAT(F6.3)
  110  FORMAT(I3)
       END
```

APPENDIX VIII

GRAIN DENSITY DISTRIBUTION FUNCTIONS

Model distributions of grain density used for comparison with the actual distributions in fiber cell walls were derived from the line-source distribution function of Salpeter, et al. (66), $f = 1/(1 + x^2/d^2)$. As introduced in the "Approach of the Thesis" section, the variables in this equation are defined as follows: f = grain density, x = distance from line source, and d = HD (Salpeter's measure of autoradiographic resolution). The d variable was considered as a constant for this analysis, since HD is a function of autoradiographic variables (isotope type, section and emulsion thickness, emulsion type, and development procedure) which were constant. According to the work of Salpeter, et al. (66), an HD value of 0.15 is correct for the conditions of this work.

Distributions describing predicted grain densities relative to solidly-labeled band sources were computed by considering a band source to be composed of line sources uniformly spaced across the width of the band. As applied in the computer program CRVFIT (see Appendix VII), these distributions were obtained by summing grain density (f) values for each line source within the band (computed from the line-source distribution function) over a defined range of distance from the source (x) and then normalizing the cumulative distribution so that the maximum grain density was unity. By varying the number of line sources per band, it was found that increasing the number of lines per band beyond 100 did not change the shape of the cumulative distribution curve even for bands as wide as 0.8 μm. Each model band source was, therefore, defined as being composed of 100 equally spaced line sources.

The model distributions for a line source and two band sources of different widths are presented in Fig. 21. In each of these plots two different distributions are drawn — the lower curve in each plot based on the theoretically derived line-source distribution function, $\underline{f} = 1/(1 + \underline{x}^2/\underline{d}^2)$, and the upper curve based on another distribution function, $\underline{f} = [0.982/(1 + \underline{x}^2/\underline{d}^2)] + [0.45/(25 + \underline{x}^2/\underline{d}^2)]$. The latter function is an empirical relation developed by Salpeter, et al. (66) to better describe grain density distributions obtained experimentally from artificial line sources. Since Gupta, et al. (67) found that experimental distributions from his biological line sources were better described by the theoretically derived function, this theoretically derived function was used in the CRVFIT computer program to generate model band-source distributions.

The concept of single band-source distribution models as shown in Fig. 21(b) and (c) was extended in the CRVFIT program to model distributions composed of as many as three distinct band sources in order to better describe the actual distributions across fiber cell walls. Three parameters (band location, width, and relative activity) that describe each band source could be varied independently for each band to affect the total cumulative distribution. Graphical outputs from the CRVFIT program are included in Appendix IX.

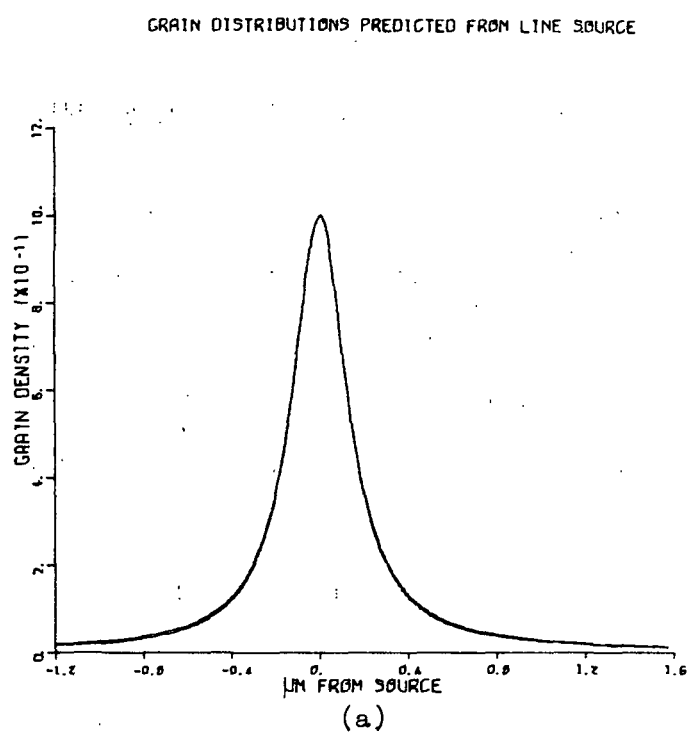

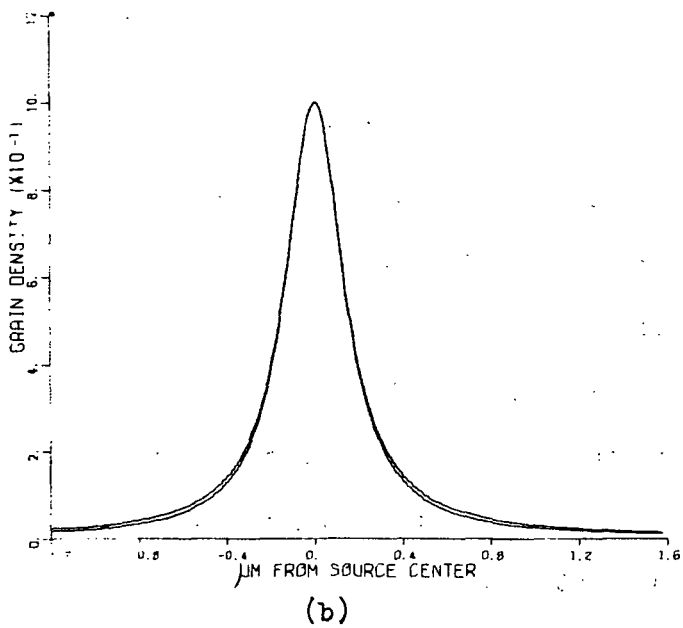

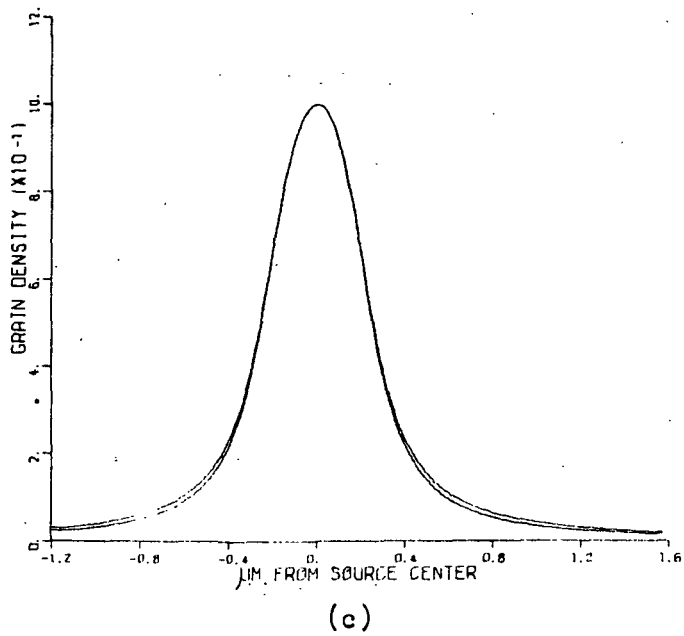

Figure 21. Line and Band Source Grain Density Distributions

APPENDIX IX

EXPERIMENTAL GRAIN DENSITY DISTRIBUTIONS

This appendix contains the graphical output of the CRVFIT program. Each graph presented is a reproduction of the plotter output for the grain density distribution of an individual fiber cell. The first line of the heading above each graph identifies — in abbreviated form — the fiber cell and electron micrograph(s) as well as the number of grains counted and the computed average wall thickness associated with that particular graph. For example, a first line of the heading of one of the graphs in Fig. 22 reads, "A3B(41-2,41-4) 574 GRAINS IN 1.243 μM WALL." This line identifies the graph with fiber cell "B" of tissue fed sugar A with a 3-hour incubation period. A total of 574 grains were counted from the two micrographs (41-2 and 41-4) of sections of this cell. Also, the average wall thickness of this cell as computed by program EMARAN is 1.243 μm.

The histogram plot in each graph is the actual grain density distribution while the smooth curve is the model distribution fitted to the actual distribution and defined by the band parameters listed in the heading above the graph. The model band sources are assigned numbers from one to three according to their relative positions in the wall. The band closest to the wall/lumen interface is designated Band 1, the next closest is designated Band 2, etc. Each band position (location and width) is indicated on the abscissa of each graph and identified by number. The band parameters for Band 1 are located on the second line of the graph heading. The parameters defining Band 2, if there is one, are located on the second line just after the parameters for Band 1. Finally, the parameters for Band 3, when present, are located at the beginning of the third line of the heading. Each set of band parameters

includes three values listed within brackets in the following order: distance (in μm) of the band midpoint from the wall/lumen interface, band width (in μm), and fractional content of the total wall activity.

The "variance" value as listed on the third line of the heading is a numerical measure of the degree of fit of the model distribution to the actual distribution (variance is defined mathematically in Appendix VII). In fitting the model to the actual distribution small variance values are desirable. A perfect fit, therefore, would have a variance of zero. Because of the nature of the autoradiographic system, however, a realistic fit for a particular distribution may not necessarily have the smallest variance value. Gupta, et al. (67) found, for example, that when a very narrow band (approximating a line) of labeled wall material lies close to the inner face of the wall, an asymmetrical distribution results in the autoradiograph. This asymmetry (skewed away from the wall) is attributed to a decrease in the average path length of β-particles traversing the relatively dense wall material (67). A visual fitting of the model to the actual distribution in the region from the wall/lumen interface to the middle lamella (0 to 1 on the relative-wall-location scale) supplements the numerical variance value in judging a "best fit." Model distributions which depart from actual distributions in the region of the cell lumen, such as for cell A in Fig. 22, might, therefore, actually be the most realistic fits.

The grain density distributions of cells from tissue fed sugar A are shown in Fig. 22-25. These include cells from tissue incubated 3 hours (Fig. 22), 24 hours (Fig. 23), and 48 hours (Fig. 24 and 25).

A3A(41-2,41-4) 367 GRAINS IN 0.657 UM WALL
(0.050, 0.100, 1.000)
VARIANCE = 953.E-05
100.0% OF ACTIVITY IN BAND 1

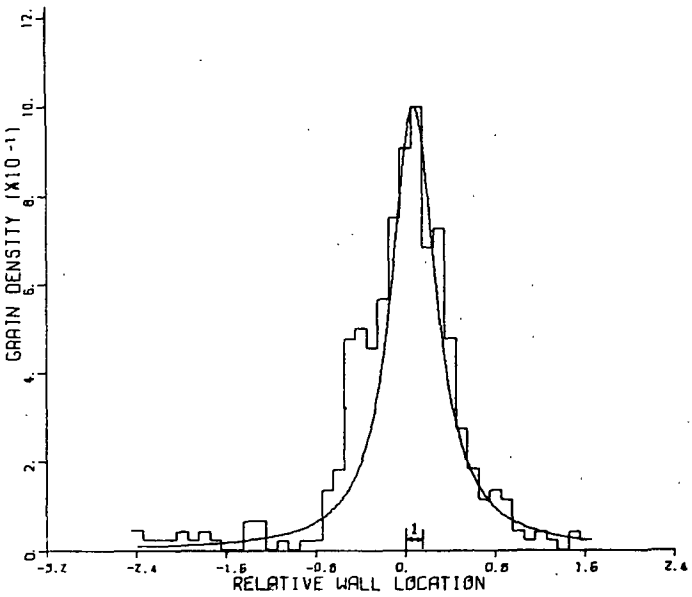

A3B(41-2,41-4) 574 GRAINS IN 1.243 UM WALL
(0.050, 0.100, 0.920) (1.400, 0.100, 0.080)
VARIANCE = 111.E-04
92.0% OF ACTIVITY IN BAND 1
8.0% OF ACTIVITY IN BAND 2

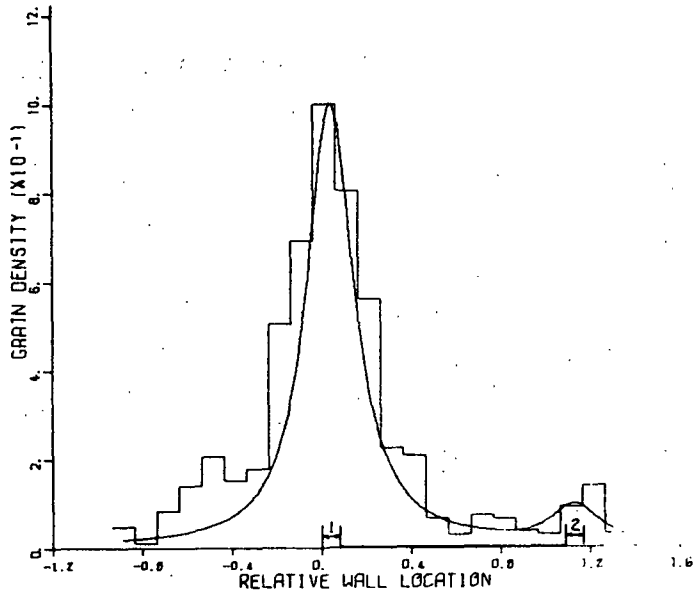

A3C(41-3,41-5) 558 GRAINS IN 1.199 UM WALL
(0.075, 0.150, 0.920) (1.250, 0.100, 0.080)
VARIANCE = 524.E-05
92.0% OF ACTIVITY IN BAND 1
8.0% OF ACTIVITY IN BAND 2

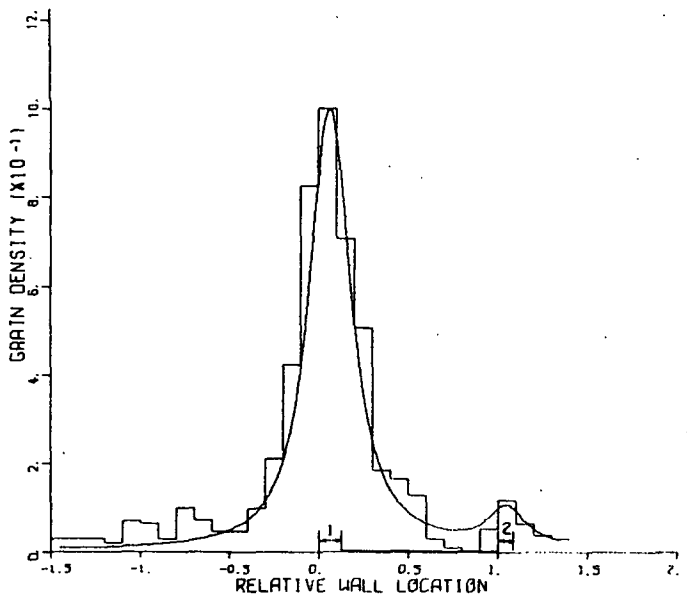

A3-D (41-1) 428 GRAINS IN 0.771 UM WALL
(0.050, 0.100, 1.000)
VARIANCE = 454.E-05
100.0% OF ACTIVITY IN BAND 1

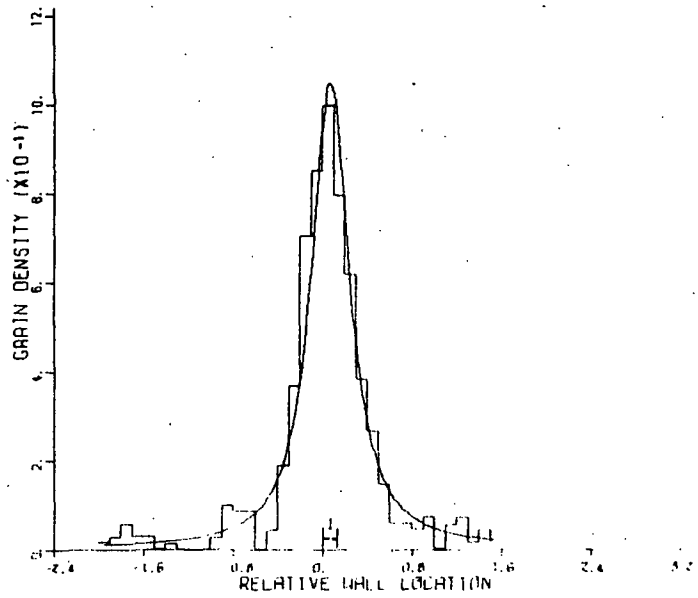

Figure 22. Grain Density Distributions in A-3 Fiber Walls

A24A (54-2) 705 GRAINS IN 1.330 UM WALL
(0.300, 0.200, 0.650) (1.000, 0.700, 0.350)
VARIANCE = 242.E-04
65.0% OF ACTIVITY IN BAND 1
35.0% OF ACTIVITY IN BAND 2

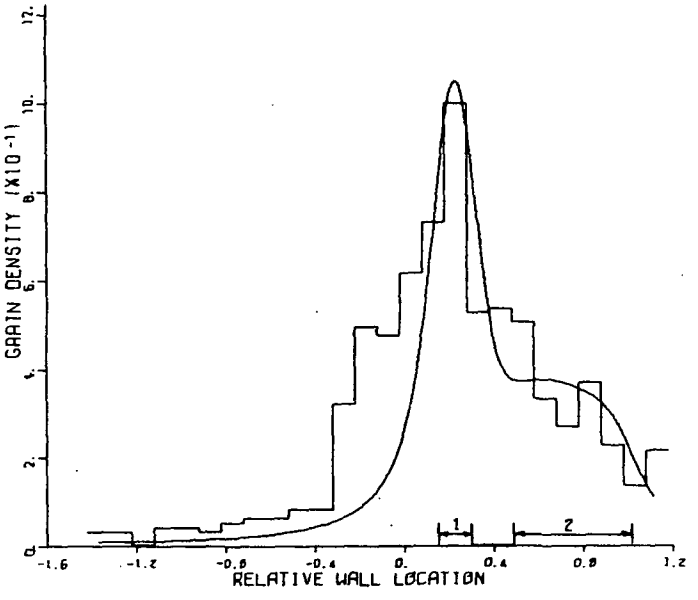

A24-B (45-1) 976 GRAINS IN 0.815 UM WALL
(0.180, 0.250, 0.940) (0.750, 0.200, 0.060)
VARIANCE = 498.E-05
94.0% OF ACTIVITY IN BAND 1
6.0% OF ACTIVITY IN BAND 2

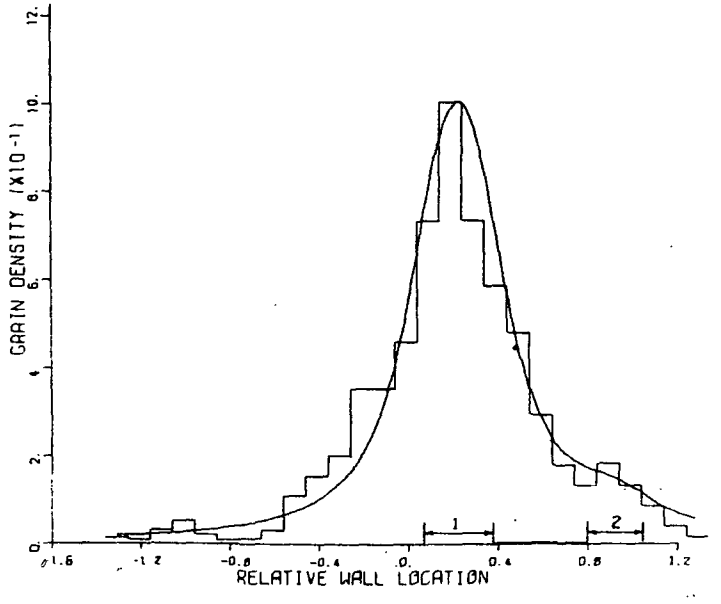

Figure 23. Grain Density Distributions in A-24 Fiber Walls

A-48A (48-1) 1163 GRAINS IN 1.616 μM WALL
(0.750, 0.500, 1.000)
VARIANCE = 284.E-05
100.0% OF ACTIVITY IN BAND 1

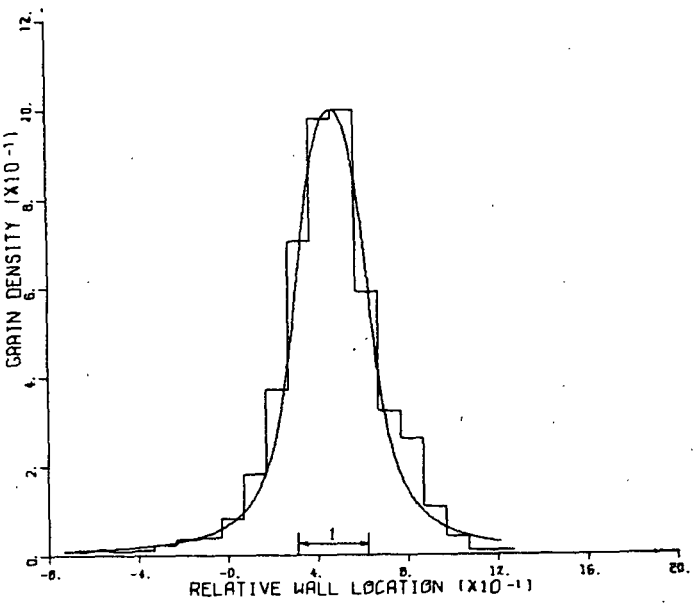

A-48B (48-4) 998 GRAINS IN 1.698 UM WALL
(0.750, 0.500, 1.000)
VARIANCE = 720.E-05
100.0% OF ACTIVITY IN BAND 1

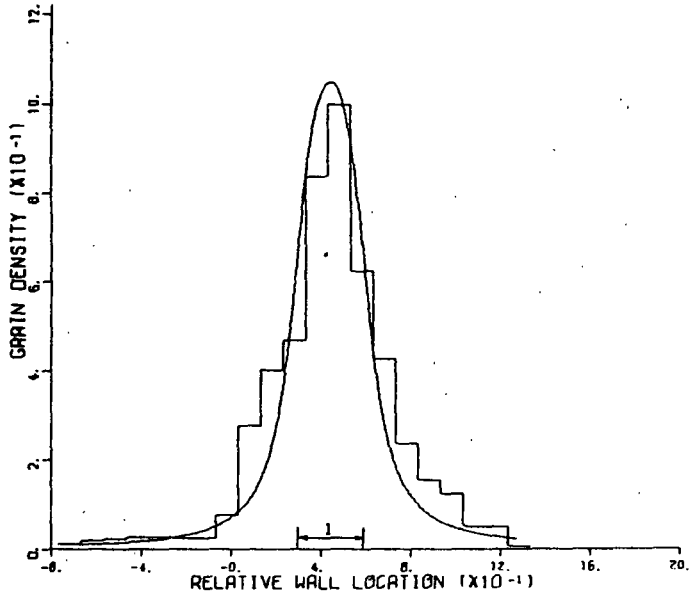

A-48C (49-3) 506 GRAINS IN 1.469 UM WALL
(0.520, 0.250, 0.960) (1.550, 0.100, 0.040)
VARIANCE = 140.E-05
96.0% OF ACTIVITY IN BAND 1
4.0% OF ACTIVITY IN BAND 2

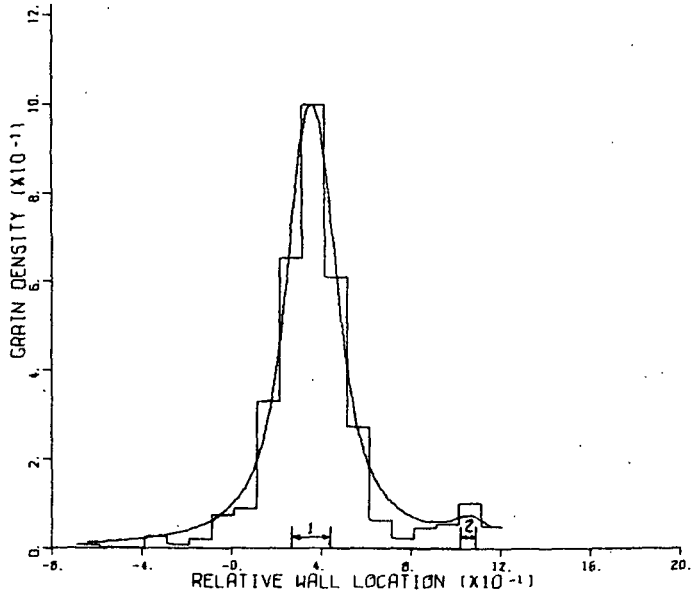

A-48E (48-5) 1064 GRAINS IN 1.720 UM WALL
(0.275, 0.450, 0.900) (1.550, 0.200, 0.100)
VARIANCE = 654.E-05
90.0% OF ACTIVITY IN BAND 1
10.0% OF ACTIVITY IN BAND 2

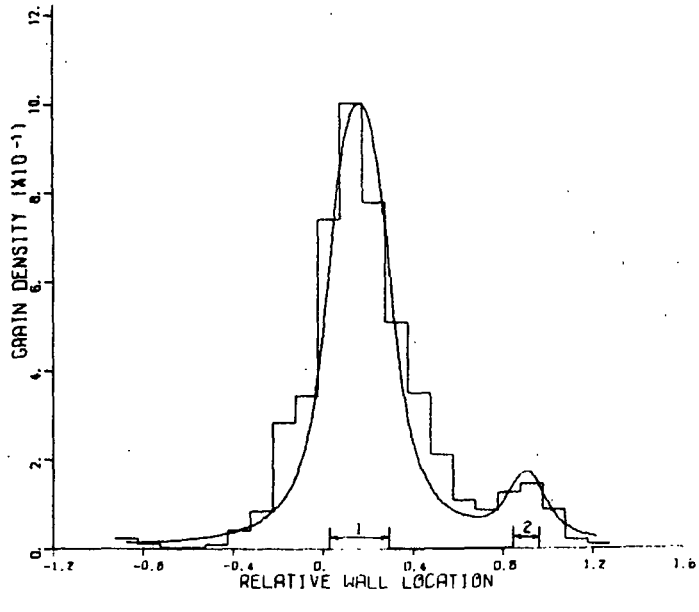

Figure 24. Grain Density Distributions in A-48 Fiber Walls (Cells A, B, C, and E)

A-48F (47-5) 841 GRAINS IN 1.392 UM WALL
(0.125, 0.250, 0.750) (0.750, 0.250, 0.250)
VARIANCE = 648.E-05
75.0% OF ACTIVITY IN BAND 1
25.0% OF ACTIVITY IN BAND 2

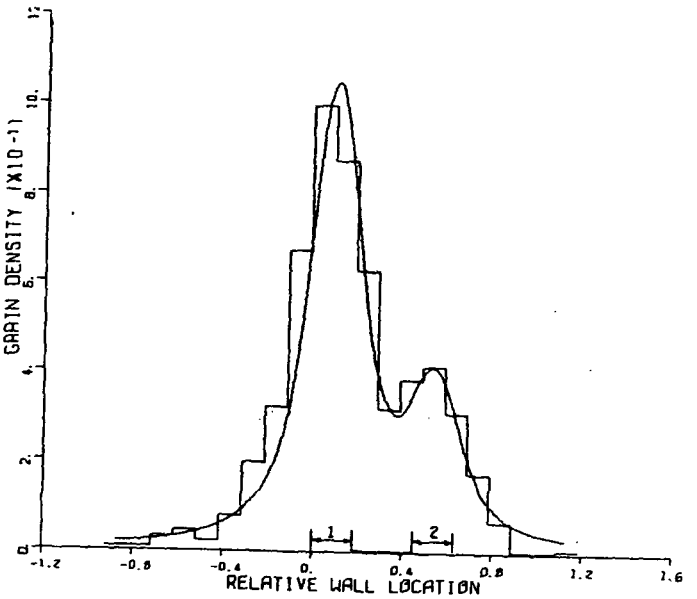

A-48G (47-3) 1202 GRAINS IN 1.878 UM WALL
(0.200, 0.400, 0.960) (1.878, 0.150, 0.040)
VARIANCE = 276.E-05
96.0% OF ACTIVITY IN BAND 1
4.0% OF ACTIVITY IN BAND 2

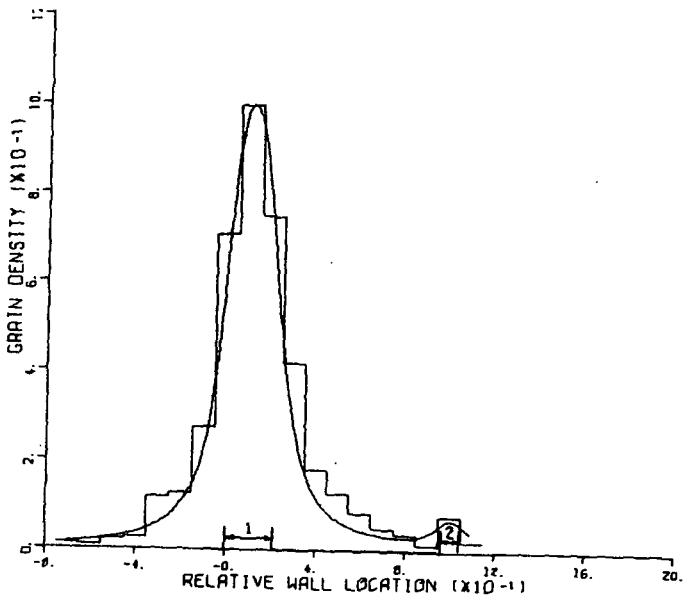

A-48H (47-4) 735 GRAINS IN 1.537 UM WALL
(0.100, 0.200, 0.900) (1.100, 0.200, 0.100)
VARIANCE = 158.E-04
90.0% OF ACTIVITY IN BAND 1
10.0% OF ACTIVITY IN BAND 2

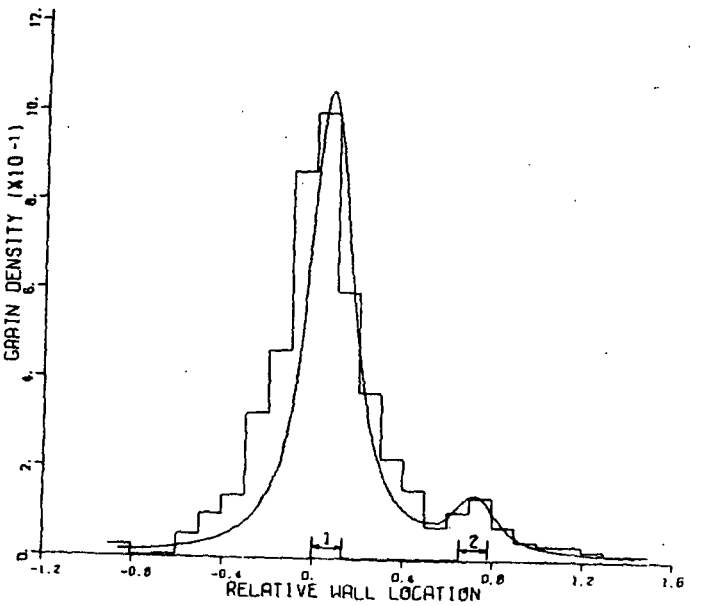

Figure 25. Grain Density Distributions in A-48 Fiber Walls (Cells F, G, and H)

Figures 26-29 illustrate the grain density distributions of cells in tissue fed sugar G6. Figures 26 and 27 show cells from tissue incubated 48 hours. Cells of delignified tissue (DG6) incubated for 24 and 48 hours are shown in Fig. 28 and 29, respectively.

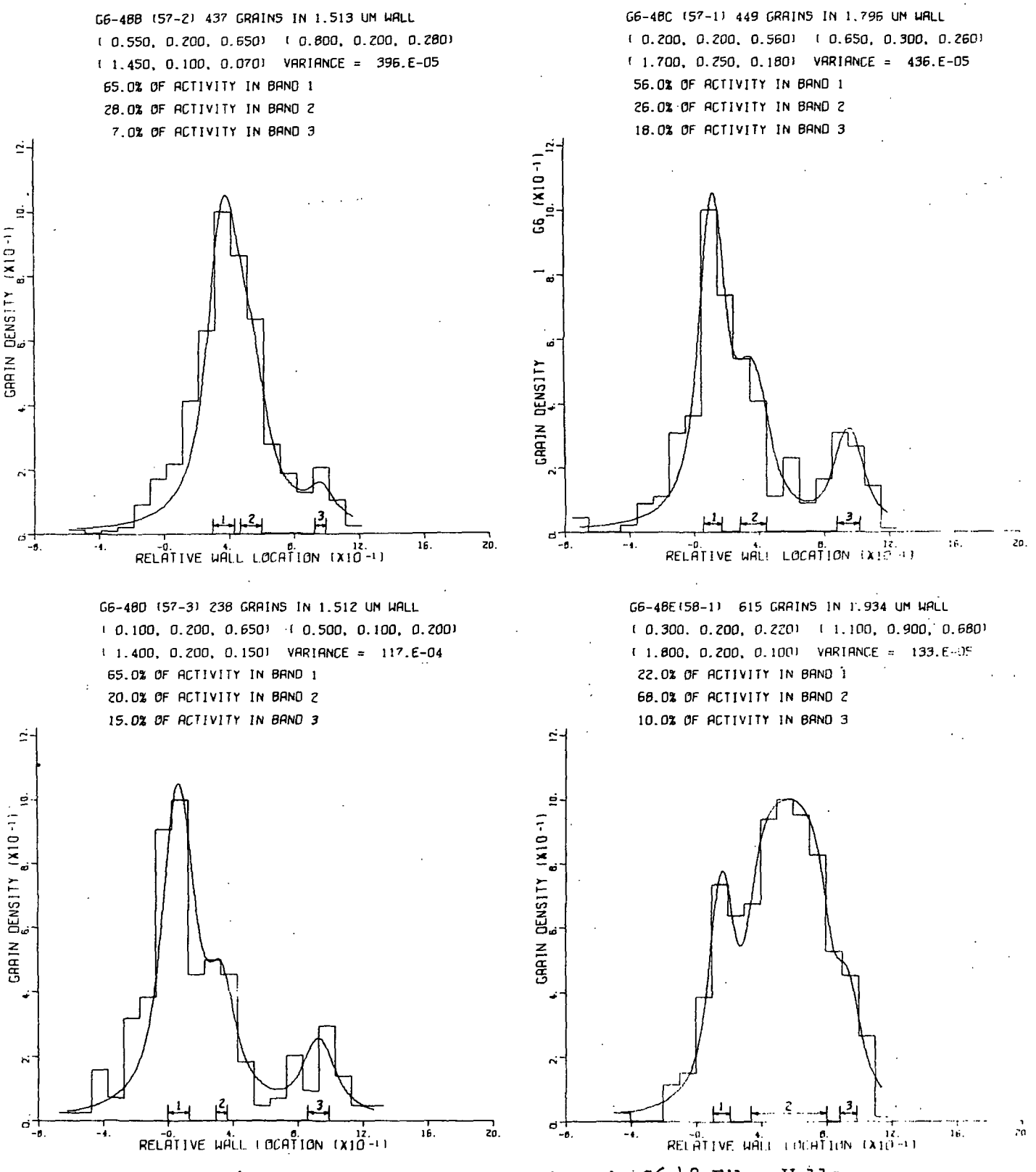

Figure 26. Grain Density Distributions in G6-48 Fiber Walls (Cells B, C, D, and E)

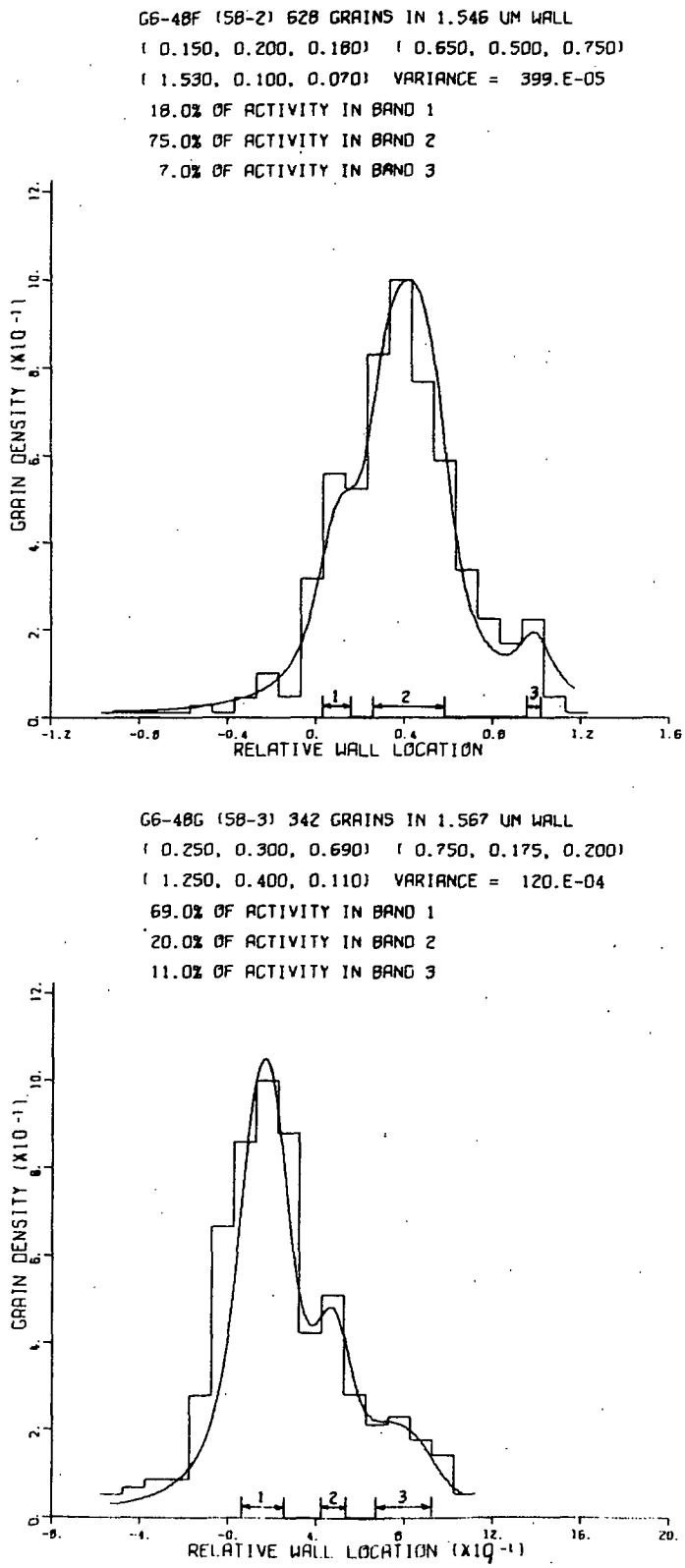

Figure 27. Grain Density Distributions in G6-48 Fiber Walls (Cells F and G)

DG6-24A (60-4) 633 GRAINS IN 1.107 UM WALL
(0.130, 0.200, 0.700) (0.450, 0.200, 0.270)
(1.200, 0.050, 0.030) VARIANCE = 659.E-05
70.0% OF ACTIVITY IN BAND 1
27.0% OF ACTIVITY IN BAND 2
3.0% OF ACTIVITY IN BAND 3

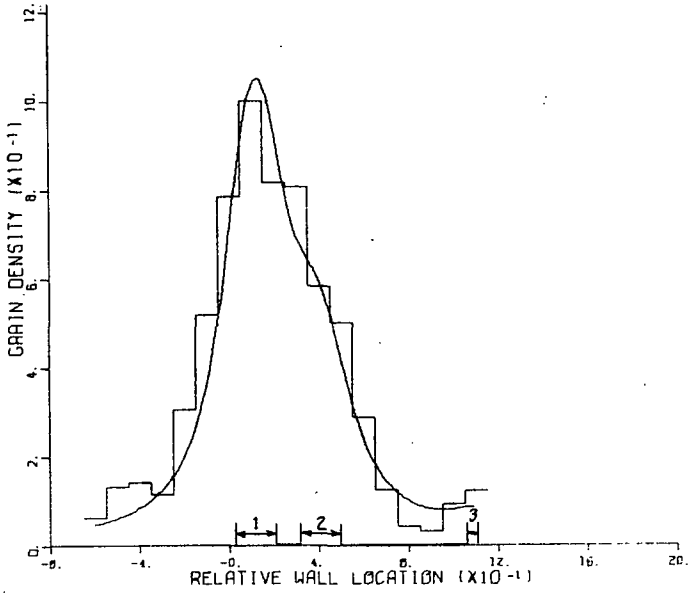

DG6-24B (60-4) 1050 GRAINS IN 1.376 UM WALL
(0.150, 0.300, 0.880) (1.000, 0.400, 0.120)
VARIANCE = 206.E-04
88.0% OF ACTIVITY IN BAND 1
12.0% OF ACTIVITY IN BAND 2

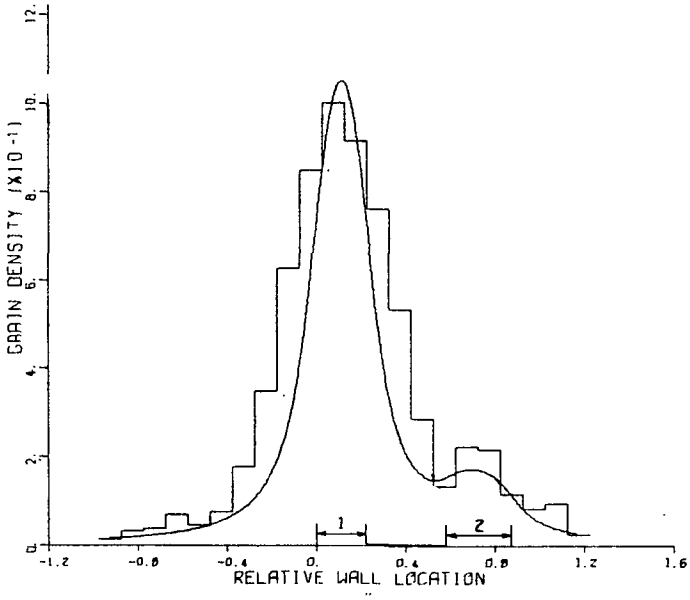

DG6-24C (60-5) 571 GRAINS IN 2.096 UM WALL
(0.200, 0.300, 0.700) (0.650, 0.500, 0.200)
(2.100, 0.200, 0.100) VARIANCE = 166.E-04
70.0% OF ACTIVITY IN BAND 1
20.0% OF ACTIVITY IN BAND 2
10.0% OF ACTIVITY IN BAND 3

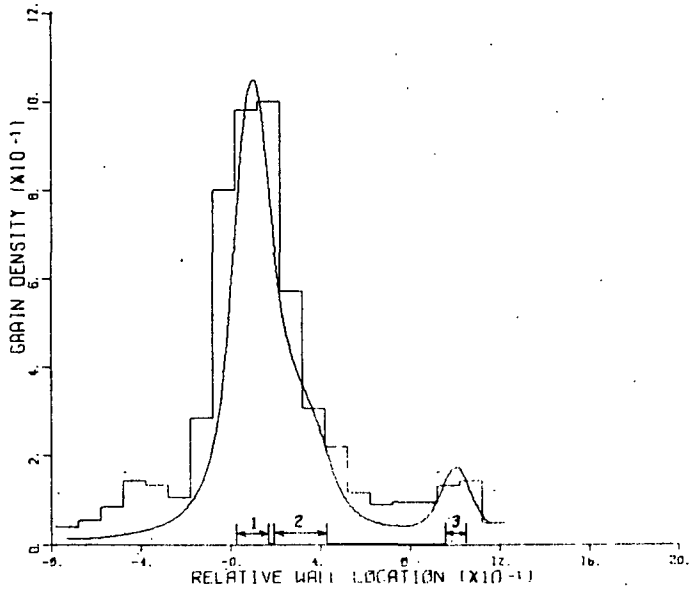

Figure 28. Grain Density Distributions in DG6-24 Fiber Walls

DG6-48A (52-4) 1216 GRAINS IN 0.804 UM WALL
(0.240, 0.200, 0.900) (0.750, 0.200, 0.100)
VARIANCE = 378.E-05
90.0% OF ACTIVITY IN BAND 1
10.0% OF ACTIVITY IN BAND 2

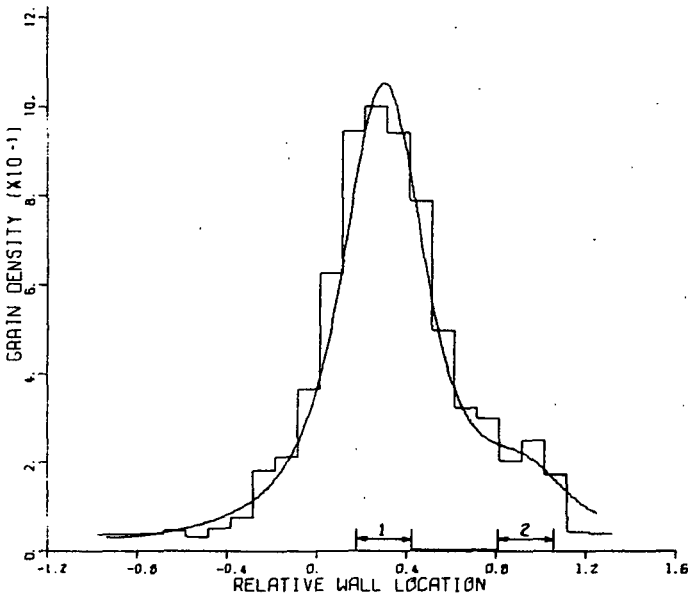

DG6-48B (52-3) 1216 GRAINS IN 0.850 UM WALL
(0.400, 0.200, 0.850) (0.750, 0.200, 0.150)
VARIANCE = 169.E-05
85.0% OF ACTIVITY IN BAND 1
15.0% OF ACTIVITY IN BAND 2

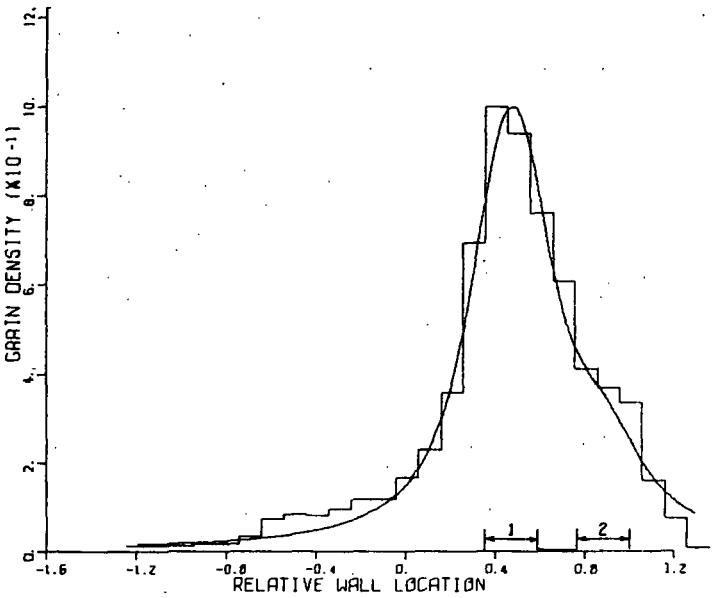

DG6-48C (52-5) 1189 GRAINS IN 1.207 UM WALL
(0.320, 0.200, 0.800) (0.580, 0.250, 0.130)
(1.100, 0.100, 0.070) VARIANCE = 486.E-05
80.0% OF ACTIVITY IN BAND 1
13.0% OF ACTIVITY IN BAND 2
7.0% OF ACTIVITY IN BAND 3

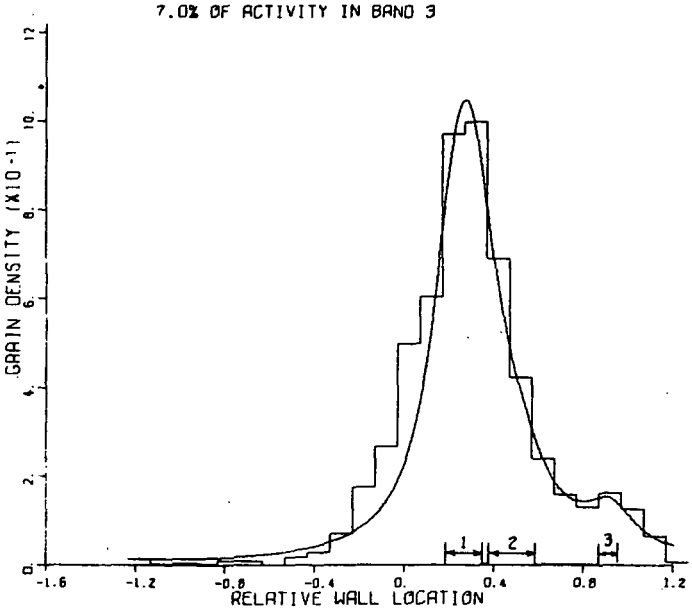

DG6-48D (52-5) 914 GRAINS IN 1.243 UM WALL
(0.180, 0.200, 0.900) (0.600, 0.300, 0.050)
(1.200, 0.200, 0.050) VARIANCE = 898.E-05
90.0% OF ACTIVITY IN BAND 1
5.0% OF ACTIVITY IN BAND 2
5.0% OF ACTIVITY IN BAND 3

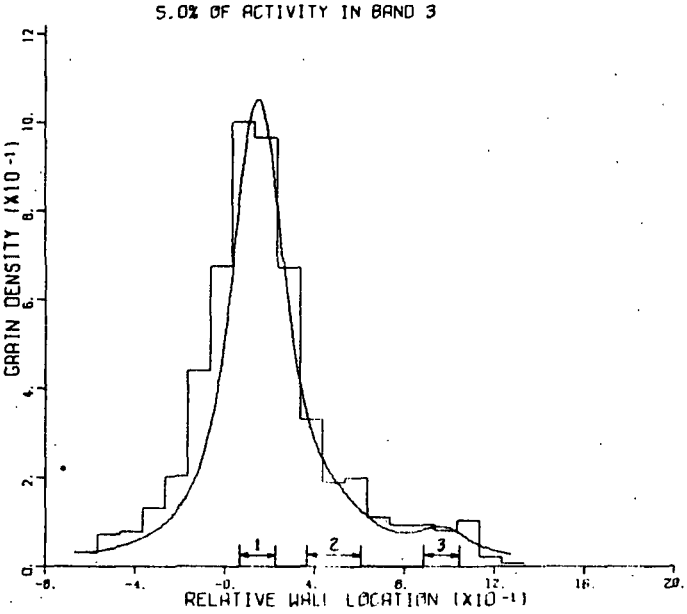

Figure 29. Grain Density Distributions in DG6-48 Fiber Walls